AN INTERNATIONAL FORUM FOR THE RAPID PUBLICATION OF ORIGINAL SCIENTIFIC ARTICLES DEALING WITH SCIENCES AND RELATED INTERDISCIPLINARY AREAS

# SOUTHERN JOURNAL OF SCIENCES

VOLUME THIRTY-THREE, NUMBER FORTY

ISSN: 2764-5967 - E-ISSN: 2764-5959

DECEMBER– 2025

# SOUTHERN JOURNAL OF SCIENCES

**ISSN: 2764-5967** **E-ISSN: 2764-5959**

**Volume 33** **Number 40** **2025**

## Dados Internacionais de Catalogação na Publicação (CIP)

S727 Southerm Journal of Sciences [recurso eletrônico] : interdisciplinary path for scientific divulgation / Araucária Associação Científica – (Fev. 2022). – Dados eletrônicos. – Nova Prata. : Araucária Associação Científica, 2024-.

Semestral
Recurso on-line
Descrição baseada em: Vol. 30, n. 33 (JUN. 2022)
Formerly known as: Southern Brazilian Journal of Chemistry
Modo de acesso: < https://sjofsciences.com>.
E-ISSN: 2764-5959
ISSN: 2764-5967

1. Química. 2. Física. 3. Biologia. 4. Ciências Naturais. 5. Farmacologia. 6. Ciências exatas. 7. Ciências aplicadas. 8. Ciências. I. Dr. D. Scientific Consulting.

UDC 001

**Bibliotecário Responsável**
Ednei de Freitas Silveira
CRB 10/1262

Journal E-mail: southbchem@gmail.com

# SOUTHERN JOURNAL OF SCIENCES

**ISSN: 2764-5967** **E-ISSN: 2764-5959**

**Volume 33** **Number 40** **2025**


# Editorial Board

**SOUTHERN JOURNAL OF SCIENCES**

**ISSN: 2764-5959 (Online)**
**ISSN: 2764-5967 (Print)**

DOI: 10.48141/2764-5959
Digital preservation: Portico

*Former Southern Brazilian Journal of Chemistry*
*Former E-ISSN 2674-6891*
*Former ISSN 0104-5431*

**Available at**
https://sjofsciences.com

**Mission**

The **SOUTHERN JOURNAL OF SCIENCES** is a double-blind peer review, open access, **multidisciplinary** Journal dedicated to publishing high-quality content and is intended to fill a gap in terms of scientific information for Southern Brazil. We have set high standards for the articles to be published by ensuring strong but fair refereeing by at least two reviewers. The Journal publishes original research articles in all the fields of Engineering, Mathematics, physics, Chemistry, Biology, Agriculture, Natural resource management, Pharmacy, Medicine, and others.

Occasionally the Journal will include review papers, interviews, and other types of communications. It will be published mainly in English, and at present, there are no page charges.

We hope this Journal will provide a forum for disseminating high-quality research in Science and are open to any questions and suggestions.

The responsibility for the articles is exclusive to the authors.

**Subjects List**
UDC 001

**Correspondências**
Av. Carlos Tarasconi, 281/202.
Bairro Sagrada Familia. CEP: 95320-000
Nova Prata – RS. Brasil.
www.sjofsciences.com
southbchem@gmail.com

# INDEX OF THE ISSUE NUMBER 40

**ISSN: 2764-5967** **E-ISSN: 2764-5959**

**Volume 33** **2025**

SOUTHERN JOURNAL OF SCIENCES

*ESTABLISHED IN 1993*

*Original research paper*

# GEOSPATIAL IDENTIFICATION OF BUILT-UP STRUCTURES ALONG THE DISCERNED KAZAURE-KARAUKARAU-KUSHAKA-ILESHA SCHIST BELT

# IDENTIFICAÇÃO GEOESPACIAL DE ESTRUTURAS EDIFICADAS AO LONGO DO CINTURÃO DE XISTO KAZAURE-KARAUKARAU-KUSHAKA-ILESHA DISCERNIDO

JONAH, Sunday Adole[1*]; ADEMU, Glory Ojone[2]; ABDULRASAQ, Ahmed Ayinde[3]; ADEOLA, Sheriff Sikiru[4]; BELLO, Abraham Oluwatobi[5]; BALOGUN, John Abiodun[6]; JOSHUA, Emmanuel Olorunleke[7]; SHOTONWA, Roagess John[8]; SAIDU, Salihu[9]

[1-8] Federal University of Technology, School of Physical Science, Department of Physics, Minna, Nigeria
[9]Federal University of Technology, School of Physical Science, Department of Geography, Minna, Nigeria.
**Corresponding author: s.jonah@futminna.edu.ng*
* ORCID: 0009-0002-2017-2611

Received 26 November 2024; received in revised form 26 September 2025; accepted 01 December 2025

## ABSTRACT

**Background:** The desire to create a database of research documents providing information about the tracts of gold deposits across the local geological province provides the impetus for a study of the kind being considered here. Geospatial identification of built-up structures within Phase I Development along the Kazaure-Karaukarau-Kushaka-Ilesha Schist Belt, trending through Minna town and its outlying districts, constitutes the veritable reference material desired in this regard. **Methods:** This study began by segmenting the area of study for ground-based and remotely sensed attribute mapping, using the key reference map from a previous study as the area-of-study guide. A handheld Garmin GPSmap78® global positioning system unit and a standard smartphone with a built-in camera were the key equipment used for the fieldwork. Polygonal-format georeferenced coordinate information was collected at conveniently detached buildings, beginning with the cluster of residential homes at the Staff Quarters, for the ground-based survey. **Result:** Nine of the ten built-up structure clusters on the path of the Belt in Phase I Development were mapped for this study, as well as six neighborhoods in the Minna built-up area beyond Phase I. The nine clusters occupy almost 40% of the *circa* 2 km$^2$ areal extent of the Phase I Development. The belt's trend and structures were north-northeast. **Discussion:** The nine cluster structures in Phase I and the six neighborhoods of Minna identified in this study have been determined to align with the path of the belt. **Conclusion:** Having now determined that the trace of the belt exits the Campus at the northern sector of the Gidan Kwano village and trends in a long arc beyond the town, this study becomes the desired reference material to be archived and consulted for information relating to gold exploitation in the Minna Area geological province.

**Keywords:** *Gold; lineament; schist-belt; georeference; remote-sensed.*

## RESUMO

**Introdução:** O desejo de criar uma base de dados de documentos de pesquisa fornecendo informações sobre os traços de depósitos de ouro ao longo da província geológica local fornece o ímpeto para um estudo do tipo aqui considerado. A identificação geoespacial de estruturas edificadas dentro do Desenvolvimento Fase I ao longo do Cinturão de Xisto Kazaure-Karaukarau-Kushaka-Ilesha que se estende através da cidade de Minna e seus distritos periféricos torna-se o material de referência verdadeiro que é desejado a este respeito. **Métodos:** Este estudo procedeu inicialmente com a segmentação da área de estudo para mapeamento de atributos baseado em solo e por sensoriamento remoto, por meio do qual o mapa de referência chave de um estudo anterior foi consultado como guia da área de estudo. Uma unidade portátil de sistema de posicionamento global Garmin GPSmap78® e um smartphone padrão com câmera embutida foram os equipamentos-chave empregados para o trabalho de campo. Informações de coordenadas georreferenciadas em formato poligonal foram coletadas em edifícios convenientemente isolados, começando no conjunto de residências no Alojamento

 
DOI: 10.48141/2764-5959.01.v33.n40.2025_01_Sunday_pgs_1_18.pdf

de Funcionários para o levantamento baseado em solo. **Resultado:** Nove dos dez agrupamentos de estruturas edificadas no caminho do Cinturão no Desenvolvimento Fase I foram mapeados para este estudo, bem como seis bairros na área construída de Minna além da Fase I. Os nove agrupamentos ocupam quase 40% da extensão areal de aproximadamente 2 km² do Desenvolvimento Fase I. A tendência do Cinturão e das estruturas nele contidas foi uma inclinação resultante norte-nordeste. **Discussão:** Os nove agrupamentos de estruturas na Fase I e os seis bairros de Minna identificados neste estudo foram determinados como alinhados no caminho do Cinturão. **Conclusão:** Tendo agora determinado que o traço do Cinturão sai do Campus no setor norte da vila Gidan Kwano e se estende em um longo arco além da cidade, este estudo torna-se o material de referência desejado para ser arquivado e consultado para informações relacionadas à exploração de ouro na província geológica da Área de Minna.

**Palavras-chave**: *Ouro; lineamento; cinturão de xisto; georreferenciamento; sensoriamento remoto*.

## 1. INTRODUCTION

The vestigial petrographic signature of the Kazaure-Karaukarau-Kushaka-Ilesha Schist Belt that is evidenced at the southern Phase II Development of the Gidan Kwano Campus, conveniently named “Jonahite” for future reference purposes (Jonah, 2021), is a geological lineament valued as the principal repository for gold deposits at the basement complex geological province of Nigeria (Obaje, 2009). Basically, the near-space of clusters of schist outcrops in a contiguous granitic basement environment is also suitable for groundwater accumulation (late Prof. P.I. Olasehinde, Department of Geology, personal communication).

The present built-up and ringed-off operational area of the Gidan Kwano Campus, conveniently termed the Phase I Development, was basically developed without much consideration for the “below-ground” geological nature of this tranche of the Campus. In hindsight, it can be argued that it was a factor of unfortunate circumstance that ensured that the knowledge-base that exists at the moment which indicates that the built-up Phase I Development is situated along a gold-bearing and groundwater-rich schist lineament was not available to the University at the moment the decision was made to develop what has become the present ringed-off land area where the core administrative and academic activities of the University are presently concentrated.

### 1.1 Research Question

Knowing that a body schist-rock lineament mapped in the predominant granitic mass of the basement complex rock of central Nigeria (especially those occurring west of longitude 8˚) is veritable gold repository (Obaje, 2009), could a dedicated study mapping the extension of one such linament through the built-up areas of Minna be the basis for re-calibrating to a higher degree of accuracy the gold-bearing character of Minna?

### 1.2 Aim

This study aims to carry out ground-based geospatial and remotely sensed mapping of built-up attributes along the Kazaure-Karaukarau-Kushaka-Ilesha Schist Belt, including the ringed-off Phase I Development of the Gidan Kwano Campus, and in the northeast and southwest directions where this belt trends beyond the built-up Phase I Development.

### 1.3 Objectives

The objectives of this study are the following: implementing ground-based, “foot-on-the-ground” geospatial data collection and archiving of built-up structures on the Kazaure-Karaukarau-Kushaka-Ilesha Schist Belt on its trending path through the Phase I Development, and applying remote-sensed satellite imaging techniques to extend the scope of attribute-identification techniques beyond the recognised Phase I Development identified for this study along the northeast path.

### 1.4 Expected Outcomes

The result of this study will be vital in the planning schedules for the near-term and long-term build-up development of the tranches of land areas contiguous to the presently-defined Phase I Development of the Gidan Kwano Campus as a useful guide to make informed decisions as to how to commit to groundwater-resources exploitation and setting a programme for eventual mining of solid minerals.

According to Jian and Philippa (2009), latitude can be defined as the angle between the equator and a line perpendicular to the ellipsoid, which ranges from $90^{\circ}$ North or south of the equator. Latitude is commonly given the Greek symbol phi ($\phi$), and longitude is lambda ($\lambda$). A line of constant latitude is known as a parallel. Parallels never meet since they are parallel to one another, whereas meridians (lines of longitude) converge at the poles. The authors also pointed

out that longitude is more complex: only east-west measurements made at the equator are true; away from the equator, where approximately the cosine of the latitude increasingly shortens the lines of latitude, measurements decrease in length. This means that at 30° north (or south), shortening is about 0.866; at 45°, 0.707; and at 60 °, 0.5. At 60° north or south, 1° of longitude will represent 55 km ground distance.

The Universal Transverse Mercator (UTM) is a *geographic coordinate system* that uses a two-dimensional (2-D) *Cartesian coordinate system* to locate points on the surface of the earth. It is a *horizontal position representation*, that is, it is used to identify locations on the earth independently of *vertical position*, but differs from the traditional method of latitude and longitude in several respects. The UTM system is not a single *map projection*. The system instead divides the earth into sixty zones, each a six-degree band of longitude, and uses a secant *transverse Mercator projection* in each zone.

Jian and Philippa (2009) stated that a further modification of the Mercator allows the production of the Universal Transverse Mercator (UTM) projection system. It is again projected on a cylinder tangent to a meridian [as in the Transverse Mercator (TM)] and by repeatedly turning the cylinder, about its polar axis, the world can be divided into 60 east-west zones, each $6^{\circ}$ longitude in width. The projection is conformal so that shapes and angles within any small area will be preserved. This system was originally adopted for large-scale military maps of the world, but it is now a global standard and is again useful for mapping large areas oriented north-south. Projected UTM grid coordinates are then established, which are identical between zones. Separate grids are also established for both northern and southern halves of each UTM zone to ensure there are no negative northings in the southern hemisphere. Hence, when quoting a UTM grid reference, it is essential to state eastings, northings, zone number and the hemisphere (north or south) to ensure clarity.

Ruihua *et al.* (2025) observed that by extending synthetic aperture technology from a microwave band to a laser wavelength, synthetic aperture ladar (SAL) achieves extremely high spatial resolution independent of target distance in long-range imaging. The authors pointed out that nonlinear phase correction is a critical challenge in SAL imaging. To address phase noise during the imaging process, they first analyzed the theoretical impact of nonlinear phase noise on imaging performance. Subsequently, a reconstruction and compensation method based on orthonormal complete basis functions was proposed to mitigate nonlinear phase noise in SAL imaging. The authors noted that the simulation results validate the accuracy and robustness of the proposed method, while experimental data demonstrate its effectiveness in improving system range resolution and reducing the peak side lobe ratio by 3 dB across various target scenarios. The authors concluded that this advancement establishes a solid foundation for the application of SAL technology in ground-based remote sensing and space target observation.

According to Yiqing *et al.* (2025), accurate, real-time, and dynamic monitoring of crop planting distributions in hilly areas with complex terrain and frequent meteorological changes is highly important for agricultural production. Thus, dual-polarization synthetic-aperture radar has significant application value in feature classification and crop distribution extraction due to its all-day, all-weather operation, large mapping bandwidth, and ease of data acquisition. The authors contended that to explore the feasibility and applicability of dual-polarization synthetic-aperture radar data in crop monitoring, their study was based on two basic methods of dual-polarization decomposition (eigenvalue decomposition and three-component polarization decomposition) to construct time series of crop dual-polarization radar vegetation indices; their study scope was full coverage analysis of crop distribution extraction in dryland mountainous areas of southeastern China. The authors noted that on the basis of the Sentinel-1 dual-polarization radar vegetation indices, the time-series classification and rapeseed distribution extraction impacts were compared using southern Hunan Province's principal rapeseed (*Brassica napus L.*) production area as the study area. The authors concluded that three-component polarization decomposition was more suitable than other methods for crop information extraction and remote sensing classification applications involving dual-polarized SAR data.

Jiaguo *et al.* (2025) remark that Spatial disparities in rangeland conditions across Kazakhstan complicate field-based assessments of livestock-carrying capacity (LCC), a critical metric for the country's food security and economic planning. Thus, the authors developed a geospatial livestock-carrying capacity (GLCC) modeling framework to quantify LCC spatio-temporal dynamics at the Oblast level, by integrating satellite-derived data on vegetation,

water resources, and terrain with in situ measurements. The authors observe that by providing ground-truth observations and contextual details, field-based measurements complement remote sensing data, helping to validate estimates and improve the reliability of the GLCC model. The modeling framework was successfully applied and validated in a case study in the Akmola Oblast, Kazakhstan, to specifically map the spatial and temporal distributions of LCC, using publicly available MODIS NPP data and in situ data from 51 field sites. The authors reported that the modeling results showed distinct spatial patterns of LCC across the Oblast, reflecting variability in rangeland productivity with higher values concentrated in southern and southeastern regions (up to 0.5 animals/ha). The results also showed significant interannual LCC fluctuations (ranging from 0.099 to 0.17 animals/ha), possibly due to rainfall variability, and thus serve as an indicator of climate-related risks for livestock management. Whilst noting that there is still room for further improvement, particularly in model parameterization to account for grazing pressures, forage quality, and livestock species, the authors concluded that the GLCC modeling framework is a simple tool for mapping livestock-carrying capacity, a more meaningful indicator for rangeland managers. Further, this work underscores the value of integrating remote sensing with field-based observations to support data-driven rangeland management planning and resilient investment strategies.

## 2. MATERIALS AND METHODS

### 2.1 Materials

#### *2.1.1 Handheld Global Positioning System (GPS) Unit*

The handheld Garmin GPSmap78® global positioning system unit shown in Figure 1 was employed to georeference built-up areas of interest in polygonal formats that were occupied for this study. The GPSmap78® is a high-sensitivity GPS with proprietary HotFix® coordinate-fixing software, an in-built 3-axis compass, and a barometric altimeter. This GPS unit also features 1.7 GB of internal memory and up to 20 hours of battery life (dual AA batteries, that is).


***Figure 1**. Handheld Garmin GPSmap78®*

#### *2.1.2 Phone with Built-in Camera*

A standard smartphone with a built-in camera was used to capture images of the corresponding georeferenced built-up polygons, as shown in Figure 2.

***Figure 2**.. Standard smartphone with built-in camera*

### 2.2 Methods

#### *2.2.1 Study Area Segmentation for Ground-based and Remotely-sensed Attribute Mapping*

At the outset, the map from the work of Jonah (2021) showing fault-trace of fracture signatures inferred from a combination of the geoelectric cross-sections and the qualitative induced polarisation tables from that study on the satellite image map of the southern Phase II Development was consulted as area-of-study guide by which investigation proceeded in the northeast-southwest sense into the built-up Phase I Development that is also visible on the map. The northeast trace beyond the Phase I Development is the extent of the area of investigation by remote-sensing techniques. The map segmentation format is as shown in Figure 3.

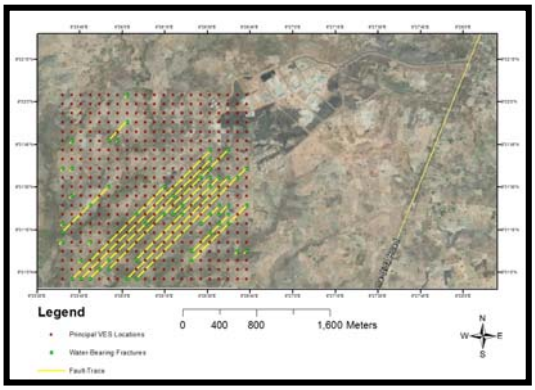


***Figure 3.*** *Map segmentation format for ground-based and remotely sensed attribute mapping (Source: Jonah, 2021)*

#### *2.2.2. Ground-Based Attribute Mapping*

Using the map of Figure 3 as a guide, built-up attributes on the northeast extension of the maximum width of the yellow-colored parallel lines (*circa* 2200 width) were georeferenced in polygonal modes, beginning from the lecturers' quarters at the extreme southwest of the ringed-off Phase I Development to the University's administration block (that is, the Senate Building) at the northeast. To adequately capture the geographic attributes of a built-up structure, such as a building, in GIS space, it is necessary to represent its spatial extent by acquiring its coordinates at the typical four corners of the building (the tetragon). However, architectural design requirements mean that many built-up structures are not necessarily tetragonal but "multi-sided" or "polygonal"; hence, the requirement to also acquire geographical attributes at the corners of such buildings.

Georeferencing built-up structures for this study was not in an arbitrary format; the map in Figure 3 served as the guide, so that buildings along the discerned schist lineament were earmarked for geographic attribute survey. Since the width of the discerned schist lineament trending through the Phase I Development is *circa* 800 m, all built-up structures (100%) along this lineament were visited for the acquisition of geographic attribute data. These attributes were chiefly latitude and longitude information (the x- and y-coordinates) determined at the corners of the buildings by the handheld Garmin GPSmap78® global positioning system unit, plus information on the date and time of visit, weather, and a local-nomenclature identifier, rendering these buildings easy to identify. Information about elevation above mean sea level (the z-co-ordinate) was considered a redundancy factor and thus ignored.

The Garmin GPSmap78, being motion-sensitive, must be held at the point of measurement in static-motion mode to extract the x- and y- coordinate information.

#### *2.2.3 Remoted-Sensed Attribute Mapping*

Remotely sensed attribute mapping of the area beyond Phase I Development was aided by recourse to QuickBird satellite imagery with 0.65 m panchromatic resolution, acquired on 20th July 2023, sourced from Datanet Services, Minna, Nigeria.

## 3. RESULTS AND DISCUSSION

### 3.1. Results

Figure 3 and Figure 4 provide the platforms upon which the data presentation aspect of the study under consideration herein rests.

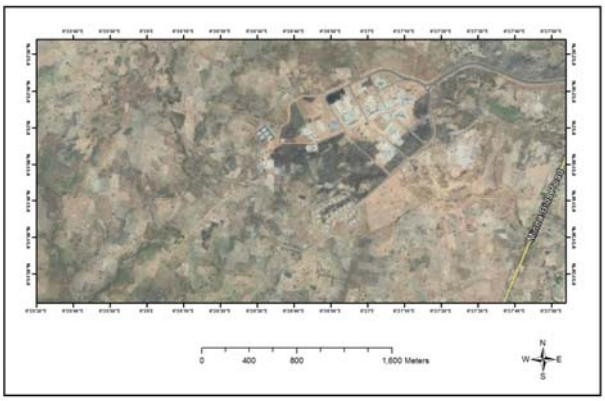


***Figure 4.*** *Satellite imagery map of the Phase I Development (Source: Jonah, 2024)*

#### *3.1.1 Ground-Based Attribute Mapping*

*3.1.1.1 Staff Quarters*

In Figure 5, the apartments of the Staff Quarters (latitude-longitude degree-minute-second coordinates for apartments 1 to 4 only are provided in the attached tables) of the Gidan Kwano Campus, located between UTM 1053700:1054300 and 219500:220000 are identified as being on the route of the northeast-trending Kazaure-Karaukarau-Kushaka-Ilesha Schist Belt.

*3.1.1.2 Works Department*

The Works Department complex shown in Figure 5, between UTM 1054300: 1054600 and 220000: 220500, although located just outside Phase I Development, lies along the northeast-

trending Kazaure-Karaukarau-Kushaka-Ilesha Schist Belt.

*3.1.1.3 School of Information and Communication Technology*

The School (that is, Faculty) of Information and Communication Technology (ICT) complex shown in Figure 5, between UTM 1054300: 1054900 and 220000: 220500, is located along the northeast-trending Kazaure-Karaukarau-Kushaka-Ilesha Schist Belt.

*3.1.1.4 School of Agriculture and Agricultural Technology*

The School of Agriculture and Agriculture Technology complex shown in Figure 5, between UTM 1054600: 1055200 and 219500: 220500, is located along the northeast-trending Kazaure-Karaukarau-Kushaka-Ilesha Schist Belt.

*3.1.1.5 Senate Building*

The Senate Building shown in Figure 5, between UTM 1054600: 1054900 and 220000: 220500, and just northeast of the School of Agriculture and Agriculture Technology complex, is located along the northeast-trending Kazaure-Karaukarau-Kushaka-Ilesha Schist Belt.

*3.1.1.6 Schools of Engineering Complex*

The built-up complex of the School of Engineering and Engineering Technology and the School of Infrastructure and Process Technology, shown in Figure 5 between UTM 1054600: 1055200 and 220000: 220500, is located along the northeast-trending Kazaure-Karaukarau-Kushaka-Ilesha Schist Belt.

*3.1.1.7 School of Environmental Technology Complex*

The built-up complex of the School of Environmental Technology and its adjunct Lecture Theatre, shown in Figure 5, between UTM 1054900: 1055200 and 220000: 220500, is located along the northeast-trending Kazaure-Karaukarau-Kushaka-Ilesha Schist Belt.

*3.1.1.8 Centre for Open and Distance e-Learning (CODeL)*

The built-up complex of the Centre for Open and Distance e-Learning (CODeL), shown in Figure 5, between UTM 1054900: 1055200 and 219500:220000, is located along the northeast-trending Kazaure-Karaukarau-Kushaka-Ilesha Schist Belt.

*3.1.1.9 Chapel of Grace*

The built-up Chapel of Grace shown in Figure 5 between UTM 1054900: 1055200 and 219000: 219500, located just outside the Phase I Development on the northwest corner, is not located along the northeast-trending Kazaure-Karaukarau-Kushaka-Ilesha Schist Belt.

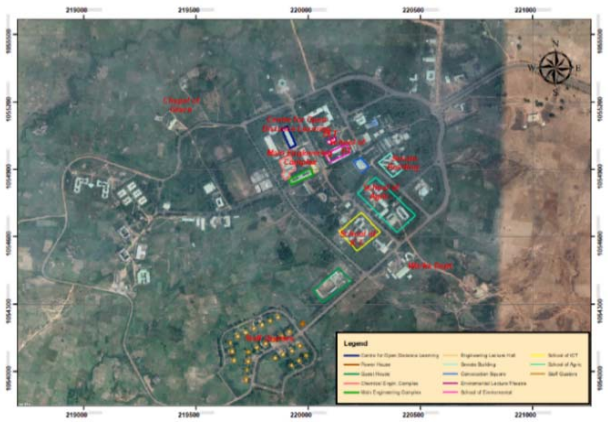

***Figure 5**. Identified built-up attributes along the diagonal vestigial trace of the Kazaure-Karaukarau-Kushaka-Ilesha Schist Belt through the Phase I Development*

***3.1.2. Remoted-Sensed Attribute Mapping***

*3.1.2.1 Northeast Sector Beyond Phase I Development*

On an extended northeast trend of the schist belt beyond the Phase I Development, the next sector for this study is the northeastern sector of Phase I Development-cum-Minna-Bida Road-cum-northern sector of Gidan Kwano Village, as shown in Figure 6.

***Figure 6**. Northeastern sector of Phase I Development-cum-Minna-Bida Road-cum-northern sector of Gidan Kwano Village captured on satellite map*

*3.1.2.2 Talba Housing Estate*

On a further extended northeast trend of the schist belt beyond the “Northeast Sector Beyond Phase I Development,” the next sector for

this schedule of study is the Talba Housing Estate area, seen in Figure 7.

***Figure 7**. The Talba Housing Estate area captured on satellite map*

*3.1.2.3 Minna South Area*

On a futher extended northeast trend of the schist belt beyond the Talba Housing Estate, the next sector for this schedule of study is the Minna South Area seen in Figure 8.

***Figure 8**. Minna South Area captured on a satellite map in its relative position to the settlement of Kpakungu*

*3.1.2.4 Central Minna*

On a further extended northeast trend of the schist belt beyond the Minna South Area, the next sector for this study is the Central Minna area, as seen in Figure 9.

***Figure 9**. Central Minna area captured on a satellite map*

*3.1.2.5 Maitumbi East*

On a further extended northeast trend of the schist belt beyond the Central Minna area, the next sector for this study is the Maitumbi East neighborhood, seen in Figure 10.

***Figure 10**. Maitumbi East neighbouhood along the Minna Eastern Bye-Pass captured on satellite map*

*3.1.2.6 Gwada*

On a futher extended northeast trend of the schist belt beyond the Maitumbi East neighborhood, the next sector for this schedule of study is the Gwada Area seen in Figure 11.

***Figure 11**. Gwada Area is a veritable distant suburb lying northeast of the Maitumbi neighborhood*

**3.2. Discussion**

***3.2.1. Ground-Based Attribute Mapping***

*3.2.1.1. Staff Quarters*

The 25 units of housing in the Staff Quarters, forming neatly separated rows in a cluster and, albeit terribly short in number, to accommodate all academics, are located at the southern fringe of the built-up and ringed-off Phase I Development, about 600 m from the centerline of the discerned Kazaure-Karaukarau-Kushaka-Ilesha Schist Belt.

*3.2.1.2 Works Department*

The Works Department complex, located on a straight northeast route from the southernmost fringe of the Staff Quarters some 500 m away across the University Golf Course and just outside the Phase I Development, is on the northeast extremity of the Kazaure-Karaukarau-Kushaka-Ilesha Schist Belt about 600 m from the centerline.

*3.2.1.3 School of Information and Communication Technology*

The School of Information and Communication Technology is located on a straight northwestern course, 100 m from the Works Department and about 500 m from the centerline of the Kazaure-Karaukarau-Kushaka-Ilesha Schist Belt.

*3.2.1.4 School of Agriculture and Agricultural Technology*

The School of Agriculture and Agricultural Technology (SAAT) is a relatively large complex of buildings across a secondary road, some 20-30 m to the northeast of the School of Information and Communication Technology complex. The northwesternmost edge of SAAT is about 300 m from the centerline of the Kazaure-Karaukarau-Kushaka-Ilesha Schist Belt.

*3.2.1.5 Senate Building*

The Senate Building grounds are located some 50 to 60 m across a roadway from the SAAT complex, in a northeasterly direction, about 250 m from the centerline of the Kazaure-Karaukarau-Kushaka-Ilesha Schist Belt.

*3.2.1.6 Schools of Engineering Complex*

The Schools of Engineering Complex, located some 300 m northwest of the School of Information and Communication Technology, lies on the centerline of the Kazaure-Karaukarau-Kushaka-Ilesha Schist Belt.

*3.2.1.7 School of Environmental Technology Complex*

The School of Environmental Technology Complex, shown as the purple rectangle in Figure 5 and located some 50 to 60 m across a roadway from the Schools of Engineering Complex, is only *circa* 70-80 m away from the centerline of the Kazaure-Karaukarau-Kushaka-Ilesha Schist Belt.

*3.2.1.8 Centre for Open and Distance e-Learning (CODeL)*

The grounds of the Centre for Open and Distance e-Learning (CODeL) is almost contiguous with the grounds of the Schools of Engineering Complex. The CODeL complex is located just northeast of the Schools of Engineering Complex, smack on the centerline of the Kazaure-Karaukarau-Kushaka-Ilesha Schist Belt.

*3.2.1.9 Chapel of Grace*

The Chapel of Grace is clearly situated within the 2200 m generic width of the Kazaure-Karaukarau-Kushaka-Ilesha Schist Belt, approximately 550 m northwest of the centerline, as illustrated in Figure 5. While the student hostel complex buildings also fall within this defined generic width, ground-based survey work in the vicinity and at the peripheries of these structures is generally inadvisable due to unsanitary conditions resulting from inadequate sanitation infrastructure and the resulting surface contamination with human waste around the buildings.

***3.2.2. Dataset of Ground-Based Attributes***

The information dataset for this study was recorded on a purpose-specific data sheet. The coordinate information from the ideal four-corner building was the targeted “polygon” sought. However, some rather large buildings are not exactly shaped like ideal tetragonal forms as determined by the architects, and for these and other built-up structures, coordinate information was obtained from the many-sided attributes of such buildings. Some of the attribute information for this study are presented in Tables 1 to 8. Some of the built-up structures, especially apartments, are more often than not restricted-access areas; thus, even for structures aligning in perfect north-south or east-west trends, slight variations are noticeable in their assumed geographic coordinate orderings.

***3.2.3. Remoted-Sensed Attribute Mapping***

*3.2.3.1 Northeast Sector Beyond Phase I Development*

In Figure 6, the Minna-Bida highway forms the principal backdrop for the clusters of shacks and hovels that comprise Gidan Kwano Village (the university campus was named in honor of this village, the *primus* settlement in those parts). The satellite imagery faithfully follows a northeast trend with great fidelity, aligning with the schist belt lineament to capture this sector for this study's schedule.

*3.2.3.2 Talba Housing Estate*

Figure 7 captures the broader area of the well-known Talba Housing Estate on the extended

northeast trend of the schist belt, as the next sector for this study. This figure shows that the Minna-Bida highway follows the northeast trend of interest in this study. However, on both sides of this roadway are dense settlement clusters that lie along the Kazaure-Karaukarau-Kushaka-Ilesha Schist Belt. The Talba Housing estate proper is opposite the Newgate College of Health Science nd Technology (now the Newgate University). Another prominent feature noted in Figure 7 is the approximate northwest-southeast course of a major seasonal stream that drains the northern segment of Minna town during the rainy season from May to October each year. Illegal gold mining by panning alluvial soil is characteristic of activities at the banks of the seasonal stream skirting the Talba Housing Estate.

*3.2.3.3 Minna South Area*

In Figure 8, it is observed that the course of the Minna-Bida highway terminates at the Kpakungu Roundabout from whence the southeast roadway leads to the neighborhoods of Barkin Sale, Sauka ka Kuta, Shango, Army Barracks, and Chanchaga. The opposite branch of the roadway, towards the northeast, leads to the neighborhoods of Oduoye Estate, Fadikpe, Dutsen Kura, Bosso, and, further out, to Maikunkele.

*3.2.3.4 Central Minna*

In Figure 9, the Eastern Bypass is now visible as the bold linear streak to the east of this illustration. The Central Minna built-up zone, as expected, is extensive, and attention in this study is focused on the rightward segment of the map in Figure 9, which is veritable east of town along the recognised northeast trend of the vestige of the Kazaure-Karaukarau-Kushaka-Ilesha Schist Belt.

*3.2.3.5 Maitumbi East*

In Figure 10, the Eastern Bypass is now centrally located, terminating at a roundabout in the Maitumbi built-up neighborhood before proceeding northward to the Maikunkele neighborhood. Much of the land area in the lower right of Figure 10 (that is, the southeast) and the upper right (that is, the northeast) along a defined northeast course is presently a beehive of illegal gold-mining activities that the government periodically cracks down on.

*3.2.3.6 Gwada*

The Gwada area in Figure 11 is on a northeasterly course away from the built-up Maitumbi neighborhood, which every resident of Minna accepts as the “edge of town.” True to form, beyond the Maitumbi “edge of town,” Gwada and its environs are shorn of vegetation covers as extensive cultivation and poor land-use practices, plus heavy wood-cutting activities for household fuel needed mainly for cooking, combine to create the bleak landscape. The Gwada area is primarily an agrarian station for weekly markets, where the principal local staple, yam, is sold on weekends at the popular open-air Gwada Yam Market. Given the rustic, countryside setting, the adobe buildings of the built-up zone almost merge with the surrounding bleak landscape on satellite imagery. Nonetheless, beneath this bleak, Mars-like landscape are indications of gold-bearing veins, as illegal gold extraction has spilled over from the capital city of Minna into the Gwada area.

## 4. CONCLUSIONS

### 4.1 Ground-Based Attribute Mapping

The Staff Quarters and Works Department complexes at the Gidan Kwano Campus “sit” on ground beneath which lies the bodies of two valuable resources that the University should have archived in its repository of assets were it not for the structural developments at this location. This Staff Quarters cluster occupies *approximately 10% or less* of the land area of the Phase I Development. The School of Information and Communication Technology building complex is situated on a surface area above prospective groundwater and gold mineral deposits. The SAAT complex, the second-largest built-up complex of buildings after the Staff Quarters and thus less that 10% of the land area of the Phase I Development, is situated on grounds beneath which lies groundwater and gold-mineral deposits. The Senate Building grounds, located near the centerline of discerned subsurface fault-traces associated with substantial groundwater accumulation, should naturally correlate with the expectation that the subsurface regime of this administrative building is hydro-centric, with aquifers. This fact was mentioned in passing to the Vice-Chancellor in March 2023 by the lead author when a presentation of the results of Jonah (2021) was made to the Vice-Chancellor to establish the basis for exploring the prospect of university-government collaboration in order to exploit the groundwater resources at the locations to the southwest of the built-up Phase I Development.

The joke there, too was the Senate Building has covered up a “gold mine.” The location of the Schools of Engineering Complex, smack on the centerline of the fault-trace extensions in a northeasterly direction, corresponding to the Kazaure-Karaukarau-Kushaka-Ilesha Schist Belt, leads to the conclusion that groundwater-prospecting locations should characterize the vicinity of this Complex.

In hindsight, the conclusion reached in Udensi *et al.* (2006) with respect to groundwater prospects identified in that study is validated by Jonah (2021) if the clusters of yellow line fault-traces are extended tthrough the area corresponding to “the north of the Staff Quarters and the east of the students’ hostels” (the area of study of Udensi *et al.,* 2006). That area, outside the study grid of Jonah (2021) and marshy-greenland, is still undeveloped but is now put to use as a veritable agronomic and botanical station. The conclusion in Udensi et al. (2006) was more upbeat about groundwater prospects than that in Udensi *et al.* (2005). The areas of study of Udensi *et al.* (2005) and Udensi *et al.* (2006) are effectively adjacent to one another. Alas, the nine identified groundwater prospect locations of Udensi *et al.* (2006) out of a total of sixty-six stations surveyed were not identified by georeferenced coordinates back then in the year 2006 (electronic GPS units were not available to investigators over here although traditional field triangulation and survey techniques should have been employed) and thus it becomes really difficult to integrate this information into the archive of database of groundwater prospects that S.A. Jonah is building for the developing portions of the Gidan Kwano Campus. From the Jonah (2021) study, gold-mineral prospects for the area of study by Udensi et al. (2006) can be inferred, information not included in the 2006 survey year.

The School of Environmental Technology (S.E.T.) complex, which currently houses the E-Exam Centre established in 2023, was not designated as "hydro-centric" in the aforementioned 2006 study due to the absence of significant fractures and insufficient thickness of the unconsolidated layer in this area. The representation in Figure 3, derived from Jonah (2021), supports this conclusion, as no yellow line fault-trace extends into the present vicinity of the E-Exam Centre.

The apparent terminations of yellow line fault-traces at the 15th stations of cross-traverses within the 2 km x 2 km grid of Figure 3 warrant clarification. During the survey campaign conducted between 2011 and 2014, which culminated in the Jonah (2021) publication, survey stations in proximity to the student hostel complex were deliberately excluded from the investigation. This decision was necessitated by health and safety considerations, as these areas were subject to unsanitary surface conditions resulting from inadequate sanitation infrastructure. The vertical electrical sounding methodology employed with the ABEM Terrameter SAS 4000 requires electrical cables to be laid along the ground surface over considerable distances to facilitate data collection at greater depths, making work in contaminated areas impractical and hazardous.

The assessment regarding gold-deposit potential applies equally to the E-Exam Centre area. Since schist bodies within the local geology constitute the favorable gold-bearing medium, the indication of granitic rock mass at this section of Phase I Development effectively eliminates the possibility of economically viable gold deposits in this tract of land.

The grounds of present-day CODeL, though located on the centreline of a schist lineament, is not crossed by extensions of yellow line fault-trace clusters (deciphered on Figure 3) in the manner that would lead to the conclusion that this complex is basically and essentially “hydro-centric.” In actuality, the fact on the ground is that in the northwest area of the CODeL grounds outside the beltway portion at this side is a spread of outcropping granitic rock masses in the general directions towards the north and northwest. It is remarkable to note here that examination of Figure 3 shows that there are virtually no remarkable yellow line fault-traces that are mapped on the far southwest side of these outcropping granitic rock masses located on the grid of the Jonah (2021) study, except for a scattering of mainly single-point prospect locations. Interestingly, this “far southwest side” encompasses the “$1\ \mathrm{km}\ \mathrm{x}\ \frac{1}{2}\ \mathrm{km}$ to the west of the students’ hostels at the Gidan Kwano Campus” study area of Salako and Udensi (2005).

The buildings of the students’ hostel complex on the northwestern end of Figure 5 were not captured for this study because they fall outside the route of the yellow line fault-traces and their extensions, that is, the vestigial trace of the Kazaure-Karaukarau-Kushaka-Ilesha Schist Belt. Salako and Udensi (2005) conclude that “the aquifer system of the survey area can be located on the north-central and northeastern portions of the area of study.” The aquifer system identified by Salako and Udensi (2005) is validated by Jonah (2021) as corresponding to the “mainly single-

point prospect locations" scattered throughout the northwestern portion of the grid shown in Figure 3, which is not encouraging for any plan to develop a groundwater exploitation and distribution system. No wonder Salako *et al.* (2010), which incorporated the seismic survey method, was designed as a follow-up study to Salako and Udensi (2005) to gain greater insights into the groundwater prospect regime in the study area. The conclusion of Salako *et al.* (2010) mirrors that of Salako and Udensi (2005). This fact is now unarguably a resounding validation of the principal conclusion of Jonah (2021) presented herein as Figure 3. Basically, the study areas of Salako and Udensi (2005) and Salako et al. (2010) are not suitable areas for prospecting for gold mineral deposits.

The Chapel of Grace is located on the larger "northwest area of the CODeL grounds outside the beltway portion" of the Phase I Development that is marked by "a spread of outcropping granitic rock masses." As can be seen in Figure 3, there are no clusters of yellow line fault-traces to the far southwest of the Chapel of Grace within the grid of the Jonah (2021) study shown in Figure 3 that would lead to designating the area of the Chapel with much confidence as "hydro-centric." This fact also eliminates any correlation with gold prospect occurrence.

### 4.2 Remoted-Sensed Attribute Mapping

The Northeast Sector remains largely undeveloped, free from the encroachment of informal settlements that characterize other areas. This zone presents significant potential for underground freshwater development schemes, as it has not yet been compromised by the widespread sanitary deterioration and environmental contamination that plague the larger Minna built-up area. The preservation of this sector's environmental integrity makes it particularly suitable for water resource development.

Activities of unauthorized miners along the banks of the seasonal stream bordering the Talba Housing Estate area have provided strong evidence of gold presence in this locality. Given the accelerating pace of structural development in these parts, further geological studies are warranted to delineate the extent of mineral prospects. Such investigations should be conducted promptly before development activities intensify further.

The extensive urbanization of the Minna South Area presents substantial challenges for gold prospecting assessment. The density of existing structures effectively precludes any large-scale mining operations, regardless of assay results. This reality underscores the importance of proactive resource planning in less developed sectors.

The portion of Central Minna designated for the "New Minna" development, as illustrated in Figure 9, remains relatively free from structural development. With construction activities currently stalled, a strategic opportunity exists to designate this zone for dedicated geological and resource studies. This window for intervention should be leveraged to establish protective measures before development resumes.

The areas of interest in Maitumbi East extend in a northeasterly direction, contiguous with the "New Minna" zone. Both areas show promise for gold occurrence and groundwater resources. The logical course of action involves designating this broader corridor as an exclusive resource zone, thereby protecting it from haphazard development while enabling systematic resource assessment.

Gwada has historically served as an agricultural service center for Minna, but Minna's urban influence has limited its growth into a major settlement. Recent findings confirm that Gwada lies along the Kazaure-Karaukarau-Kushaka-Ilesha Schist Belt. Should further geological studies and assaying work indicate commercially viable gold deposits, the designation of the greater Gwada area as a dedicated economic zone becomes imperative for strategic resource development.

### 4.3 Recommendations

It is recommended that the Federal University of Technology, Minna, fully adopt the observations arising from this study to enhance or further refine physical development schemes for the University, especially in the built-up Phase I Development. Moreover, the University should integrate the observations made herein with in-house endeavors that have identified gold-mineral potential along the southwest extension of the trace of the Kazaure-Karaukarau-Kushaka-Ilesha Schist Belt. In the same vein, the Niger State Government should fully adopt the observations arising from this study to enhance or further refine physical development schemes for the built-up Minna town. By this, then, prospective

groundwater areas can be cleared and relocated so that large-scale exploitation of the continuous line of groundwater points can be initiated as a supplement to the insufficient surface-water supply system for Minna town. The areas on the trace of the Kazaure-Karaukarau-Kushaka-Ilesha Schist Belt that have not yet been heavily built-up can be set aside as veritable and protected “economic-mineral zones” for modern mining activities.

## 5. DECLARATIONS

### 5.1 Study Limitations

Actually, the full diagonal traverse of the Kazaure-Karaukarau-Kushaka-Ilesha Schist Belt across Nigeria is approximately 700 km (Jonah, 2021). Given the importance of this traverse for groundwater and gold repositories, a comprehensive study of the nature presented herein would have followed this traverse across various towns and villages in southwest Nigeria, from Ilesha to northeast Nigeria, at Kazaure, to highlight the previously unknown economic potential of these settlements. On the back of a full-body study such as this, it becomes even more crucial for security planners to narrow the banditry threat zones to specific corridors, as indications of alluvial gold deposits along this belt have attracted armed marauders to invade and engage in illegal mining. A federal government grant must necessarily sponsor a full-body study of this nature. In the absence of any such grant, this study has compiled the requisite information for the Minna Area geological province, which can be consulted by the Federal University of Technology, Minna, and the Niger State Government, whose administrative headquarters is located in Minna.

### 5.2 Acknowledgements

The authors express their sincere gratitude to the Federal University of Technology, Minna, for providing the institutional support and research facilities that made this study possible. We would like to acknowledge the Department of Physics, School of Physical Sciences, for granting us access to laboratory equipment and field research permissions on the Gidan Kwano Campus.

We extend our appreciation to the university administration for facilitating access to various locations across the Phase I Development for our geospatial surveys. Special thanks are due to the Department of Physics technical staff for their assistance with equipment maintenance and calibration.

The authors also acknowledge support from the University's research infrastructure, including library resources and computational facilities, which were essential for data analysis and manuscript preparation.

### 5.3. Funding Source

This research was conducted with personal funding from the authors, without any external grants or institutional research funding being secured for this study. The authors acknowledge that all fieldwork expenses, laboratory analyses, and equipment usage were covered through personal resources of the research team.

In accordance with the principles of transparent scientific communication, we declare that this work was conducted using the research infrastructure and facilities provided by the Federal University of Technology, Minna, Nigeria. The University provided essential support through access to laboratory equipment, field research permissions within the Gidan Kwano Campus, and computational facilities. However, no direct financial support was allocated specifically for this project.

The authors confirm that no commercial interests, external funding bodies, or third-party organizations influenced the design, execution, or interpretation of this research. This independence ensures that all findings and conclusions presented herein reflect solely the scientific evidence gathered and analyzed by the research team, maintaining complete integrity in the research process and data interpretation.

In accordance with the ethical guidelines of the Southern Journal of Sciences, which do not allow donations from authors with manuscripts under evaluation (even when research funds are available) or in cases of authors' financial constraints, publication costs were fully absorbed by the journal under our Platinum Open Access policy, through the support of the Araucária Scientific Association (https://acaria.org/). This policy aims to ensure complete independence between the editorial process and any financial aspects, reinforcing our commitment to scientific integrity and equity in knowledge dissemination.

### 5.4 Competing Interests

The authors declare that there exists no conflict of interest whatsoever arising from the preparation of this manuscript for publication with any other competing interests, whether they be of the authors’ or of second parties and third parties thereof. The data employed in the enunciation of

the textual material herein are original, having been duly acquired by the authors as part of the annual undergraduate schedule of project supervision here at the Federal University of Technology, Minna, Nigeria. This body of data field, duly archived for validation and reference purposes, are available for integrity checks anytime.

### 5.5. Open Access



### 5.6. Author Contributions

S.A.J. conceived the study design, conducted field surveys, and wrote the manuscript. G.O.A. contributed to data collection and GPS measurements. A.A.A. assisted with satellite imagery analysis and interpretation. S.S.A. and A.O.B. participated in field data collection and equipment calibration. J.A.B. and E.O.J. contributed to data analysis and manuscript review. R.J.S. assisted with remote sensing analysis. S.S. provided geographical expertise and manuscript review. All authors read and approved the final manuscript.

## 6. REFERENCES:

1. Adesoye, S.A. (1986). Master Plan of the Federal University of Technology's Permanent Site, Minna, Adesoye and Partners, Kaduna, Nigeria.
2. Jiaguo, Q., Zihan, L., Weltz, M. A., Spaeth, K. E., Iskakova, G., Nesbit, J., ...Toledo, D. (2025). A geospatial livestock-carrying capacity model (GLCC) in the Akmola Oblast, Kazakhstan. *Remote Sensing, 17*(8), 1477. doi.org/10.3390/rs17081477
3. Jian, G.L., & Philippa, J.M. (2009). Essential Image Processing and GIS for Remote Sensing, Wiley-Blackwell, United Kingdom (UK).
4. Jonah, S.A. (2021). Series of 1-D ER and IP traverses reveal vestige of regional geological structure. Applied Journal of Physical Science, 3(2), 37-60. (Paper ID: EA9433402)
5. Jonah, S.A. (2024). Dual Geoelectrical Survey Regime to Profile Groundwater Occurrence at an East-Central Tranche of the Gidan Kwano Campus, Minna, Nigeria, Unpublished Synopsis for PhD Thesis, Federal University of Technology, Minna, Nigeria.
6. Obaje, N.G. (2009). Geology and mineral resources of Nigeria. In Lecture Notes in Earth Sciences. Springer-Verlag, Berlin.
7. Ruihua, S., Juanying, Z., Dong, W., Wei, L., Yinshen, W., Bingnan, W., & Maosheng, X. (2025). Nonlinear phase reconstruction and compensation method based on orthonormal complete basis functions in synthetic aperture ladar imaging technology. Remote Sensing, 17(8),1480.doi.org/10.3390/rs17081480
8. Salako, K.A., & Udensi, E.E. (2005). Vertical electrical sounding investigation of the western part of the Federal University of Technology, Minna. Proc: First Annual School of Science Education Conference (Federal University of Technology, Minna), 1, 69-78.
9. Udensi, E.E., Ogunbajo, M.I., Nwosu, J.E., Jonah, S.A., Kolo, M.T., Onoduku, U.S., ... Crown, I.E. (2005). Hydrogeological and geophysical surveys for groundwater at designated premises of the main Campus of the Federal University of Technology, Minna. Zuma Journal of Pure and Applied Science, 7(1), 52-58.
10. Udensi, E.E., Unuevho, C.I., Jonah, S.A., Ofor, P.N., Adetona, A.A., Salako, K.A., ... Gana, C.S. (2006). Geoelectrical survey for groundwater at the Gidan Kwano Campus of the Federal University of Technology, Minna. Environmental Technology and Science Journal, 1(1), 16-48.
11. Yiqing, Z., Hong, C., Shangrong, W., Yongli, G., & Qian, S. (2025). Rapeseed area extraction based on time-series dual-polarization radar vegetation indices. Remote Sensing, 17(8), 1479. doi.org/10.3390/rs17081479

***Table 1**. Attribute Information of Staff Apartment Number 1*

DEPARTMENT OF PHYSICS
SCHOOL OF PHYSICAL SCIENCES
FEDERAL UNIVERSITY OF TECHNOLOGY, MINNA, NIGER STATE

**Title of Project:** Geospatial Identification of Built-up Structures in Phase I Development of the Gidan Kwano Campus and Beyond Along the Kazaure-Karaukarau-Kushaka-Ilesha Schist Belt
Date: ……*8th July, 2023*……. Time: ……*11:27 a.m.*……
Weather: ……*Fine*……
Principal Information:

1. **Geospatial Info**

**Polygon 1**

| S/N | LATITUDE | LONGITUDE |
|---|---|---|
| 1. | 09˚31′31.50″ | 006˚26′49.70″ |
| 2. | 09˚31′31.60″ | 006˚26′49.20″ |
| 3. | 09˚31′32.10″ | 006˚26′49.40″ |
| 4. | 09˚31′32.00″ | 006˚26′49.90″ |

2. **Location Attributes**
   Local-nomenclature Identifier:- *Staff Apartment Designated #1*

***Table 2**. Attribute Information of Staff Apartment Number 2*

DEPARTMENT OF PHYSICS
SCHOOL OF PHYSICAL SCIENCES
FEDERAL UNIVERSITY OF TECHNOLOGY, MINNA, NIGER STATE

**Title of Project:** Geospatial Identification of Built-up Structures in Phase I Development of the Gidan Kwano Campus and Beyond Along the Kazaure-Karaukarau-Kushaka-Ilesha Schist Belt
Date: …… *8th July, 2023*…… Time: ……*11:34 a.m.*……
Weather: …… *Fine* ……
Principal Information:

1. **Geospatial Info**

**Polygon 2**

| S/N | LATITUDE | LONGITUDE |
|---|---|---|
| 1. | 09˚31′32.90″ | 006˚26′49.97″ |
| 2. | 09˚31′32.80″ | 006˚26′49.97″ |
| 3. | 09˚31′33.40″ | 006˚26′49.50″ |
| 4. | 09˚31′33.30″ | 006˚26′50.00″ |

2. **Location Attributes**
   Local-nomenclature Identifier:- *Staff Apartment Designated #2*

***Table 3**. Attribute Information of Staff Apartment Number 3*

DEPARTMENT OF PHYSICS
SCHOOL OF PHYSICAL SCIENCES
FEDERAL UNIVERSITY OF TECHNOLOGY, MINNA, NIGER STATE

**Title of Project:** Geospatial Identification of Built-up Structures in Phase I Development of the Gidan Kwano Campus and Beyond Along the Kazaure-Karaukarau-Kushaka-Ilesha Schist Belt
Date: …… *8th July, 2023*…… Time: ……*11:43 a.m.*……
Weather: …… *Fine* ……
Principal Information:

1. **Geospatial Info**

**Polygon 3**

| S/N | LATITUDE | LONGITUDE |
|---|---|---|
| 1. | 09˚31′33.60″ | 006˚26′49.90″ |
| 2. | 09˚31′33.70″ | 006˚26′49.90″ |
| 3. | 09˚31′35.00″ | 006˚26′50.00″ |
| 4. | 09˚31′35.00″ | 006˚26′49.70″ |

2. **Location Attributes**
   Local-nomenclature Identifier:- *Staff Apartment Designated #3*

***Table 4**. Attribute Information of Staff Apartment Number 4*

DEPARTMENT OF PHYSICS
SCHOOL OF PHYSICAL SCIENCES
FEDERAL UNIVERSITY OF TECHNOLOGY, MINNA, NIGER STATE

**Title of Project:** Geospatial Identification of Built-up Structures in Phase I Development of the Gidan Kwano Campus and Beyond Along the Kazaure-Karaukarau-Kushaka-Ilesha Schist Belt
Date: …… *8th July, 2023*…… Time: ……*11:50 a.m.*……
Weather: …… *Fine* ……
Principal Information:

1. **Geospatial Info**

**Polygon 4**

| S/N | LATITUDE | LONGITUDE |
|---|---|---|
| 1. | 09˚31′35.50″ | 006˚26′49.60″ |
| 2. | 09˚31′35.90″ | 006˚26′49.40″ |
| 3. | 09˚31′36.20″ | 006˚26′49.90″ |
| 4. | 09˚31′35.70″ | 006˚26′50.20″ |

2. **Location Attributes**
   Local-nomenclature Identifier:- *Staff Apartment Designated #4*

***Table 5**. Attribute Information of SICT Complex*

DEPARTMENT OF PHYSICS
SCHOOL OF PHYSICAL SCIENCES
FEDERAL UNIVERSITY OF TECHNOLOGY, MINNA, NIGER STATE

**Title of Project:** Geospatial Identification of Built-up Structures in Phase I Development of the Gidan Kwano Campus and Beyond Along the Kazaure-Karaukarau-Kushaka-Ilesha Schist Belt

Date: ……*8th July, 2023*…… Time: ……*1:26 p.m.*……

Weather: ……*Fine*……

Principal Information:

1. **Geospatial Info**

**Polygon 21**

| S/N | LATITUDE | LONGITUDE |
|---|---|---|
| 1. | 09˚31′50.60″ | 006˚27′08.70″ |
| 2. | 09˚31′51.60″ | 006˚27′07.50″ |
| 3. | 09˚31′52.20″ | 006˚27′08.00″ |
| 4. | 09˚31′51.70″ | 006˚27′09.30″ |
| 5. | 09˚31′51.40″ | 006˚27′09.30″ |

2. **Location Attributes**

Local-nomenclature Identifier:- *School of Information and Communication Technology (SICT)*

***Table 6**. Attribute Information of SET Complex*

DEPARTMENT OF PHYSICS
SCHOOL OF PHYSICAL SCIENCES
FEDERAL UNIVERSITY OF TECHNOLOGY, MINNA, NIGER STATE

**Title of Project:** Geospatial Identification of Built-up Structures in Phase I Development of the Gidan Kwano Campus and Beyond Along the Kazaure-Karaukarau-Kushaka-Ilesha Schist Belt

Date: ……*8th July, 2023*…… Time: ……*1:41 p.m.*……

Weather: …… *Fine* ……

Principal Information:

1. **Geospatial Info**

**Polygon 23**

| S/N | LATITUDE | LONGITUDE |
|---|---|---|
| 1. | 09˚31′03.0″ | 006˚27′0.08″ |
| 2. | 09˚31′04.1″ | 006˚27′0.03″ |
| 3. | 09˚31′05.3″ | 006˚27′03.5″ |
| 4. | 09˚31′04.8″ | 006˚27′04.1″ |

2. **Location Attributes**

Local-nomenclature Identifier:- *School of Environmental Technology (SET)*

***Table 7****. Attribute Information of E-Exam Centre*

DEPARTMENT OF PHYSICS
SCHOOL OF PHYSICAL SCIENCES
FEDERAL UNIVERSITY OF TECHNOLOGY, MINNA, NIGER STATE

**Title of Project:** Geospatial Identification of Built-up Structures in Phase I Development of the Gidan Kwano Campus and Beyond Along the Kazaure-Karaukarau-Kushaka-Ilesha Schist Belt
Date: ……*8th July, 2023*…… Time: ……*1:56 p.m.*……
Weather: …… *Fine*……
Principal Information:

1. **Geospatial Info**

**Polygon 25**

| S/N | LATITUDE | LONGITUDE |
|---|---|---|
| 1. | 09˚31′08.5″ | 006˚27′01.3″ |
| 2. | 09˚31′09.2″ | 006˚27′00.7″ |
| 3. | 09˚31′08.0″ | 006˚27′59.0″ |
| 4. | 09˚31′07.5″ | 006˚27′59.2″ |
| 5. | 09˚31′07.8″ | 006˚27′58.8″ |
| 6. | 09˚31′09.7″ | 006˚27′58.3″ |
| 7. | 09˚31′09.9″ | 006˚27′57.2″ |
| 8. | 09˚31′09.9″ | 006˚27′57.7″ |
| 9. | 09˚31′11.1″ | 006˚27′59.6″ |
| 10. | 09˚31′11.3″ | 006˚27′59.6″ |
| 11. | 09˚31′11.1″ | 006˚27′59.9″ |
| 12. | 09˚31′11.5″ | 006˚27′59.9″ |
| 13. | 09˚31 09.4″ | 006˚27′00.5″ |
| 14. | 09˚31′09.2″ | 006˚27′01.6″ |

2. **Location Attributes**

Local-nomenclature Identifier:- *E-Exam Centre*

***Table 8**. Attribute Information of Chemical Engineering Complex*

DEPARTMENT OF PHYSICS
SCHOOL OF PHYSICAL SCIENCES
FEDERAL UNIVERSITY OF TECHNOLOGY, MINNA, NIGER STATE

**Title of Project:** Geospatial Identification of Built-up Structures in Phase I Development of the Gidan Kwano Campus and Beyond Along the Kazaure-Karaukarau-Kushaka-Ilesha Schist Belt
Date: ……*8th July, 2023*…… Time: ……*2:37 p.m.*……
Weather: …… *Fine*……
Principal Information:

1. **Geospatial Info**

**Polygon 28**

| S/N | LATITUDE | LONGITUDE |
|---|---|---|
| 1. | 09°31′00.6″ | 006°27′54.6″ |
| 2. | 09°31′01.3″ | 006°27′54.1″ |
| 3. | 09°31′03.3″ | 006°27′53.8″ |
| 4. | 09°31′04.1″ | 006°27′53.8″ |
| 5. | 09°31′02.0″ | 006°27′55.2″ |
| 6. | 09°31′02.2″ | 006°27′56.3″ |

2. **Location Attributes**

Local-nomenclature Identifier:- *Chemical Engineering Complex*

SOUTHERN JOURNAL OF SCIENCES

*ESTABLISHED IN 1993*

*Review paper*

# ANALYTICAL METHODS FOR METHANOL DETECTION IN ALCOHOLIC BEVERAGES: A COMPARATIVE REVIEW OF CLASSICAL, COLORIMETRIC, AND CHROMATOGRAPHIC APPROACHES

# MÉTODOS ANALÍTICOS PARA DETECÇÃO DE METANOL EM BEBIDAS ALCOÓLICAS: UMA REVISÃO COMPARATIVA DE ABORDAGENS CLÁSSICAS, COLORIMÉTRICAS E CROMATOGRÁFICAS

DE BONI, Luis Alcides Brandini[1*]; FERNANDES, Rochele da Silva[2];

[1] Southern Journal of Sciences. Brazil. ORCID: 0009-0000-8102-6197

[2] Universidade Federal do Rio Grande do Sul, Instituto de Química. Brazil. ORCID: 0009-0008-5454-0287

*Corresponding author: labdeboni@gmail.com

Received 29 October 2025; received in revised form 20 November 2025; accepted 11 December 2025

## ABSTRACT

**Introduction:** The detection of methanol in alcoholic beverages represents a critical public health issue, particularly in light of the recent outbreak of poisonings in Brazil, which registered 58 confirmed cases and 15 deaths through October 2025. Methanol's toxicity, with an estimated lethal dose ranging from 0.5 to 1.5 g/kg, requires reliable analytical methods for health surveillance. Brazilian legislation establishes a maximum limit of 20 mg/100 mL of anhydrous alcohol; however, the need for accessible screening methods in field settings remains an important challenge. **Objective:** To critically compare three analytical methods for methanol determination: classical qualitative methods (Lucas Test and dichromate/Schiff), Brazilian colorimetric method, and gas chromatography with flame ionization detector (GC-FID), evaluating their performance and applicability in resource-limited contexts. **Methods:** Theoretical-comparative approach through critical analysis of specialized literature and normative technical documentation. Methods were evaluated according to: operational principle, sensitivity (LOD/LOQ), selectivity, operational complexity, analysis time, and practical applicability. **Results:** The Lucas Test is not applicable for methanol detection. Colorimetric methods showed moderate sensitivity (LOD ~20-160 mg/100 mL), a 10-30-minute execution time, low operational complexity, and excellent portability. The Brazilian method presented chemical equivalence with international standards, differing only in the type of reading performed. GC-FID has shown superior sensitivity (LOD ≤ 1 mg/100 mL) and high specificity, but it requires extended time (~45-60 minutes), complex laboratory infrastructure, and specialized operators. Sugars interfere with colorimetric methods. **Conclusions:** The methods are complementary within a hierarchical system. Colorimetric methods enable rapid field screening, while GC-FID serves as the confirmatory method for forensic analyses. We recommend implementing integrated protocols that combine in situ colorimetric screening with GC-FID confirmation in accredited laboratories for effective health surveillance.

**Keywords**: *Methanol, Alcoholic beverages, Analytical methods, Health surveillance, Public health.*

## RESUMO

**Introdução**: A detecção de metanol em bebidas alcoólicas representa uma questão crítica de saúde pública, particularmente à luz do recente surto de intoxicações no Brasil, que registrou 58 casos confirmados e 15 mortes até outubro de 2025. A toxicidade do metanol, com dose letal estimada entre 0,5 e 1,5 g/kg, exige métodos analíticos confiáveis para vigilância sanitária. A legislação brasileira estabelece limite máximo de 20 mg/100 mL de álcool anidro; entretanto, a necessidade de métodos de triagem acessíveis em condições de campo permanece um desafio importante. **Objetivo**: Comparar criticamente três métodos analíticos para determinação de metanol: métodos qualitativos clássicos (Teste de Lucas e dicromato/Schiff), método colorimétrico brasileiro

 
DOI: 10.48141/2764-5959.02.v33.n40.2025_02_Rochele_pgs_19_48.pdf

e cromatografia gasosa com detector de ionização em chama (CG-DIC), avaliando seu desempenho e aplicabilidade em contextos com recursos limitados. **Métodos**: Abordagem teórico-comparativa através de análise crítica de literatura especializada e documentação técnica normativa. Os métodos foram avaliados segundo: princípio operacional, sensibilidade (LD/LQ), seletividade, complexidade operacional, tempo de análise e aplicabilidade prática. **Resultados**: O Teste de Lucas não é aplicável para detecção de metanol. Métodos colorimétricos apresentaram sensibilidade moderada (LD ~20-160 mg/100 mL), tempo de execução de 10-30 minutos, baixa complexidade operacional e excelente portabilidade. O método brasileiro apresentou equivalência química com padrões internacionais, diferindo apenas no tipo de leitura realizada. CG-DIC demonstrou sensibilidade superior (LD ≤ 1 mg/100 mL) e alta especificidade, porém requer tempo prolongado (~45-60 minutos), infraestrutura laboratorial complexa e operadores especializados. Açúcares interferem nos métodos colorimétricos. **Conclusões**: Os métodos são complementares dentro de um sistema hierárquico. Métodos colorimétricos possibilitam triagem rápida em campo, enquanto CG-DIC serve como método confirmatório para análises forenses. Recomenda-se implementar protocolos integrados que combinem triagem colorimétrica in situ com confirmação por CG-DIC em laboratórios credenciados para vigilância sanitária efetiva.

**Palavras-chave**: *Metanol, Bebidas alcoólicas, Métodos analíticos, Vigilância sanitária, Saúde pública*.

## 1. INTRODUCTION

### 1.1. The Problem of Methanol Intoxication

Accurate detection of methanol in alcoholic beverages is a critical public health issue, given the high toxicity of this compound. As demonstrated by Gosselin *et al*. (1984), the estimated lethal dose for a 70 kg human is only 0.5 to 1.5 g/kg, highlighting the danger even at relatively small quantities.

The urgency of this monitoring was tragically illustrated recently when Brazil's Ministry of Health reported an outbreak of intoxications, with 108 notifications registered up to October 24, 2025. Of these, 58 cases were confirmed, 50 remain under investigation, and 635 notifications were ruled out. São Paulo state has the highest number of confirmed cases (44), followed by Pernambuco (5), Paraná (6), Rio Grande do Sul (1), Mato Grosso (1), and Tocantins (1). To date, 15 deaths have been confirmed, distributed among São Paulo (9), Paraná (3), and Pernambuco (3), with another 9 deaths still under investigation (Ministry of Health, 2025). This situation clearly reveals the pressing need for effective health surveillance.

### 1.2. Characteristics of Methanol

To understand the risks involved and the importance of accurate detection, it's important to know the physicochemical and toxicological characteristics of methanol. Methanol ($CH_3OH$), also known as methyl alcohol, carbinol, or wood alcohol, is an organic chemical compound with a molecular mass of 32.04 g/mol, characterized as a colorless, polar, volatile, and highly flammable liquid with a mild alcoholic odor when pure (World Health Organization [WHO], 1997). It is the simplest alcohol in the homologous series of aliphatic alcohols, being completely miscible in water and most organic solvents (International Labour Organization [ILO] & World Health Organization [WHO], 2018).

From a physicochemical perspective, methanol has a boiling point of 64.7 °C, melting point of -97.8 °C, relative density of 0.79 (water = 1), and vapor pressure of 12.3 kPa at 20 °C (ILO & WHO, 2018). Its flammability characteristics include a flash point of 12.2 °C (closed cup) and autoignition temperature of 470 °C, with explosive limits in air ranging from 5.5% to 44% by volume (WHO, 1997). Its vapors mix easily with air, forming explosive mixtures (limits between 6-50% by volume). Methanol has a low flash point (9 °C c.c.) and is dangerous due to its violent reactivity with strong oxidizers, acids, and reducing agents, posing a risk of fire and explosion (ILO, 2018).

Modern industrial production of methanol is based exclusively on the catalytic conversion of pressurized synthesis gas (hydrogen, carbon monoxide, and carbon dioxide) in the presence of heterogeneous metallic catalysts (WHO, 1997). The chemical sector accounted for 66% of global methanol consumption in 2024 (Mordor Intelligence, 2025).

In terms of occupational safety and human health, methanol is an important risk. The substance is classified by the UN GHS as a highly flammable liquid and vapor, and is toxic if swallowed and harmful if inhaled, causing damage to the central nervous system (CNS). Absorption can occur through inhalation, ingestion, or dermal contact, and evaporation at 20 °C can quickly lead to harmful atmospheric contamination (ILO, 2018).

Acute exposure through inhalation, ingestion, or percutaneous absorption can result in central nervous system depression, metabolic acidosis, visual disturbances, blindness, coma,

and death, with symptoms potentially delayed by 12 to 24 hours (WHO, 1997). Short-term exposure irritates the eyes, skin, and respiratory tract, and may cause loss of consciousness and, possibly blindness and death. Symptoms include dizziness, headache, visual disturbances, and seizures, and effects may be delayed, indicating the need for medical observation. Methanol is readily absorbed through respiratory, oral, and dermal routes, being slowly metabolized to formate, which is considered primarily responsible for the characteristic visual damage of intoxication (WHO, 1997).

Repeated or prolonged exposure can result in dermatitis and cause chronic effects on the CNS, such as recurring headaches and impaired vision. Specific treatment is necessary in case of poisoning, and periodic medical examination is suggested, depending on the degree of exposure (ILO, 2018).

### 1.3. Regulatory Framework

This risk scenario is acknowledged by Brazilian legislation, which establishes specific limits for methanol in distilled beverages. Normative Instruction No. 13, dated June 29, 2005, from the Ministry of Agriculture, Livestock and Food Supply (MAPA) approves the Technical Regulation for Establishing Identity and Quality Standards for Sugarcane Spirit and Cachaça, setting the limit at 20 mg of methanol per 100 mL of anhydrous alcohol. In 2009, the National Institute of Metrology, Quality and Technology (INMETRO) approved Ordinance No. 276, dated September 24, 2009, which instituted the Conformity Assessment Regulation for cachaça. In 2022, MAPA published Ordinance No. 539, dated December 26, 2022, establishing new identity and quality standards for sugarcane spirit and cachaça, maintaining the limit of 20 mg of methanol per 100 mL of anhydrous alcohol.

### 1.4. Context of Cachaça Production

Within the context of national production of distilled beverages, the efficiency of the distillation process in cachaça production is a critical factor for the quality and safety of the final product. During distillation, methanol, due to its high volatility, is mostly removed in the initial phase, known as the head fraction. Studies have shown that discarding 1-2% of the total distillate volume is sufficient to eliminate most of this unwanted compound (SCANAVINI *et al*., 2012). As a result of this control practice, commercial cachaça presents a low methanol content.

A benchmark analysis in the sector identified an average value of approximately 6 mg per 100 mL of anhydrous alcohol in the final product, a level lower than that found in other spirits, such as wine-based spirits, confirming the effectiveness of separation during distillation (BOSCOLO *et al*., 2000).

### 1.5. Global Overview of Methanol Poisonings

The recent case of methanol poisoning in Brazil (MS, 2025) is not an isolated incident globally. Table 1 presents a compilation of similar incidents across more than 20 countries. Typically, these methanol poisoning incidents are related to the consumption of adulterated alcoholic beverages; however, a case with distinct characteristics occurred in the USA during the pandemic, where hand sanitizer containing ethanol mixed with methanol was ingested (Konkel *et al*., 2024).

### 1.6. Study Objective and Approach

Given the context of toxicological risks, regulatory frameworks, production-related technical challenges, and the global occurrence of outbreaks, this article adopts a theoretical-comparative approach to analyze three representative analytical methods for methanol detection. The goal is to provide a critical foundation for selecting control measure methodologies, including in resource-limited settings.

#### 1.6.1. General Objective

To critically compare the three analytical methods for determining methanol in alcoholic beverages - classical qualitative teaching methods, national colorimetric method, and the gold standard (gas chromatography) - evaluating their performance and applicability in resource-limited contexts.

#### 1.6.2. Specific Objectives

To describe the operational principles, advantages, and limitations of the three selected paradigmatic methods.

To characterize the performance of the methods based on key analytical parameters: sensitivity (LOD/LOQ), selectivity against ethanol, cost, operational complexity, and analysis time.

To evaluate the feasibility of the classical and national colorimetric methods for applications in rapid screening and health surveillance, contrasting their results with the gold standard method.

To synthesize the trade-offs identified in the comparison, highlighting technological gaps and opportunities for developing accessible methodologies for the Brazilian scenario.

## 2. METHODOLOGICAL APPROACH

To address the proposed objectives, particularly the need to compare methods applicable in resource-limited contexts with the gold-standard method, this article adopts a theoretical and comparative research strategy. The critical analysis focuses on three representative analytical approaches, selected for their relevance across different application scenarios: combined classical organic chemistry methods, a validated national colorimetric method, and the chromatographic method considered the gold standard.

### 2.1. Method Selection and Rationale

The selection was intentional, aiming to cover a significant spectrum of complexity, cost, and applicability:

#### 2.1.1. Combined Classical Methods (Lucas Test followed by Dichromate/Schiff Oxidation)

These correspond to the traditional didactic approach, commonly used in teaching organic chemistry at the university level. Although they consist of two distinct tests, they are performed sequentially within the same analysis:

- Lucas Test: a screening method by exclusion that classifies alcohols by structure (primary, secondary, tertiary). Since methanol does not react in this test (a negative result is expected for simple primary alcohols), it serves to rule out the presence of secondary and tertiary alcohols that could interfere.
- Dichromate Oxidation + Schiff's Reagent: a confirmatory method that specifically identifies methanol through the formation of formaldehyde, which reacts with Schiff's reagent, producing a characteristic pink-violet coloration.

Inclusion rationale: To assess whether established didactic protocols can be adapted for low-cost health surveillance screening.

#### 2.1.2. Brazilian Colorimetric Method (Modesto, 2020)

A colorimetric technique developed and validated in Brazil specifically for alcoholic beverage analysis. It is based on the oxidation of methanol to formaldehyde, followed by reaction with chromotropic acid, allowing visual or instrumental detection.

Inclusion rationale: It is an effort to develop an accessible methodology, with potential for field application or laboratories with limited infrastructure.

#### 2.1.3. Gold Standard Method (Gas Chromatography with Flame Ionization Detector - GC-FID)

An analytical technique described in international standards (ASTM E681, AOAC 972.11, IAL and OIV methods) and recognized by MAPA as the official method for forensic and regulatory analyses.

Inclusion rationale: It is a reference for sensitivity, specificity, and accuracy against which simpler methods will be evaluated.

### 2.2. Information Sources

Method characterization was based on a comprehensive review of specialized literature in analytical chemistry and method validation, complemented by national and international normative technical documentation. The analysis also incorporated peer-reviewed scientific publications and official beverage analysis manuals from recognized institutions such as MAPA (Ministry of Agriculture, Livestock and Food Supply), IAL (Adolfo Lutz Institute), and OIV (International Organisation of Vine and Wine).

To survey documented cases of methanol poisoning worldwide, a systematic search was conducted in the Science.gov database (https://www.science.gov/scigov/desktop/en/results.html) using the search term "methanol outbreak". The search yielded 462 records.

The document selection criteria were: a) relevance according to the database's own classification, b) contribution to presenting a broad overview of methanol poisoning cases in different geographical and temporal contexts. And the

exclusion of duplicate or too-similar records.

### 2.3. Parameters for Comparative Analysis

For systematic comparison, the methods were evaluated according to criteria extracted from specialized literature on analytical method validation and aligned with the study's specific objectives:

1. Operating principle (chemical mechanism)
2. Sensitivity (LOD/LOQ relative to the regulatory limit of 20 mg/100 mL)
3. Selectivity against interferents (ethanol, sugars, other compounds)
4. Operational complexity (equipment, reagents, training)
5. Cost per analysis and initial investment
6. Total analysis time (preparation + execution + reading)
7. Practical applicability and recommended use context (laboratory vs. field)

### 2.4. Analysis Structure

The results of this comparison will be organized in three stages:

a. Detailed description of each method (Section 3), including procedures, reagents, and chemical fundamentals

b. Comparative synthesis in tabular format (Section 4), presenting side-by-side performance of each method according to established criteria

c. Critical discussion (Section 5) that will highlight the trade-offs inherent in choosing each methodology, especially considering Brazilian health surveillance scenarios with different levels of available resources

This structure will allow us to identify technological gaps and opportunities to develop or adapt accessible methodologies without compromising the analytical reliability required for public health protection.

## 3. Analytical Methods

In this section, the three methods selected for comparison are described in detail: the combined classical organic chemistry methods, the colorimetric method developed in Brazil, and gas chromatography with flame ionization detector. For each method, the chemical fundamentals, experimental procedures, required reagents, and criteria for interpreting results are presented.

### 3.1. Combined Classical Methods

The classical method combines two sequential analyses commonly performed in organic chemistry practical classes: the Lucas Test followed by dichromate oxidation, with confirmation using Schiff's reagent. This didactic approach, extensively documented in organic chemistry experimental compendia (Furniss *et al*., 1989), establishes a screening protocol followed by confirmation, based on the following analytical reasoning:

**Protocol Logic:**

1. The Lucas Test (Lucas, 1905) classifies alcohols by structure (primary, secondary, or tertiary)
2. Since methanol is a primary alcohol that does not react in the Lucas Test, a negative result in this test rules out the presence of secondary and tertiary alcohols that could cause false-positive results in subsequent tests
3. Once the presence of a primary alcohol (or mixture containing primary alcohols) is confirmed, oxidation with dichromate proceeds
4. The formaldehyde formed specifically from methanol is then identified by Schiff's reagent (Schiff, 1866)

Why perform the Lucas Test if it doesn't detect methanol?

The Lucas Test functions as a "gatekeeper" for the analytical protocol. Although it does not directly detect methanol, it plays a crucial role as an exclusion screening step:

**NEGATIVE Result (absence of turbidity):** Confirms that there are NO secondary or tertiary alcohols in the sample. This increases the reliability of subsequent tests by excluding potential interferents.

**POSITIVE Result (presence of turbidity):** Alerts that secondary or tertiary alcohols are present, requiring caution in interpreting the tests.

This prior exclusion of potential interferents

reduces the likelihood of false-positive or ambiguous results in the confirmatory stage with Schiff's reagent, serving as a quality-control measure integrated into the analytical protocol.

Figure 1 presents the complete flowchart of this combined analytical protocol.

### 3.1.1. Step 1 – Lucas Test (Exclusion Screening)

**Purpose and Principle:** The Lucas Test (Lucas, 1905) is used for classifying primary, secondary, and tertiary alcohols, based on the difference in reactivity of these compounds toward hydrochloric acid (HCl) in the presence of zinc chloride ($ZnCl_2$) as a Lewis acid catalyst. In this protocol, the test functions as an exclusion screening step: a negative result (absence of turbidity) indicates that the sample does not contain secondary or tertiary alcohols, allowing safe progression to the confirmatory steps specific for methanol.

The reaction occurs according to Equation 1:

$$R\text{-}OH + HCl + ZnCl_2 \rightarrow R\text{-}Cl + H_2O \quad \text{(Eq. 1)}$$

The reaction rate depends on the alcohol structure:

- Tertiary alcohols: immediate reaction (instantaneous turbidity)
- Secondary alcohols: 5-10 minutes (gradual turbidity)
- Primary alcohols: do not react at room temperature
- Methanol: does not react (simple primary alcohol) – expected result to proceed

#### Reagents

Lucas Reagent composition anhydrous $ZnCl_2$ (136 g), concentrated HCl (105 mL). Preparation: dissolve in an ice bath; store in an amber bottle.

#### Procedure

The procedure requires basic laboratory glassware, including clean, dry test tubes with a 10 mL capacity, Pasteur pipettes for precise liquid transfer, and a stopwatch for time control.

The analytical procedure begins by adding 2 mL of Lucas reagent to a test tube, followed by the addition of 3-4 drops (approximately 0.2 mL) of the alcoholic sample to be tested. The mixture is then shaken vigorously for 10 seconds to ensure proper contact between the reagent and the sample. After shaking, the test tube is allowed to stand at room temperature and observed for up to 60 minutes for any signs of turbidity or phase separation.

#### Expected Results and Interpretation

Table 2 presents the typical results obtained with the Lucas Test for different alcohols.

**Decision criterion:** If turbidity occurs (positive result), the sample contains secondary or tertiary alcohols, which may interfere with subsequent stages. If there is no turbidity after 60 minutes (negative result), proceed to Stage 2.

### 3.1.2. Stage 2 – Dichromate Oxidation and Confirmation with Schiff's Reagent

**Purpose and Principle**: This stage specifically identifies methanol by forming formaldehyde as an oxidation product. The technique is based on the selective oxidation of primary alcohols with potassium dichromate in an acidic medium, followed by confirmation with Schiff's reagent (Schiff, 1866). Schiff's reagent reacts specifically with aldehydes, being highly sensitive to formaldehyde (the oxidation product of methanol) and much less reactive to acetaldehyde (the oxidation product of ethanol), thus allowing differentiation between the two primary alcohols.

#### Oxidation of primary alcohols:

Methanol: $CH_3OH \rightarrow HCHO$ (formaldehyde) $\rightarrow HCOOH$ (formic acid)

Ethanol: $CH_3CH_2OH \rightarrow CH_3CHO$ (acetaldehyde) $\rightarrow CH_3COOH$ (acetic acid)

#### Dichromate reaction (Eq. 2):

$$3\ CH_3OH + Cr_2O_7^{2-} + 8\ H^+ \rightarrow 3\ HCHO + 2\ Cr^{3+} + 7\ H_2O \quad \text{(Eq. 2)}$$ (orange → green)

#### Reagents

The required reagents include an oxidizing solution and Schiff's reagent. The oxidizing

solution is prepared by first dissolving 5 g of $K_2Cr_2O_7$ in 90 mL of distilled water, then carefully adding 10 mL of concentrated $H_2SO_4$ while stirring continuously to dissipate heat. Schiff's reagent is prepared by dissolving 0.1 g of basic fuchsin in 100 mL of distilled water and treating with $SO_2$ or bisulfite until the solution becomes colorless; it should be stored in an amber bottle for stability.

**Procedure**

**Part A – Alcohol oxidation:**

1. In a clean, dry test tube, add 1 mL of dichromate/$H_2SO_4$ solution
2. Add 3-5 drops of the sample (previously tested in Stage 1)
3. Gently shake
4. Observe color change (orange → green) and development of characteristic odor
5. Wait 2-3 minutes

Table 3 presents the expected oxidation results for different alcohols.

**Part B – Confirmation with Schiff's Reagent:**

1. Transfer 0.5 mL of the oxidized solution to a new tube
2. Add 1 mL of Schiff's reagent
3. Shake and wait 5-10 minutes
4. Observe color development

Table 4 presents the results of the confirmation test with Schiff's reagent.

**Result Interpretation**

Methanol identification relies on a characteristic analytical profile across multiple tests. A positive result presents as negative turbidity in the Lucas test (confirming the primary alcohol structure), an efficient orange-to-green color transition during dichromate oxidation, development of formaldehyde's distinctive pungent odor, and, most critically, an intense pink-violet coloration in Schiff's test, which serves as confirmatory evidence. Ethanol, conversely, shares some features with methanol—both show no Lucas test turbidity and similar oxidation color changes—but differs critically in producing acetaldehyde's sweet odor and yielding either a very faint or absent pink coloration in Schiff's test, thus excluding methanol presence.

**Quality Control**

Analytical validation requires systematic inclusion of control samples in each batch. Known methanol standards serve as positive controls to verify reagent functionality, while ethanol or water serves as negative controls to exclude false positives. Reagent blanks assess potential contamination, and parallel analysis of both methanol and ethanol reference solutions provides direct comparative standards for interpreting unknown samples and ensuring accurate alcohol differentiation.

Standard solutions should yield expected results, as outlined in Tables 2, 3, and 4, to validate reagent quality and correct procedure execution, following the practices documented in experimental organic chemistry protocols (Furniss *et al.*, 1989).

**3.2. Brazilian Colorimetric Method**

This colorimetric method was developed and validated in Brazil specifically for the determination of methanol in various alcoholic matrices, including beverages (Modesto, 2020). The technique indicates an effort to develop a low-cost, highly portable analytical methodology suitable for both laboratory analyses and field screening.

A distinctive feature of this method is its chemical equivalence with recognized international protocols, such as the OIV-MA-AS315-27 standard from the International Organisation of Vine and Wine. Both employ oxidation followed by reaction with chromotropic acid, differing essentially in the type of reading: while international standards prescribe spectrophotometry at 575 nm, the Brazilian method allows visual reading or RGB analysis with low-cost portable devices (smartphone or portable photometers), making it especially suitable for resource-limited contexts.

**3.2.1. Objective**

To detect and/or quantify the presence of methanol in alcoholic beverages (vodka, whisky, cachaça) through a colorimetric method based on the oxidation of methanol to formaldehyde, followed by reaction with chromotropic acid, with

the possibility of field execution.

### 3.2.2. Method Principle

Methanol in the sample is oxidized to formaldehyde in an acidic medium using an oxidizing agent (potassium dichromate or potassium permanganate). The generated formaldehyde reacts with chromotropic acid in a strongly acidic medium ($H_2SO_4$ 16.5-18 mol/L), forming a violet/purple complex whose intensity is proportional to the methanol concentration (Modesto, 2020). The reading can be performed visually or with the aid of color analysis devices. Figure 2 presents the complete flowchart of both protocols.

**Selectivity:** Ethanol is also oxidized, but its products (acetaldehyde and acetic acid) do not react meaningfully with chromotropic acid, ensuring selectivity for methanol.

**Method variants:** Two oxidizing routes can be used:

- Method A (Dichromate): $K_2Cr_2O_7$ as oxidizing agent
- Method B (Permanganate): $KMnO_4$ as oxidizing agent (more sensitive, better visual contrast)

### 3.2.3. Reagents and Materials

#### 3.2.3.1. Reagents

The analytical procedure requires concentrated sulfuric acid at different molarities: 18 mol/L for the dichromate-based approach (method A) and 16.5 mol/L for the permanganate-based approach (method B). The oxidizing agent varies according to the selected method. Method A employs a potassium dichromate solution prepared by dissolving 1 g of $K_2Cr_2O_7$ in 40 mL of water, followed by the addition of 10 mL of concentrated $H_2SO_4$. Method B utilizes a potassium permanganate solution consisting of 0.75 g of $KMnO_4$ dissolved in water with 2 mL of orthophosphoric acid ($H_3PO_4$), adjusted to a final volume of 50 mL. This second method additionally requires a 0.05 mol/L sodium sulfite solution, prepared by dissolving 0.315 g of $Na_2SO_3$ in 50 mL of distilled water. Both methods use chromotropic acid as the colorimetric reagent, prepared at 0.5% (w/w) by dissolving 0.5 g of the disodium salt dihydrate ($C_{10}H_8O_8S_2$) in 49.5 g of sulfuric acid at the molarity specified for the chosen method. Distilled water is used throughout for solution preparation and dilution.

#### 3.2.3.2. Materials

- Test tubes (10–15 mL)
- Graduated pipettes or micropipettes
- Stopwatch
- Optional: smartphone with camera, portable photometer, or spectrophotometer

Note: A water bath is not required in the optimized versions of the method (Modesto, 2020).

### 3.2.4. Experimental Procedure

**Method A – Oxidation with Potassium Dichromate ($K_2Cr_2O_7$)**

Step 1 – Oxidation

1. In a clean, dry test tube, add 5 mL of the alcoholic beverage (vodka, whiskey, or non-sweetened cachaça)
2. Add 4 mL of potassium dichromate oxidizing solution
3. Gently shake and let stand for 5 minutes at room temperature

Note: The solution should turn green (reduction of $Cr^{6+}$ to $Cr^{3+}$), indicating alcohol oxidation.

Step 2 – Colorimetric Reaction

1. Transfer 1 mL of the oxidized solution to a new test tube
2. Add 3 mL of chromotropic acid solution in 18 mol/L $H_2SO_4$
3. Wait 10 minutes at room temperature
4. Observe color formation

**Method B – Oxidation with Potassium Permanganate ($KMnO_4$) [Recommended]**

Step 1 – Oxidation

1. In a test tube, add 1 mL of the alcoholic beverage
2. Add 1.6 mL of $KMnO_4$ oxidizing solution (0.75 g in 50 mL with $H_3PO_4$)
3. Wait 5 minutes at room temperature

Note: Formation of $MnO_2$ (brown precipitate).

Step 2 – Decolorization

1. Add 4 mL of sodium sulfite solution (0.05 mol/L)
2. Shake until the solution becomes colorless (reduction of excess $MnO_4^-$ and $MnO_2$)

Step 3 – Colorimetric Reaction

1. Transfer 1 mL of the decolorized solution to a new tube
2. Add 3 mL of chromotropic acid solution in 16.5 mol/L $H_2SO_4$
3. Wait 10 minutes at room temperature
4. Observe the developed color

### 3.2.5. Result Interpretation

Regulatory limit (MAPA): ≤ 20 mg/100 mL of methanol in vodka, whiskey, and cachaça. Table 5 presents the visual interpretation of results for both methods.

**Comparison between methods:**

- Method B ($KMnO_4$): More sensitive with better color contrast (yellow → clean violet), recommended for visual screening
- Method A ($K_2Cr_2O_7$): Resulting color is a mixture (green + violet = brown), requiring more careful reading or use of auxiliary devices

**Important limitation:** Do not apply to samples containing sugar (cocktails, sweetened cachaças, liqueurs) – sugar interferes by generating dark brown coloration that prevents accurate reading.

**Recommendation for quantification:** Use digital RGB analysis (smartphone camera and software) or a portable photometer for greater objectivity at concentrations near the regulatory limit (20 mg/100 mL). Portable devices allow the construction of calibration curves and quantification with reasonable precision (Modesto, 2020).

### 3.2.6. Controls and Validation

Quality assurance protocols require systematic inclusion of control samples in each analytical batch. Positive controls are prepared by spiking beverages with methanol to achieve 20 mg/100 mL, the regulatory threshold set by MAPA, thereby confirming the method's sensitivity at the critical concentration. Negative controls use either GC-FID-verified methanol-free beverages or analytical-grade ethanol to exclude false positives. Reagent blanks assess baseline interference and contamination potential. For quantitative applications employing instrumental detection, calibration standards at known methanol concentrations enable construction of analytical curves for accurate quantification.

Performance characteristics established by Modesto (2020) demonstrate the method's fitness for purpose. Selectivity validation encompassed multiple beverage matrices including vodka, whiskey, and non-sweetened cachaça, confirming applicability across typical distilled spirit compositions. Detection capabilities vary with the measurement approach: visual observation achieves approximately 160 mg/100 mL (0.2% v/v) detection limits, whereas instrumental measurements with RGB colorimeters or spectrophotometers achieve approximately 20 mg/100 mL, aligning with regulatory requirements. The complete analytical procedure, from sample introduction through final measurement, requires 20 to 30 minutes, facilitating rapid screening applications.

### 3.2.7. Applicability and Context of Use

This method offers advantages for health surveillance through its portability, low cost, operational simplicity, rapid 20-30 minute analysis time, and versatility in providing both visual and instrumental reading options. All reagents and materials are transportable and accessible, requiring no complex equipment for basic screening applications. However, limitations include moderate visual sensitivity, unsuitable for precise quantification; susceptibility to sugar interference, which restricts use in sweetened beverages; and inherent subjectivity in visual readings, though auxiliary colorimetric devices can mitigate this concern.

The method finds optimal application in three key contexts: field screening during inspections, events, and at retail locations where rapid results support immediate public safety decisions; routine analyses in resource-limited laboratories seeking

cost-effective alternatives to chromatographic methods; and educational settings where the technique's simplicity and visual nature facilitate demonstrations and training in analytical chemistry and methanol detection principles.

**Important Note on Confirmation:** These colorimetric methods are qualitative/semi-quantitative and intended for rapid screening in the field or teaching laboratory. For official, forensic analyses or precise quantification, confirmation by gas chromatography (GC-FID) is recommended according to MAPA/ABNT NBR 16041 standards (Modesto, 2020).

### 3.3. Gas Chromatography with Flame Ionization Detection (GC-FID)

Gas chromatography with flame ionization detection is the gold standard method for the quantitative determination of methanol in alcoholic beverages, recognized by national and international regulatory bodies as the reference technique for forensic and fiscal analyses.

The analytical superiority of GC-FID is based on three fundamental characteristics: (1) exceptional specificity provided by the physical separation of volatile compounds in the chromatographic column, eliminating interferences from other alcohols and matrix components; (2) high sensitivity with detection limits on the order of 1 mg/100 mL, well below the regulatory limit of 20 mg/100 mL; and (3) accuracy and precision that allow exact and reproducible quantification, which are necessary for technical reports with legal value.

Several standardized methods employ GC-FID for methanol determination, all based on the same chromatographic principles but with variations in instrumental parameters. The AOAC 972.11 method (Methanol in Distilled Liquors) is widely used internationally (AOAC, 1972). In Brazil, the IAL 228/IV method (Instituto Adolfo Lutz, 2008) is particularly suitable for national laboratories, as it provides specific validation for the characteristics of Brazilian beverages. The International Organisation of Vine and Wine provides methods OIV-MA-AS315-27 (OIV, 2016a) and OIV-MA-BS-14 (OIV, 2016b) for analysis of volatile compounds including methanol. The Ministry of Agriculture and Livestock recognizes these methods in its Manual of Official Methods for Analysis of Wines, Beverages and Acetic Fermented Products (MAPA, 2025).

The detailed description that follows is based on the IAL 228/IV method (IAL, 2008), chosen for its suitability to the Brazilian context and the availability of complete technical documentation.

#### 3.3.1. Objective

To quantitatively determine the concentration of methanol in distilled alcoholic beverages (aguardente, cachaça, whiskey, vodka, rum) by gas phase chromatography with flame ionization detection, using internal standardization with 3-pentanol (IAL, 2008).

#### 3.3.2. Method Principle

The method is based on the chromatographic separation of the sample's volatile components on a capillary column with a polar stationary phase (polyethylene glycol, commercially known as Carbowax), followed by flame ionization detection (FID).

**Separation principle:** Volatile compounds are vaporized in the heated injector and transported by carrier gas (hydrogen) through the capillary column. The polar stationary phase differentially retains compounds based on their polarity and volatility, thereby promoting physical separation. Methanol, being highly polar, has a characteristic retention time that allows its unequivocal identification.

**Detection principle:** In the FID detector, organic compounds are burned in a hydrogen/air flame, generating ions that produce an electric current proportional to the amount of carbon present. The chromatographic peak area is directly proportional to the compound concentration.

**Quantification by internal standardization:** 3-pentanol is used as internal standard, added at a known concentration to both the sample and calibration standards. This procedure eliminates variations in injection volume, volatile losses, and instrumental fluctuations, ensuring precision superior to simple external calibration. Figure 3 presents the complete flowchart of the analytical procedure.

#### 3.3.3. Equipment and Materials

##### 3.3.3.1. Equipment

- Gas chromatograph equipped with: ○ Flame ionization detector (FID) ○ Split/splitless injector with precise

temperature control ○ Data acquisition system and integration software

- Capillary column: Carbowax (polyethylene glycol) – 30 m × 0.53 mm i.d. × 1 µm film thickness (or similar)
- Analytical balance: 0.1 mg resolution
- Microsyringe: 10 µL (compatible with GC injector)

**3.3.3.2. Gases (high purity)**

The chromatographic analysis requires three high-purity gases at 99.999% minimum purity. Hydrogen serves dual purposes as both carrier gas and flame supply for the detector. Synthetic air functions as the oxidant in the flame ionization detector (FID). Nitrogen is employed as auxiliary gas (make-up) to optimize detector performance. Due to hydrogen's highly flammable nature, special safety precautions are mandatory, including the use of leak detectors and ensuring adequate laboratory ventilation.

**3.3.3.3. Glassware**

Precise volumetric glassware is needed for accurate solution preparation. Class A volumetric flasks in 10 mL and 100 mL capacities are required for standard preparation. Class A volumetric pipettes of 1 mL and 10 mL sizes ensure accurate volume transfers during analytical procedures.

**3.3.4. Reagents**

All chemical reagents must meet chromatographic-grade specifications with a minimum purity of 99.5%. The required materials include methanol as the calibration reference standard, 3-pentanol as the internal standard, absolute ethyl alcohol at ≥99.5% purity as the primary solvent, and distilled or ultrapure water for dilutions and auxiliary preparations.

**3.3.5. Solution preparation**

All analytical solutions are prepared using gravimetric (weight-based) methodology rather than volumetric methods to achieve maximum precision, following protocols established by IAL (2008). This approach eliminates volumetric errors associated with temperature variations and meniscus reading.

**3.3.5.1. Methanol Stock Standard Solution (A)**

A 100 mL volumetric flask containing approximately 40 mL of absolute alcohol is first tared on an analytical balance. Approximately 2.0 mL of methanol is then added and precisely weighed. The flask is brought to volume with absolute alcohol, weighed again, and the final mass is recorded. The methanol concentration in mg/100 g is calculated from the mass difference between the initial and final weighings.

**3.3.5.2. Internal Standard Stock Solution (B)**

A 100 mL volumetric flask containing approximately 40 mL of absolute alcohol is tared on an analytical balance. Approximately 2.5 mL of 3-pentanol is added and precisely weighed. After diluting to volume with absolute alcohol, the flask is weighed again to record the final mass. The 3-pentanol concentration, in mg/100 g, is determined from the mass difference.

**3.3.5.3. 40% v/v Alcohol Solution** Dilute 40 mL of absolute alcohol to 100 mL with distilled water (to simulate beverage matrix).

**3.3.5.4. Working Standard Solution (C) – for calibration**

1. In a tared 100 mL flask with ~40 mL of 40% alcohol, add: ○ 1 mL of solution A (methanol) – weigh ○ 1 mL of solution B (internal standard) – weigh
2. Make up to volume with 40% alcohol
3. Weigh and record masses for exact concentration calculation

**3.3.5.5. Working Internal Standard Solution (E) – for samples**

1. In a tared 100 mL flask with ~40 mL of 40% alcohol: ○ Pipette 10 mL of solution B
2. Make up to volume with 40% alcohol
3. Weigh and record masses

**Storage:**

- All solutions: 4-8°C in well-sealed amber bottles
- Stability: Solutions A and B (stocks) – 6 months; Solutions C and E (working) – 1 month

### 3.3.6. Procedure

#### 3.3.6.1. Sample Preparation

1. Tare a 10 mL volumetric flask
2. Add 9 mL of sample (weigh precisely)
3. Add 1 mL of solution E (internal standard) – weigh
4. Homogenize by gentle shaking
5. Record all masses for calculations

Critical note: Beverages with dry residue > 0.4 g/100 mL (sweetened drinks, liqueurs) must be distilled beforehand to avoid contamination of the chromatographic column.

#### 3.3.6.2. Chromatographic Conditions

Table 6 presents the optimized instrumental parameters for methanol separation.

#### 3.3.6.3. Analysis

1. Calibration: ○ Inject standard solution C at least 4 times (replicates) ○ Determine retention time of methanol and internal standard ○ Calculate correction factor (see section 3.3.7.1)
2. Sample analysis: ○ Inject each prepared sample at least 4 times (replicates) ○ Identify methanol peak by comparison with the standard retention time ○ Record peak areas of methanol and internal standard

### 3.3.7. Calculations

#### 3.3.7.1. Methanol Correction Factor (CF)

The correction factor relates the detector response to methanol versus the internal standard:

$$CF_{methanol} = (C_{methanol} \times A_{IS}) / (C_{IS} \times A_{methanol})$$

Where:

- $C_{methanol}$ = Methanol concentration in solution C (mg/100 g)
- $C_{IS}$ = Internal standard concentration in solution C (mg/100 g)
- $A_{methanol}$ = Methanol peak area in solution C
- $A_{IS}$ = Internal standard peak area in solution C

#### 3.3.7.2. Methanol Concentration in Sample (mg/100 g)

Using the correction factor, the concentration in the sample is calculated:

$$C_{methanol,sample} = (A_{methanol,sam} \times CF_{methanol} \times C_{IS,sam}) / A_{IS,sam}$$

Where:

- $A_{methanol,sam}$ = Methanol peak area in the sample
- $A_{IS,sam}$ = Internal standard peak area in the sample
- $C_{IS,sam}$ = Internal standard concentration in the sample (mg/100 g)

#### 3.3.7.3. Result in mg/100 mL of Anhydrous Alcohol (Regulatory format)

To express according to MAPA requirements:

$$C = (C_{methanol,sample} \times d_{abs} \times 100) / G$$

Where:

- C = Final methanol concentration (mg/100 mL of anhydrous alcohol)
- $d_{abs}$ = Absolute density of the sample (g/mL)
- G = Alcoholic strength of the sample (% v/v)

### 3.3.8. Expression of Results

Express the result in mg/100 mL of anhydrous alcohol, with one decimal place (eg. 8.5 mg/100 mL).

Regulatory limit (MAPA): Maximum of 20.0 mg/100 mL of anhydrous alcohol for aguardente, cachaça, vodka, and whiskey.

### 3.3.9. Quality Control

#### 3.3.9.1. Acceptance Criteria

To ensure result reliability, these criteria must be met:

- Coefficient of variation between injections: < 5%
- Chromatographic resolution: between methanol and adjacent peaks > 1.5
- Peak asymmetry factor: 0.8 - 1.5 (indicator of column efficiency)
- Spike recovery: 95-105%

### 3.3.10. Advantages and Limitations of the Method

Table 7 summarizes the distinctive characteristics of GC-FID.

### 3.3.11. Applicability and Context of Use

**Ideal application context:**

- Forensic and fiscal analyses (legal value)
- Confirmation of screening method results
- Precise quantification for industrial quality control
- Research and development of new products
- Audits and certifications

**Not recommended for:**

- Rapid field screening
- High-volume routine analyses (low throughput)
- Laboratories without adequate infrastructure
- Situations requiring immediate results

**Role in the Health Surveillance System**

GC-FID does not replace screening methods; rather, it complements the analytical system. Its function is to confirm, with legal authority, the suspicious or positive results obtained by simpler methods (e.g., colorimetric), ensuring legal certainty for regulatory actions such as seizures, fines, and criminal proceedings.

## 4. RESULTS

### 4.1. Contextualization: The Reference Method

Gas Chromatography with Flame Ionization Detection (GC-FID) is the reference method for the determination of methanol in alcoholic beverages. This prominent position is recognized by the Ministry of Agriculture, Livestock and Food Supply (MAPA), which establishes it as the official technique for fiscal and forensic analyses. The technical superiority of GC-FID is founded on three analytical pillars: exceptional specificity provided by chromatographic separation, superior sensitivity with detection limits below 1 mg/100 mL, and accuracy that confers legal value to the results.

Even so, this analytical robustness imposes substantial practical limitations. The operational complexity, the need for specialized laboratory infrastructure, and the impossibility of field execution restrict its application to accredited laboratories. This scenario reveals a critical gap: the lack of analytical methods that reconcile reliability with portability and accessibility for on-site health surveillance. In contrast, colorimetric methods emerge as viable alternatives for field screening, enabling analyses at the collection point without the need for sample transport or complex laboratory infrastructure.

### 4.2. Comparative Analysis of Colorimetric Methods

The systematic investigation of colorimetric methods revealed fundamental differences in their chemical principles, sensitivity, applicability, and limitations. The Brazilian Method (Modesto, 2020) encompasses two oxidizing routes: Method A employs potassium dichromate ($K_2Cr_2O_7$) as oxidant, while Method B uses potassium permanganate ($KMnO_4$). Both routes converge on the same chromogenic detection step using chromotropic acid in strongly acidic medium, resulting in chemically equivalent analytical performance. The critical difference lies in visual interpretability: Method A generates a violet color superimposed on residual green from chromium(III) species, producing a brownish- tan appearance that complicates visual assessment. In contrast, Method B exhibits a clean yellow-to-violet color transition with minimal background interference. This superior visual contrast makes Method B the preferred choice for field screening applications where instrumental reading is

unavailable, while Method A remains viable for laboratory use with colorimetric devices.

Table 8 summarizes the analytical characteristics of all evaluated colorimetric methods, including both Brazilian Method variants, enabling systematic comparison of their capabilities and limitations.

### 4.3. Functional Classification of Methods

The analysis of data presented in Table 8 allowed classification of the methods into two distinct functional categories. The Lucas Test proved inapplicable for methanol determination, as it is intended solely for structural classification of alcohols (primary, secondary, and tertiary). This method does not detect methanol but functions as an exclusion screening step in the combined protocol, eliminating potential interferents before confirmatory stages.

The three remaining methods share the same analytical strategy: oxidation of methanol to formaldehyde, followed by colorimetric detection of the formed aldehyde. However, they diverge significantly in the oxidant/detector reagent pairs employed. The method with dichromate and Schiff's reagent uses a distinct chemical system from those based on permanganate and chromotropic acid, resulting in differences in sensitivity and in the color pattern developed.

### 4.4. Chemical Equivalence between Brazilian Method and OIV Standard

A relevant finding from this analysis was the verification that the Brazilian Method (Modesto, 2020) and the OIV-MA-AS315-27 Standard are chemically identical in their oxidation and chromogenic detection steps. Both employ potassium permanganate as oxidizing agent and chromotropic acid as a detection reagent, and follow essentially equivalent protocols.

The fundamental difference between them lies exclusively in the mode of reading the final result: the Brazilian Method allows visual analysis or with the aid of portable devices (smartphones with RGB analysis or benchtop photometers), conferring greater flexibility and portability; the OIV Standard, in turn, rigorously prescribes the use of spectrophotometry at 575 nm for instrumental quantification, ensuring maximum precision and interlaboratory reproducibility. This chemical equivalence validates the national method as a technically sound alternative to international protocols, with the additional advantage of adaptability to resource-limited contexts.

### 4.5. Limitations from Analytical Interferences

Investigation of interferences revealed a critical restriction common to methods based on chromotropic acid (the Brazilian Method and the OIV Standard). The presence of sugars and reducing compounds in the sample matrix promotes parallel reactions that generate dark brown coloration, masking or distorting the characteristic violet analytical signal of the methanol-chromotropic complex. This interference notably limits the applicability of these methods to non-sweetened beverages, such as vodka, whiskey, and pure cachaça. Consequently, cocktails, liqueurs, sweetened cachaças, and other beverages containing added sugar cannot be analyzed by these protocols without prior sample treatment (e.g., distillation or extensive dilution).

### 4.6. Comparative Synthesis: Analytical Performance and Applicability

To contextualize colorimetric methods relative to the gold standard, Table 9 presents a comprehensive comparison of critical analytical parameters, operational aspects, costs, and application contexts.

### 4.7. Integrated Interpretation of Results

The comparative analysis shows that the investigated methods do not compete with one another but rather occupy complementary niches within a hierarchical analytical system. The classical colorimetric methods and the Brazilian Method stand out for their portability, low cost, and speed of execution—characteristics essential for field screening during inspections, health surveillance actions, and response to public health emergencies. Their moderate sensitivity (LOD ~20-160 mg/100 mL) is sufficient to detect significant contamination above the regulatory limit of 20 mg/100 mL, enabling rapid decision-making regarding the recall of suspect products.

On the other hand, GC-FID maintains its unquestionable superiority in specificity (LOD ≤ 1 mg/100 mL) and accuracy, characteristics indispensable for confirmatory analyses, technical expertise, and precise quantification in legal reports. Its operational complexity and high cost are justified when absolute precision is mandatory, but make it impractical for routine high-volume screening or in locations without laboratory

infrastructure.

Finally, the finding that sugars interfere with methods based on chromotropic acid clearly delimits the scope of application: these protocols are suitable for non-sweetened distilled beverages (vodka, whiskey, pure cachaça) but require prior treatment for complex matrices such as liqueurs and cocktails. This limitation does not compromise their utility in health surveillance, since outbreaks of methanol poisoning frequently involve adulterated distilled beverages—precisely the type of matrix in which these methods perform best.

## 5. DISCUSSION

### 5.1. Analytical Hierarchy: Complementarity between Methods

The classification of GC-FID as a reference method derives from its undeniable analytical advantages. The specificity allows physical separation of methanol from other matrix components, such as ethanol and acetaldehyde, eliminating interferences that can lead to false-positive or false-negative results in colorimetric methods. The technique's sensitivity, capable of detecting concentrations on the order of 1 mg/100 mL, is vital for identifying contamination well below the regulatory limit of 20 mg/100 mL, providing a robust analytical safety margin. Finally, the accuracy and precision of instrumental analysis remove the subjectivity of visual interpretation, ensuring reproducible, reliable results that are required for forensic reports with legal value.

The complexity of GC-FID—which includes high equipment costs (R$ 100-300 thousand), the need for high-purity gases, specialized chromatographic columns, and highly qualified operators—makes it a confirmatory and quantitative method. In contrast, colorimetric methods are more appropriately classified as screening and semi-quantitative methods. The comparison between them, therefore, is not one of absolute quality but rather of function within a hierarchical control system.

The limitation of GC-FID regarding field use is, in practice, what creates the need and defines the role of simpler methods. A fiscal agent cannot transport a chromatograph to an inspection at a party, artisanal distillery, or border inspection post. In this scenario, colorimetric methods are valuable tools, enabling rapid, immediate assessment. A positive or suspicious field result justifies sample collection, which is then sealed and sent to an accredited laboratory for confirmatory analysis by GC-FID, ensuring both operational agility and regulatory compliance.

### 5.2. Chemical Equivalence and Cross-Validation: Brazilian Method versus International Standard

One of the most relevant findings of this study was the verification that the Brazilian Method developed by Modesto (2020) is chemically identical to the OIV-MA-AS315-27 Standard in its oxidation and chromogenic detection steps. Both employ potassium permanganate as the oxidizing agent and chromotropic acid as the detection reagent, following protocols that are nearly identical in reagent concentrations, reaction times, and experimental conditions.

This chemical equivalence has important practical implications. First, it technically validates the national method as a solid alternative to international protocols, conferring scientific credibility supported by standards recognized by the International Organisation of Vine and Wine. Second, it shows that the fundamental difference between the methods lies exclusively in the reading mode: while the OIV standard rigorously prescribes spectrophotometry at 575 nm, the Brazilian method offers flexibility, allowing visual reading or portable devices (smartphones with RGB analysis or benchtop photometers).

This instrumental flexibility is a strategic advantage in resource-limited contexts, enabling protocol adaptation to available infrastructure without compromising the chemical foundation of the analysis. Equipped laboratories can opt for spectrophotometric reading for maximum precision and interlaboratory comparability; field agents can employ visual analysis or portable devices for rapid screening; small distilleries can implement quality control with minimal investment in equipment.

### 5.3. Analytical Limitations: Sugar Interferences and Practical Implications

The interference of sugars and reducing compounds in methods based on chromotropic acid is a relevant but not critical technical limitation when properly contextualized. This interference restricts the direct application of these methods to non-sweetened distilled beverages (vodka, whiskey, pure cachaça), requiring prior treatment (distillation or extensive dilution) for complex matrices such as liqueurs, cocktails, and

sweetened cachaças.

While this limitation does not substantially compromise the utility of these methods in health surveillance for two reasons. First, the epidemiology of methanol poisoning outbreaks shows that most cases are associated with consumption of adulterated distilled beverages (artisanal cachaças, clandestine vodkas, counterfeit whiskeys)—precisely the type of matrix where colorimetric methods show best performance. Table 1 documents outbreaks in 22 countries, predominantly involving non-sweetened distilled beverages.

Second, for situations where analysis of sweetened beverages is necessary, the protocol can be adapted through prior sample distillation. This relatively simple procedure removes sugars and other volatile interferents, allowing subsequent colorimetric analysis of the distillate. This additional step, while reducing portability, keeps the method more accessible and faster than GC-FID.

### 5.4. Analytical Trade-offs: Sensitivity versus Portability

The comparative analysis revealed a fundamental trade-off between analytical sensitivity and portability/accessibility. Colorimetric methods exhibit moderate sensitivity (LOD ~20-160 mg/100 mL) compared with GC-FID (LOD ≤1 mg/100 mL), but this difference should be interpreted in light of the application context and regulatory limits.

The Brazilian regulatory limit established by MAPA is 20 mg/100 mL of anhydrous alcohol. The Brazilian Method, when aided by RGB reading devices or portable photometers, achieves an LOD of approximately 20 mg/100 mL, which matches the regulatory limit exactly. This sensitivity is analytically adequate for screening, as it detects contaminations at the critical level that separates compliant from non-compliant products.

The lower sensitivity of colorimetric methods implies a smaller safety margin for detecting discrete contaminations below the regulatory limit. Samples with 5-15 mg/100 mL of methanol, although compliant, could go unnoticed in visual screening. This is precisely the scenario where the hierarchical approach is justified: colorimetric methods identify gross contaminations (outbreaks, adulterations), while GC-FID ensures fine control for quality certification and detailed forensic investigations.

### 5.5. Well-Produced Cachaça: Safety Context and Real Risk

Methanol toxicity is a potential public health risk, with a lethal dose estimated between 0.5 and 1.5 g/kg body weight for adult humans (Gosselin *et al.*, 1984). Studies demonstrate that well-produced commercial cachaça has an average methanol content of approximately 6 mg per 100 mL of anhydrous alcohol (Boscolo *et al.*, 2000), a value much lower than the regulatory limit of 20 mg/100 mL. To contextualize this value in terms of real risk, we calculated the amount of beverage necessary to reach the lethal dose.

To estimate the lethal methanol dose for a 70 kg adult, we start from the lower end of the toxicity range (0.5 $g \cdot kg^{-1}$). This gives 35 g — i.e. 35 000 mg — of methanol, an amount that could theoretically be fatal. The next question is how much cachaça would have to be consumed to reach this figure. First, we consider the concentration in anhydrous alcohol (6 mg per 100 mL, or 60 mg $L^{-1}$). Dividing the lethal dose by this concentration shows that 583 L of pure alcohol would be required. Yet cachaça is only about 40 % ABV, so every 100 mL of spirit contains 40 mL of anhydrous alcohol. The methanol content therefore, drops to 2.4 mg per 100 mL (24 $mg \cdot L^{-1}$) and the volume needed rises to 1.458 L.

This implausible volume becomes even more remote when we compare it with ethanol toxicity. The human lethal dose of ethanol is reported to be 5–8 $g \cdot kg^{-1}$ (Vonghia et al., 2008), corresponding to 350–560 g for a 70 kg person. With ethanol density at 789 $g \cdot L^{-1}$, a litre of 40 % ABV cachaça delivers 316 g of pure ethanol. Consequently, death from ethanol would occur after 1.1–1.8 L of cachaça — orders of magnitude below the 1.458 L required for methanol.

Water toxicity provides a second biological ceiling. Roughly 60 % of cachaça is water, so the hypothetical 1.458 L would include about 875 L of water. The acute lethal volume of water is approximately 6 L for an adult (Farrell & Bower, 2003), meaning water intoxication would occur long before methanol reached dangerous levels.

These back-of-the-envelope calculations ignore pharmacokinetic nuances such as absorption and metabolic rate, but they clearly show that the naturally low methanol content of well-produced cachaça poses no practical threat when the beverage is consumed in moderation. Real danger arises only from criminal adulteration or sloppy distillation in which the “heads” fraction is not discarded, pushing methanol concentrations tens or hundreds of times above normal levels.

### 5.6. Recent Outbreaks and the Urgency of Rapid Detection

The Brazilian outbreak of October 2025, with 58 confirmed cases and 15 deaths reported by the Ministry of Health (2025), reinforces the urgency of accessible analytical methods for rapid response in public health emergencies. Table 1 documents outbreaks in more than 22 countries, with alarming fatality rates—80% in Uganda (2017), 44% in Estonia (2001), 37% in Czech Republic (2012-2014)—demonstrating that the time window for intervention is critical.

In these emergency scenarios, the portability and speed of colorimetric methods become decisive attributes. The ability to perform on-site analyses in distributors, bars, events, and households allows:

1. Rapid identification of contamination source, reducing time between first cases and product recall;
2. Mass screening of multiple suspect samples within hours, impossible with GC-FID due to analysis time (~45-60 min/sample);
3. Immediate mobilization of resources for recall of contaminated batches before additional consumption;
4. Effective risk communication to the population, based on quickly obtained analytical data.

The Iranian experience during the COVID-19 pandemic is emblematic: between February and May 2020, Iran recorded 534-800 deaths from methanol poisoning associated with consumption of adulterated alcoholic beverages supposedly "protective" against the virus (Hassanian-Moghaddam *et al.*, 2020). Rapid detection and risk communication could have significantly mitigated the number of victims.

### 5.7. Integrated Hierarchical System: Protocol Proposal for Health Surveillance

Based on the findings of this study, we propose implementing an integrated hierarchical system that combines colorimetric screening methods with GC-FID for confirmation, optimizing inspection resources, and balancing operational agility with analytical reliability. The suggested protocol consists of three levels:

**Level 1 – Field Screening (Colorimetric Methods):**

- Objective: Rapid identification of suspect samples
- Method: Brazilian Method ($KMnO_4$ + Chromotropic) with visual reading or portable device
- Decision criterion: Positive result (violet coloration) → Suspect sample
- Action: Immediate collection, sealing, and forwarding to Level 2
- Time: 20-30 minutes

**Level 2 – Laboratory Confirmation (GC-FID):**

- Objective: Precise quantification for forensic report
- Method: GC-FID according to IAL 228/IV or AOAC 972.11 method
- Decision criterion: Concentration > 20 mg/100 mL → Confirmed non-compliance
- Action: Issuance of technical report, definitive seizure, administrative/criminal sanctions
- Time: 45-60 minutes/sample

**Level 3 – Counterproof (Reference Laboratory):**

- Objective: Resolution of challenges and litigation
- Method: GC-FID or GC-MS in a certified laboratory (INMETRO, MAPA)
- Action: Final judicial decision

This hierarchical protocol offers concrete operational advantages:

- Resource efficiency: Expensive analyses (GC-FID) are reserved for confirmation of suspect cases, not for mass screening;
- Operational agility: Field decisions based on analytical evidence within minutes;
- Legal security: Forensic reports by GC-FID ensure legal value for administrative and criminal proceedings;

- Scalability: Multiple teams can perform simultaneous screening at different locations;
- Cost-effectiveness: Reduction of operational costs without compromising reliability.

### 5.8. Technological Gaps and Development Opportunities

Despite the advances introduced by the Brazilian Method (Modesto, 2022), some technological gaps persist and are opportunities for research and development:

#### 5.8.1. Development of Integrated Portable Devices

The integration of RGB analysis systems, whether on smartphones or dedicated portable photometers, can enhance the sensitivity of colorimetric methods, bringing them closer to the regulatory limit of 20 mg/100 mL while maintaining objectivity and reproducibility superior to visual reading. Devices with automated calibration and an intuitive interface would further reduce subjectivity and training requirements, democratizing access to reliable semi-quantitative analyses.

#### 5.8.2. Treatment of Complex Samples

The development of simplified pre-treatment protocols for sweetened beverages (flash distillation, solid-phase extraction, or controlled dilution) would expand the scope of application of colorimetric methods without excessively compromising portability. Portable micro-distillers or disposable purification cartridges could enable analysis of liqueurs and cocktails in the field.

#### 5.8.3. Ready-to-Use Kits

The commercialization of standardized colorimetric kits containing pre-dosed reagents, positive/negative controls, and visual instructions would facilitate large-scale adoption by small producers, health inspectors, and laboratories with limited resources. These kits, validated and certified, would ensure reproducibility among different users and contexts.

#### 5.8.4. Interlaboratory Validation

Collaborative interlaboratory validation studies of the Brazilian Method in accordance with ISO/IEC 17025 standards would strengthen its official acceptance and international comparability, thereby consolidating it as a recognized alternative for screening in resource-limited contexts.

### 5.9. Brazilian Context: Implications for Public Policies

Brazil has unique characteristics that make the implementation of hierarchical protocols especially relevant. With more than 40,000 cachaça-producing establishments (including small artisanal distilleries), a continental territory with remote, difficult-to-access regions, and limited inspection resources, the country faces meaningful challenges in ensuring food safety for distilled alcoholic beverages.

The adoption of colorimetric methods for field screening would enable:

- Decentralized inspection in municipalities without accredited laboratories;
- Training of artisanal producers for quality self-control;
- Rapid response to outbreaks in regions far from urban centers;
- Resource optimization of surveillance agencies (ANVISA, State Surveillance, MAPA).

The experience of the October 2025 outbreak, concentrated in São Paulo but with cases in six states, shows the need for analytical capillarity that simple methods can provide, complementing the network of certified laboratories.

## 6. CONCLUSIONS

This study critically compared analytical methods for methanol determination in alcoholic beverages, evaluating the combined classical methods, the Brazilian colorimetric method, and gas chromatography (GC-FID) with respect to performance and applicability in resource-limited contexts.

The results confirm that the methods are not competitors but rather complementary within a hierarchical system. GC-FID maintains its position as the reference method for confirmatory analyses (LOD ≤1 mg/100 mL, accuracy and legal value),

while colorimetric methods stand out as field screening tools (portability, low operational cost, execution in 20-30 minutes).

It was verified that the Brazilian Method is chemically equivalent to the OIV Standard, differing only in the type of reading, which technically validates the national protocol as an alternative to international methods. The Lucas Test proved inapplicable for methanol detection, being restricted to structural classification of alcohols. Sugar interference limits the use of chromotropic methods to non-sweetened distilled beverages, which is consistent with the epidemiological profile of outbreaks (adulterated distilled beverages).

The implementation of integrated protocols—colorimetric field screening followed by GC-FID confirmation in the laboratory— is an efficient operational strategy that optimizes inspection resources, ensuring operational agility and legal security. This approach is especially relevant in the Brazilian context, where the October 2025 outbreak (58 cases, 15 deaths) underscores the need for accessible, rapid-response methods in health surveillance.

As a limitation, this study adopted a theoretical-comparative approach without its own experimental validation. Future studies should include interlaboratory validation of the Brazilian Method, the development of portable devices with automated reading, and the development of simplified protocols for complex beverages.

We conclude that public health protection requires not only precise methods but also accessible ones that can be implemented at scale, making colorimetric methods a strategic tool for effective health surveillance in countries with limited resources.

## 7. DECLARATIONS

### 7.1. Study Limitations

This study adopted a theoretical-comparative approach based on a critical review of specialized literature and normative documentation, without its own experimental validation of the methods. The main limitations include:

- Absence of experimental validation directly comparing the three methods with real contaminated beverage samples;
- Lack of field studies evaluating the practical applicability of colorimetric methods under real inspection conditions;
- Limited scope to non-sweetened distilled beverages, with a superficial approach to complex matrices (liqueurs, cocktails);
- Absence of primary data on interlaboratory precision, robustness, and measurement uncertainty of colorimetric methods.

Despite these limitations, the study provided a solid, critical, and comparative foundation for analytical methods for methanol detection, clearly identifying the advantages, limitations, and applicability contexts of each technique, contributing to informed selection of methodologies for health surveillance and quality control in the Brazilian context.

### 7.2. Future Perspectives

Future studies could strengthen the conclusions through: (i) experimental validation with real fortified samples; (ii) field studies during inspections; (iii) interlaboratory validation of the Brazilian Method according to ISO/IEC 17025; (iv) development of portable devices with automated reading; (v) protocols for beverages not covered in this study. Additionally, emerging technologies (electrochemical sensors, portable Raman spectroscopy, microfluidic devices) may expand the arsenal of tools for health surveillance in resource-limited contexts.

### 7.3. Acknowledgments

The author thanks the Brazilian research and health surveillance institutions whose technical work provided the documentary basis for this review: the Ministry of Agriculture, Livestock and Food Supply (MAPA), the Instituto Adolfo Lutz (IAL), and the Ministry of Health for epidemiological data. Recognition to the international scientific community whose research on analytical methods and poisoning outbreaks provided the necessary global context for this analysis.

### 7.4. Funding Source

The author funded this research with personal resources. There was no external funding from development agencies, public or private institutions. In accordance with the ethical

guidelines of the Southern Journal of Sciences, which do not allow donations from authors with manuscripts under evaluation (even when research funds are available) or in cases of authors' financial constraints, publication costs were fully absorbed by the journal under our Platinum Open Access policy, through the support of the Araucária Scientific Association (https://acaria.org/). This policy aims to ensure complete independence between the editorial process and any financial aspects, reinforcing our commitment to scientific integrity and equity in knowledge dissemination.

### 7.5. Conflicts of Interest

The authors declare the absence of financial or commercial conflicts of interest related to this study. The analytical methods described are in the public domain or widely documented in scientific literature. There is no commercial relationship with manufacturers of equipment, reagents, or analysis kits. This work is strictly academic in nature and does not promote specific products or services. The author did not receive any form of compensation from organizations that might have interest in the results presented.

### 7.6. Open Access



### 7.7. Author Contributions

Luis Alcides Brandini De Boni (LABD) conceived the study design, conducted the literature review, critically analyzed the analytical methods, developed the theoretical comparisons, prepared the tables and figures, and wrote the manuscript. Rochele da Silva Fernandes (RSF) critically reviewed the manuscript, identified inconsistencies in data presentation, verified technical accuracy of analytical method descriptions, and provided substantive suggestions for improving methodological clarity and standardization. Both authors reviewed and approved the final version of the manuscript and are accountable for all aspects of the work.

### 7.8. AI Use declaration

This manuscript was prepared with assistance from artificial intelligence tools. ChatGPT (OpenAI), Claude AI (Anthropic), and Grammarly were used to support literature organization, improve text clarity, and refine grammar and style. All technical content, data interpretation, comparative analysis, and scientific conclusions are the sole responsibility of the author. The AI tools served exclusively as writing assistants and did not generate original scientific content or analysis. The author critically reviewed, verified, and validated all information presented.

## 8. HUMAN AND ANIMAL-RELATED STUDIES

### 8.1. Ethical Approval

Not plicable.

### 8.2. Informed Consent

Not plicable.

## 9. REFERENCES:

1. AOAC. (1972). Official Method 972.11: Methanol in distilled liquors. AOAC International. Retrieved from https://www.aoac.org/wp-content/uploads/2023/07/Index-of-Method-Numbers.pdf
2. Birungi Doreen, Eyu, P., Okethwangu, D., Biribawa, C., Kizito, S., Nakanwagi, M., Nguna, J., Nkonwa, I. H., Opio, D. N., Aceng, F. L., Alitubeera, P. H., Kadobera, D., Kwesiga, B., Bulage, L., Ario, A. R., & Zhu, B.-P. (2020). Fatal methanol poisoning caused by drinking adulterated locally distilled alcohol: Wakiso District, Uganda, June 2017. Journal of Environmental and Public Health, 2020, Article ID 5816162. https://doi.org/10.1155/2020/5816162
3. Boscolo, M., Bezerra, C. W. B., Cardoso, D. R., Lima Neto, B. S., & Franco, D. W. (2000). Identification and dosage by HRGC of minor alcohols and esters in Brazilian sugar-cane spirit. Journal of the Brazilian Chemical Society, 11(1), 86–90. https://doi.org/10.1590/s0103-50532000000100015

4. Brasil. Instituto Nacional de Metrologia, Qualidade e Tecnologia – INMETRO. (2009, September 24). Portaria nº 276, de 24 de setembro de 2009: Aprova o RTAC 001497/… Diário Oficial da União. http://www.inmetro.gov.br/legislacao/rtac/pdf/RTAC001497.pdf
5. Brasil. Ministério da Agricultura, Pecuária e Abastecimento. (2005, June 29). Instrução Normativa nº 13: Aprova o Regulamento Técnico para Fixação dos Padrões de Identidade e Qualidade para Aguardente de Cana e para Cachaça. Diário Oficial da União. https://pesquisa.in.gov.br/imprensa/jsp/visualiza/index.jsp?data=30/06/2005&jornal=1&pagina=3&totalArquivos=256
6. Brasil. Ministério da Agricultura, Pecuária e Abastecimento. (2022, December 26). Portaria MAPA nº 539, de 26 de dezembro de 2022: Estabelece os Padrões de Identidade e Qualidade da aguardente de cana e da cachaça. Diário Oficial da União, Seção 1, ed. 243, p. 13. https://www.in.gov.br/en/web/dou/-/portaria-mapa-n-539-de-26-de-dezembro-de-2022-453828778
7. Eskandrani, R., Almulhim, K., Altamimi, A., Alhaj, A., Alnasser, S., Alawi, L., Aldweikh, E., Alaufi, K., & Mzahim, B. (2022). Methanol poisoning outbreak in Saudi Arabia: a case series. Journal of Medical Case Reports, 16(1), 357. https://doi.org/10.1186/s13256-022-03600-7
8. Farrell, D. J., & Bower, L. (2003). Fatal water intoxication. Journal of Clinical Pathology, 56(10), 803-804. https://doi.org/10.1136/jcp.56.10.803-a
9. Furniss, B. S., Hannaford, A. J., Smith, P. W. G., & Tatchell, A. R. (1989). Vogel's textbook of practical organic chemistry (5th ed.). Wiley.
10. González, C. (1999, March 12). Mortes na BA foram causadas por metanol. Folha de S.Paulo. https://www1.folha.uol.com.br/fsp/cotidian/ff12039945.htm
11. Gosselin, R. E., Smith, R. P., & Hodge, H. C. (1984). Clinical toxicology of commercial products (5th ed.). Williams & Wilkins.
12. Hassanian-Moghaddam, H., Zamani, N., Kolahi, A. A., McDonald, R., & Hovda, K. E. (2020). Double trouble: methanol outbreak in the wake of the COVID-19 pandemic in Iran—a cross-sectional assessment. Critical Care, 24(1), 402. https://doi.org/10.1186/s13054-020-03140-w
13. Hovda, K. E., Hunderi, O. H., Tafjord, A.-B., et al. (2005). Methanol outbreak in Norway 2002–2004: epidemiology, clinical features and prognostic signs. Journal of Internal Medicine, 258(2), 181–190. https://doi.org/10.1111/j.1365-2796.2005.01521.x
14. Instituto Adolfo Lutz. (2008). Métodos físico-químicos para análise de alimentos (4th ed., 1st digital ed.). São Paulo: Instituto Adolfo Lutz. Retrieved from https://wp.ufpel.edu.br/nutricaobromatologia/files/2013/07/NormasADOLFOLUTZ.pdf
15. International Labour Organization. (2018, May). ICSC 0057: Methanol. International Programme on Chemical Safety. https://chemicalsafety.ilo.org/dyn/icsc/showcard.display?p_lang=en&p_card_id=0057&p_version=2
16. International Labour Organization & World Health Organization. (2018). Methanol: International Chemical Safety Card 0057. Geneva: International Programme on Chemical Safety. Retrieved from https://chemicalsafety.ilo.org
17. Jacobsen, D., Wils, K., Smedsaas, E., & Bredesen, J. E. (1982). Studies on Methanol Poisoning. Acta Medica Scandinavica, 212(1–2), 5–10. https://doi.org/10.1111/j.0954-6820.1982.tb03160.x
18. Konkel, K., Burkhart, K., Cheng, C., Lee, R., Michele, T., Mentari, E., Diak, I.-L., & MCCulley, L. (2023). Methanol poisonings from contaminated hand sanitizers identified by the United States Food and Drug Administration. Clinical Toxicology, 61(12), 1065–1067. https://doi.org/10.1080/15563650.2023.2288809
19. Lucas, H. O. (1905). A new method for the determination of the constitution of alcohols. Journal of the American Chemical Society, 27(2), 1032–1035.
20. MAPA. (2025). Manual de métodos oficiais de análises de vinhos, bebidas e fermentados acéticos: Métodos físico-químicos. Ministério da Agricultura e Pecuária, Secretaria de Defesa Agropecuária. Retrieved from https://wikisda.agricultura.gov.br/pt-br/Laboratórios/Metodologia/Bebidas/Manual_IQA_BEV

21. Ministério da Saúde. (2025, October 24). Metanol: 58 casos confirmados de intoxicação após consumo de bebidas alcoólicas. https://www.gov.br/saude/pt-br/assuntos/noticias/2025/outubro/metanol-58-casos-confirmados-de-intoxicacao-apos-consumo-de-bebidas-alcoolicas
22. Modesto, L. A. M. (2020). Desenvolvimento de método colorimétrico para determinação de metanol em etanol hidratado combustível, gasolina automotiva, bebidas alcoólicas e vinagre [Master's thesis, Universidade Estadual Paulista]. UNESP Institutional Repository. http://hdl.handle.net/11449/236222
23. Mordor Intelligence. (2025, July 28). Methanol Market Size, Share, Trends Analysis & Industry Report, 2030. https://www.mordorintelligence.com/industry-reports/methanol-market
24. OIV. (2016a). OIV-MA-AS315-27: Analysis of volatile compounds in wine by gas chromatography (Resolution Oeno 553/2016). Organisation Internationale de la Vigne et du Vin. Retrieved from https://www.oiv.int/public/medias/5159/oiv-ma-as315-27.pdf
25. OIV. (2016b). OIV-MA-BS-14: Determination of principal volatile substances. Organisation Internationale de la Vigne et du Vin. Retrieved from https://www.oiv.int/public/medias/2674/oiv-ma-bs-14.pdf
26. Paasma, R., Hovda, K. E., Tikkerberi, A., & Jacobsen, D. (2007). Methanol mass poisoning in Estonia: outbreak in 154 patients. Clinical Toxicology, 45(2), 152–157. https://doi.org/10.1080/15563650601031680
27. Rahimi, R., et al. (2021). Methanol poisoning in Klang Valley, Malaysia: Autopsy findings in sixteen fatal cases. Forensic Science International: Reports, 3, 100170. https://doi.org/10.1016/j.fsir.2021.100170
28. Rostrup, M., Edwards, J. K., Abukalish, M., Ezzabi, M., Some, D., Ritter, H., & Hovda, K. E. (2016). The methanol poisoning outbreaks in Libya 2013 and Kenya 2014. PLoS ONE, 11(3), e0152676. https://doi.org/10.1371/journal.pone.0152676
29. Rulisek, J., Balik, M., Polak, F., et al. (2017). Cost-effectiveness of hospital treatment and outcomes of acute methanol poisoning during the Czech Republic mass poisoning outbreak. Journal of Critical Care, 39, 190–198. https://doi.org/10.1016/j.jcrc.2017.03.001
30. Sarıbaş, K., Akpınar, A. A., Özşeker, P. E., Taşkın, Ö., Dişel, N. R., & Devecioğlu, G. F. (2025). Methanol poisoning in the emergency department: methanol blood levels, prognosis, and sequelae outcomes. Irish Journal of Medical Science, 194, 1461–1470. https://doi.org/10.1007/s11845-025-03982-9
31. Scanavini, H. F. A., Ceriani, R., & Meirelles, A. J. A. (2012). Cachaça distillation investigated on the basis of model systems. Brazilian Journal of Chemical Engineering, 29(2), 429–440. https://doi.org/10.1590/s
32. 32. Schiff, H. (1866). Mittheilungen aus dem Universitäts-Laboratorium in Pisa [Communications from the University Laboratory in Pisa]. Annalen der Chemie und Pharmacie, 140(1), 93–109.
33. Schwartz, M. (2019, February 23). Bootleg liquor kills scores in India's latest mass outbreak of alcohol poisoning. NPR. https://www.npr.org/2019/02/23/697317095/bootleg-liquor-kills-scores-in-indias-latest-mass-outbreak-of-alcohol-poisoning
34. Šejvl, J., Barták, M., Gavurová, B., Mašlániová, M., Petruželka, B., Rogalewicz, V., Zacharov, S., & Miovský, M. (2019). Public health response to methanol mass poisoning in the Czech Republic in 2012: a case study. Central European Journal of Public Health, 27(Suppl), S29–S39. https://doi.org/10.21101/cejph.a5764
35. Venegas-Justiniano, Y., Rosales-Mendoza, K., Enríquez-Almanza, B., Valdivia-Infantas, M., Barboza-Pastrana, A., & Hurtado-Aréstegui, A. (2024). Intoxicación por metanol: análisis de una serie de casos en dos Hospitales Públicos. ACTA MEDICA PERUANA, 41(1). https://doi.org/10.35663/amp.2024.411.2775
36. Voice of America. (2022, July 19). Methanol found in 21 youths who died at bar in South Africa. https://www.voanews.com/a/methanol-found-in-21-youths-who-died-at-bar-in-south-africa/6665203.html
37. Vonghia, L., Leggio, L., Ferrulli, A., Bertini, M., Gasbarrini, G., & Addolorato, G. (2008). Acute alcohol intoxication. European Journal of Internal Medicine,

19(8), 561-567. https://doi.org/10.1016/j.ejim.2007.06.033
38. World Health Organization. (1997). Methanol: Health and safety guide (Health and Safety Guide No. 105). Geneva: World Health Organization.
39. World Health Organization (WHO). (2020, July 29). INFOSAN Quarterly Summary – 2020 #2. https://www.who.int/news/item/29-07-2020-infosan-quarterly-summary-2020-2
40. 40. Zakharov, S., Pelclova, D., Urban, P., Navratil, T., Diblik, P., Kuthan, P., et al. (2014). Czech mass methanol outbreak 2012: epidemiology, challenges and clinical features. Clinical Toxicology, 52(10), 1013–1024. https://doi.org/10.3109/15563650.2014.974106
41. Zniber, A., Benhadda, S., Badrane, N., Ennaïri, M., Chaoui, H., & Tahri, M. Y. (2025). Methanol poisoning outbreak in a northwestern Moroccan town: report of 22 cases treated with hemodialysis. Clinical Toxicology. https://doi.org/10.1080/15563650.2025.2525410

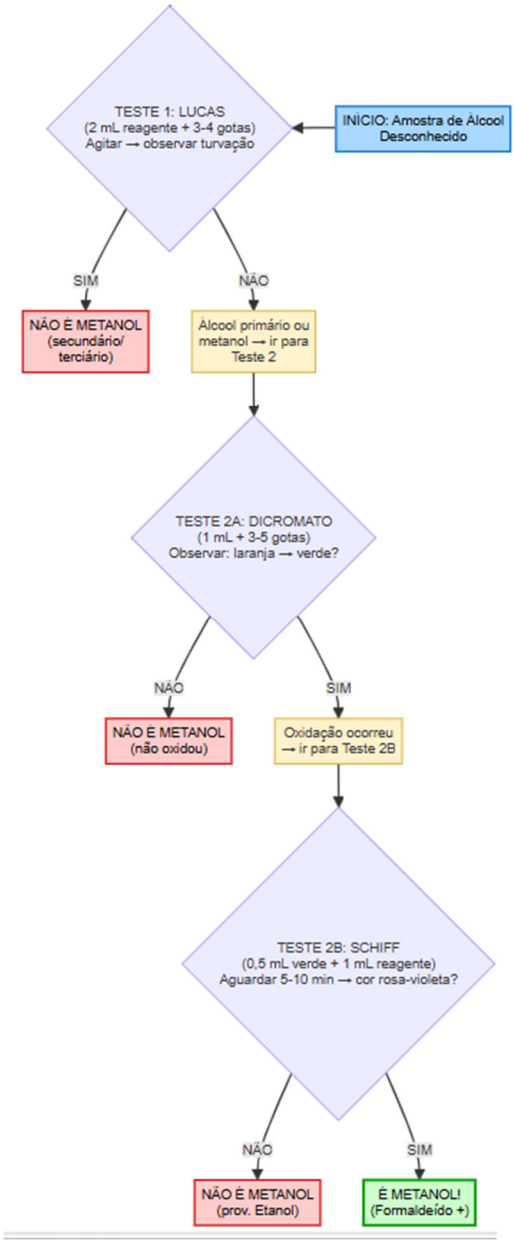


**Figure 1.** *Flowchart of the combined analysis protocol for methanol detection in alcoholic beverages using classical methods. The process consists of initial screening with Lucas Test (elimination of secondary and tertiary alcohols), followed by dichromate oxidation and specific confirmation with Schiff's reagent.*

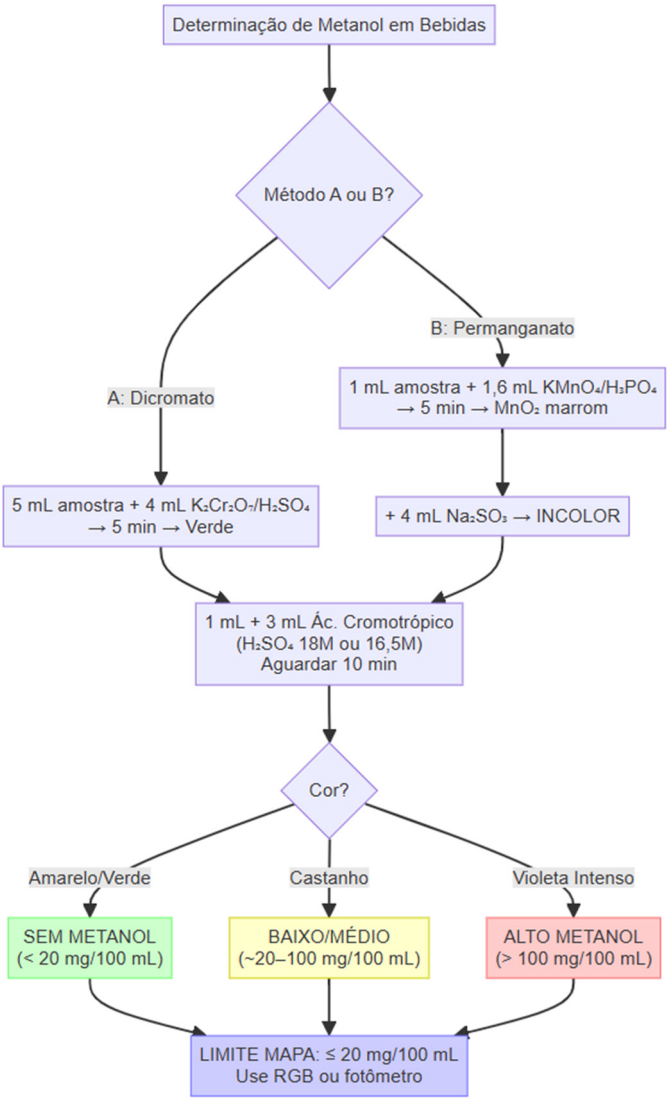


**Figure 2.** *Flowchart of Brazilian colorimetric methods for methanol determination in alcoholic beverages. The method offers two oxidizing routes (A: dichromate or B: permanganate), both followed by a chromogenic reaction with chromotropic acid. The violet color intensity is proportional to methanol concentration, allowing visual screening or quantification with portable devices.*

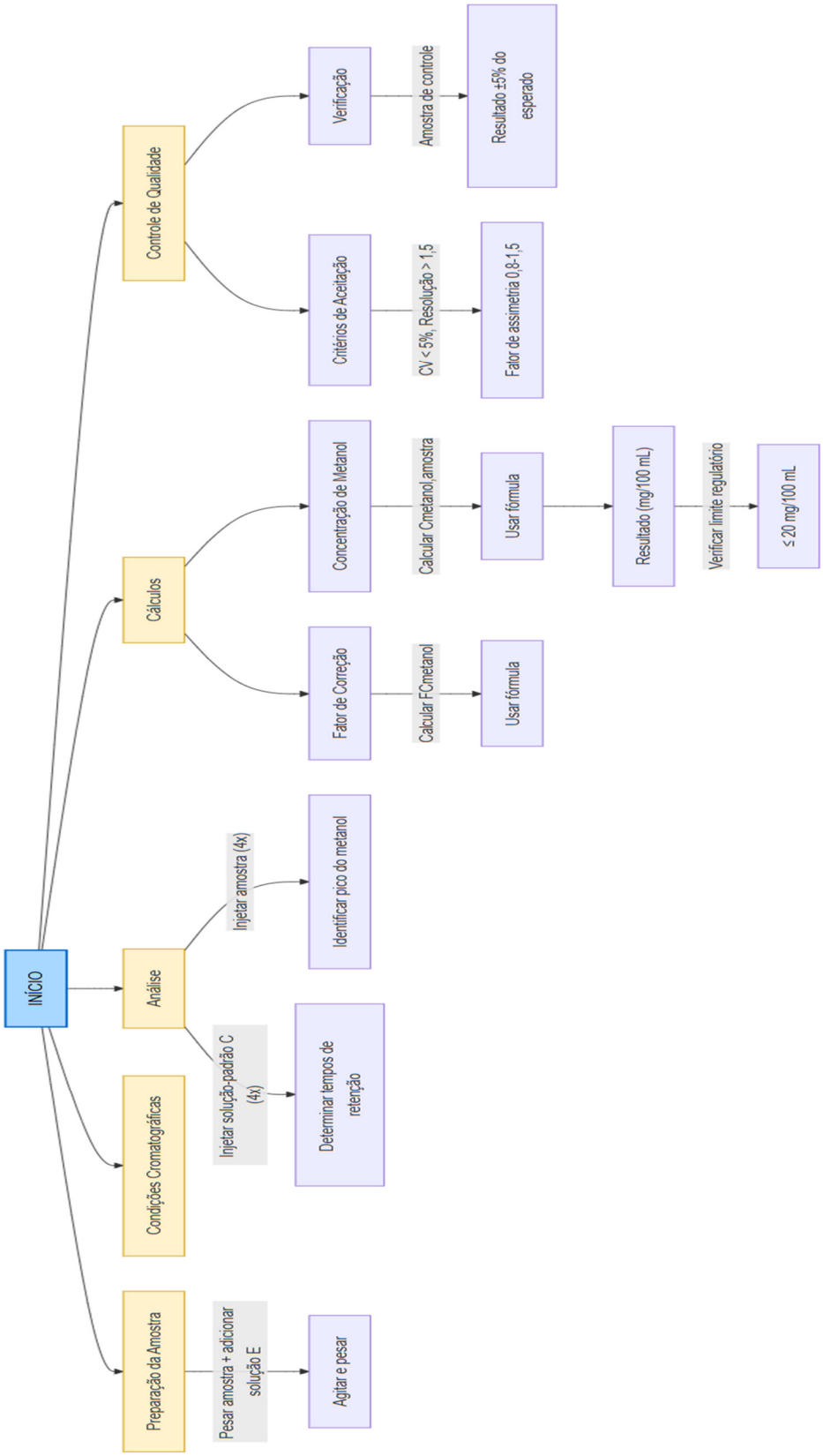


**Figure 3.** *Flowchart of the method for methanol determination by gas chromatography with flame ionization detection (GC-FID). The process includes sample preparation with internal standard addition, conditioning of chromatographic conditions, instrumental analysis, quantification calculations, and rigorous quality control.*

**Table 1.** *Methanol Poisoning Outbreaks*

| Location (Country) | Outbreak Year(s) | Victims / Reported Fatalities | APA Reference(s) |
|---|---|---|---|
| **Brazil (Oct 2025)** | 2025 | 108 records; 15 reported deaths | Ministério da Saúde, 2025 |
| **Iran** | Feb-May 2020 (COVID-19 Peak) | 534-800 deaths (13.6% mortality) | Hassanian-Moghaddam *et al.*, 2020 |
| **Czech Republic** | 2012-2014 (Mass outbreaks) | 137 confirmed cases; 51 deaths (37% mortality) | (Rulisek *et al.*, 2017; Šejvl *et al.*, 2019; Zakharov *et al.*, 2014) |
| **Malaysia (Klang Valley)** | Sep-Oct 2018 | 64 fatalities; 16 fatal cases autopsied | (Rahimi *et al.*, 2021) |
| **Uganda (Wakiso District)** | June 2017 | 15 cases; 12 deaths (80% fatality) | (Birungi Doreen *et al.*, 2020) |
| **Estonia** | 2001 | 154 patients; 68 deaths (44% mortality) | (Paasma *et al.*, 2007; Šejvl *et al.*, 2019) |
| **Libya** | 2013 | 1,066 cases; ~90 deaths (10% fatality) | (Rostrup *et al.*, 2016) |
| **Kenya** | 2014 | Documented outbreaks | (Rostrup *et al.*, 2016) |
| **Norway (Kristiansand)** | October 1979 | 11 hemodialyzed patients; 3 deaths (non-dialyzed) | (Jacobsen *et al.*, 1982) |
| **Norway (Prolonged epidemic)** | 2002-2004 | 53 cases | (Hovda *et al.*, 2005; Šejvl *et al.*, 2019) |
| **Turkey** | 1993-2002 | 113 cases | (Šejvl *et al.*, 2019) |
| **Turkey (Istanbul, Ankara)** | Nov 2024 - Feb 2025 | >235 cases (Istanbul); >94 cases (Ankara) | (Sarıbaş *et al.*, 2025) |
| **Saudi Arabia (Riyadh)** | Not specified | Approximately 25 individuals affected | (Eskandrani *et al.*, 2022) |
| **Morocco** | Recent (Published 2025) | 22 cases treated with hemodialysis | (Zniber *et al.*, 2025) |
| **Poland** | 2009-2013 | 49 cases (peak of 15 in 2013) | (Šejvl *et al.*, 2019) |
| **Russia** | Dec 2016 | 88 deaths | (Šejvl *et al.*, 2019) |
| **Brazil** | 1999 | 35 deaths | González, C. (1999, March 12). |
| **Dominican Republic** | Dec 2020 | 199 deaths | World Health Organization (WHO). (2020, July 29). |
| **Peru** | 2018-2022 | 9 deaths | Venegas-Justiniano *et al.*, 2024 |
| **South Africa** | 2022 | 21 adolescents killed | Voice of America. (2022, July 19). |
| **India (Assam)** | Feb 2019 | 150+ deaths | Schwartz, M. (2019, February 23). |
| **Mexico** | May and June 2020 | 100 deaths | World Health Organization (WHO). (2020, July 29). |
| **Cambodia** | June 2020 | 43 | World Health Organization (WHO). (2020, July 29). |
| **USA (Hand Sanitizer)** | May 2020 - Nov 2021 | 58 cases; 23 fatalities (40%) | (Konkel *et al.*, 2024) |

**Table 2. Lucas Test results for different types of alcohols.**

| Alcohol | Time | Observation | Interpretation for the protocol |
|---|---|---|---|
| Methanol | >60 min | No reaction, solution remains clear | Proceed to Stage 2 |
| Ethanol | >60 min | No reaction | Proceed to Stage 2 |
| n-Propanol | >60 min | No reaction | Proceed to Stage 2 |
| Isopropanol | 5-10 min | Gradual turbidity | Secondary alcohol present |
| tert-Butanol | Immediate | Immediate turbidity, phase separation | Tertiary alcohol present |

**Table 3.** Dichromate oxidation results for different alcohols.

| Alcohol | Color change | Odor | Product |
|---|---|---|---|
| Methanol | Orange → green | Pungent, irritating | Formaldehyde |
| Ethanol | Orange → green | Sweet, fruity | Acetaldehyde |
| Isopropanol | Orange → green | Acetone-like | Acetone |
| tert-Butanol | No change | - | Does not oxidize |

**Table 4.** Schiff's test results for formaldehyde confirmation.

| Product formed | Color developed | Diagnosis |
|---|---|---|
| Formaldehyde (methanol) | Intense pink-violet | POSITIVE |
| Acetaldehyde (ethanol) | Very faint pink or none | Negative |
| Acetone (isopropanol) | None (not an aldehyde) | Negative |

**Table 5.** Visual interpretation of results from Brazilian colorimetric methods.

| Method | Observed color | Color intensity | Diagnosis | Estimated concentration |
|---|---|---|---|---|
| A (Dichromate) | Yellow/Green | - | Negative | < 20 mg/100 mL |
| A (Dichromate) | Brown-tan | Weak to moderate | Positive | ~20-100 mg/100 mL |
| A (Dichromate) | Violet + green | Intense | Positive | > 100 mg/100 mL |
| B (Permanganate) | Light yellow | - | Negative | < 20 mg/100 mL |
| B (Permanganate) | Light violet | Weak | Positive | ~20-50 mg/100 mL |
| B (Permanganate) | Intense violet | Strong | Positive | > 100 mg/100 mL |

**Table 6.** Chromatographic conditions for methanol determination by GC-FID (IAL 228/IV method).

| **Parameter** | **Condition** |
|---|---|
| Injector temperature | 200°C |
| Detector temperature | 250°C |
| Oven programming: | |
| - Initial temperature | 40°C (hold 4 min) |
| - Ramp 1 | 15°C/min to 60°C (hold 5 min) |
| - Ramp 2 | 30°C/min to 170°C (hold 10 min) |
| Carrier gas ($H_2$) | 1 mL/min (constant flow) |
| $H_2$ for flame (FID) | 20 mL/min |
| Synthetic air (FID) | 175 mL/min |
| $N_2$ make-up (FID) | 25-30 mL/min |
| Injection mode | Split 1:100 |
| Injection volume | 1.0 µL |
| Total run time | ~45-60 minutes |

**Table 7.** Advantages and limitations of the GC-FID method for methanol determination.

| **Advantages** | **Limitations** |
|---|---|
| Exceptional specificity: Physical separation eliminates interferences | High cost: Equipment (R$ 100-300 thousand) |
| Superior sensitivity: LOD ≤ 1 mg/100 mL | Complex infrastructure: Gases, ventilation, space |
| Precision and accuracy: CV < 5%, recovery 95-105% | Specialized operator: Extensive training required |
| Exact quantification: Results with legal value | Analysis time: 45-60 min per sample |
| Official recognition: Accepted by MAPA, AOAC, OIV | Not portable: Impossible to use in the field |
| Multicomponent analysis: Detects other volatiles simultaneously | Operating cost: Gases, maintenance, standards |

**Table 8.** Comparative analytical characteristics of colorimetric methods for methanol detection.

| Analytical Criterion | Lucas Test | Dichromate + Schiff | Brazilian A ($K_2Cr_2O_7$) | Brazilian B ($KMnO_4$) | OIV Standard |
|---|---|---|---|---|---|
| **Fundamental Principle** | Nucleophilic substitution (SN1) | Oxidation to formaldehyde + colorimetric reaction | Oxidation to formaldehyde + chromotropic reaction | Oxidation to formaldehyde + chromotropic reaction | Oxidation to formaldehyde + chromotropic reaction |
| **Oxidizing Agent** | $ZnCl_2$ (catalyst) | $K_2Cr_2O_7$ | $K_2Cr_2O_7$ | $KMnO_4$ | $KMnO_4$ |
| **Detection Agent** | Visual turbidity | Schiff's Reagent | Chromotropic Acid | Chromotropic Acid | Chromotropic Acid |
| **Primary Objective** | Alcohol classification | Methanol identification | Semi-quantitative screening | Semi-quantitative screening | Precise quantification |
| **Reading Type** | Visual (turbidity time) | Visual (color intensity) | Visual or RGB/photometer | Visual or RGB/photometer | Spectrophotometer (575 nm) |
| **Observed Sensitivity** | N/A (not for methanol) | Moderate (~160 mg/100 mL visual) | ~20-160 mg/100 mL | ~20-160 mg/100 mL | ~20 mg/100 mL |
| **Color Developed** | Turbidity (cloudy) | Pink-violet | Violet + green (brownish) | Clean violet | Violet |
| **Visual Contrast** | Good (clear→cloudy) | Moderate | Poor (mixed colors) | Excellent (yellow→violet) | N/A (instrumental) |
| **Main Interferences** | 2° and 3° alcohols | Other aldehydes (weak) | Sugars, reducing compounds | Sugars, reducing compounds | Sugars, reducing compounds |
| **Execution Complexity** | Low | Moderate | Moderate | Moderate | High |
| **Analysis Time** | 5-60 min | 15-30 min | 20-30 min | 20-30 min | 20-30 min |
| **Portability** | Excellent | Excellent | Excellent | Excellent | Poor (lab only) |
| **Typical Applicability** | Exclusion screening | Laboratory screening | Field/lab screening | **Field screening (recommended)** | Laboratory confirmation |

LOD = Limit of Detection; RGB = Red-Green-Blue color analysis via digital imaging; N/A = Not applicable. *Method B (permanganate-based) is recommended for field screening due to superior visual contrast. Method A (dichromate-based) is suitable for laboratory settings with colorimetric reading devices. **All methods based on chromotropic acid are not applicable to sugar-containing beverages without prior sample treatment (distillation or dilution).

**Table 9.** Comparison of analytical performance and applicability of classical colorimetric methods, national method, and gold standard (GC-FID).

| **Criterion** | **Combined Classical Methods** | **National Method (Modesto, 2020)** | **Gold Standard Method (GC-FID)** |
|---|---|---|---|
| Principle | Oxidation with dichromate + reaction with Schiff or chromotropic acid | Colorimetry with chromotropic acid after oxidation | Chromatographic separation with flame ionization detection |
| LOD (mg/100 mL) | ~160 (without optical aid) | ~20 (with RGB reading or photometer) | ≤1 |
| LOQ (mg/100 mL) | ~200 | ~30 | ~5 |
| Selectivity | Medium – ethanol also oxidizes but does not react with dye | Good – ethanol does not interfere in final reading | High–efficiency chromatographic separation |
| Analysis time | 15–30 min | 20–30 min | ~45–60 min (including preparation and run) |
| Initial investment | Minimal (tubes, basic reagents) | Low (photometer or smartphone) | High (chromatograph, gases, column) |
| Training required | Basic – technical level | Basic to intermediate | Advanced – specialized analyst |
| Field applicability | Excellent – portable, no electricity | Excellent – can use a smartphone | Poor – requires laboratory |
| Suitability for screening | Yes | Yes | Not recommended |
| Suitability for confirmation | Not recommended | Possible, with validation | Ideal |
| MAPA compliance | Not officially quantitative | Semi-quantitative – accepted with validation | Fully compliant |
| Main limitations | Low sensitivity, subjective interpretation | Sugar interference, calibration necessary | High cost, time, and requires infrastructure |
| | | | |

Legend: LOD = Limit of Detection; LOQ = Limit of Quantification; RGB = Color analysis via digital image; MAPA = Ministry of Agriculture, Livestock and Food Supply (regulatory limit: 20 mg/100 mL of anhydrous alcohol); ✓ = Suitable; ✗ = Unsuitable; △ = Partially suitable.

SOUTHERN JOURNAL OF SCIENCES

*ESTABLISHED IN 1993*

*Original research paper*

# INQUIRY FOR SUITABLE LOCATIONS FOR A DRILLING REGIME AT AN UPSLOPE ROCKY KNOLL OF LAWU ESTATE, WESTERN BYPASS, MINNA, NIGERIA

# PROSPECÇÃO DE LOCAIS APROPRIADOS PARA PERFURAÇÃO EM ELEVAÇÃO ROCHOSA DA PROPRIEDADE LAWU, VIA DE CONTORNO OESTE, MINNA, NIGÉRIA

JONAH, Sunday Adole[1]*; ABUTU, Oche[1]; ADESANMI, Solomon Glory[1]; OMONZANE, Favour Osaze[1]; OBODOAGU, Virginia Chidimma[1]; ABDULRAHEEM, Jamiu Adeiza[1]; ALHASSAN, Musa[1]; ENIETAN, Endurance Emmanuel[1]; SAIDU, Salihu[2]

[1] Federal University of Technology, School of Physical Science, Department of Physics, Minna. Nigeria. ORCID: 0009-0002-2017-2611

[2] Federal University of Technology, School of Physical Science, Department of Geography, Minna. Nigeria.

*Corresponding author: s.jonah@futminna.edu.ng

Received 25 March 2025; received in revised form 25 September 2025; accepted 11 December 2025

## ABSTRACT

**Background**: A client requested that the study group help determine suitable locations for a drilling regime on his lot, located on an upslope rocky knoll in Lawu Estate, Minna, Nigeria. There is no luxury of conducting an unimpeded wide-area survey for this housing Estate, as it is built up almost entirely. Therefore, the constrained area to be surveyed necessitated the adoption of the "electrical drilling," or vertical electrical sounding, mode of the geoelectrical method to satisfy the client's inquiry. **Aim**: To carry out a purpose-specific survey to pinpoint the best location in a built-up property at the upmarket Lawu Estate that would be suitable for a drilling regime targeted for household consumption. The specific objectives are to determine the subsurface layer structure, to identify fracture zones with potential for water accumulation, and to estimate the depths of potential aquifers. **Methods**: The survey crew reconnoitered the study area to georeference locations for the VES survey within the 30 m x 20 m lot. Owing to the extensive build-up at this lot, only a four-point traverse along the 30-metric dimension of the building's frontage was demarcated in the northeasterly direction, thereby limiting the survey crew's desire to define an appropriate survey grid. The VES data acquisition followed the "traditional" sequence of Schlumberger array layout measurements, in which the current and potential probes are maintained at the same relative spacing and the whole spread is progressively expanded about a fixed central point. **Results**: Log-log and pseudosection plots were generated from the acquired data, from which the conventional three-layer structure is deciphered, with a desired 193 Ωm for VES Station 4 at the third layer. **Discussion**: The acquired and processed data for this study were subjected to a suite of empirical rules-of-thumb procedures for interpreting VES data in the Nigerian Basement Complex geological province, with VES Station 4 showing the most encouraging 100% result. **Conclusion**: Drilling to a depth of 100 m at Station 4 is recommended based on the identified fractured basement at this depth.

**Keywords**: *Geoelectric; VES; traverse; groundwater; aquiferous*

## RESUMO

**Introdução**: Um cliente solicitou ao grupo de estudo auxílio para determinar locais adequados para um regime de perfuração em seu lote localizado em uma elevação rochosa na encosta superior da Propriedade Lawu, Minna, Nigéria. Não há possibilidade de conduzir levantamento de área ampla sem impedimentos, pois esta propriedade residencial está quase totalmente edificada. Portanto, a área restrita a ser levantada necessitou a adoção da "perfuração elétrica", ou modo de sondagem elétrica vertical (SEV), do método geoelétrico para satisfazer a consulta solicitada pelo cliente. **Objetivo**: Realizar levantamento específico para identificar o melhor local em uma propriedade edificada na Propriedade Lawu adequado para regime de perfuração destinado ao

 
DOI: 10.48141/2764-5959.03.v33.n40.2025_03_Sunday_pgs_49_61.pdf

consumo doméstico. Os objetivos específicos incluem determinar a estrutura das camadas subsuperficiais, identificar zonas de fratura com potencial para acumulação de água e estimar as profundidades de aquíferos potenciais. **Métodos**: A área de estudo foi reconhecida pela equipe de levantamento para georreferenciar os locais a serem ocupados para levantamento SEV no lote de 30 m x 20 m. Devido à extensa edificação neste lote, apenas uma travessia de quatro pontos ao longo da dimensão de 30 metros da fachada do edifício foi demarcada na direção nordeste, limitando assim o desejo da equipe de levantamento de definir uma grade de levantamento apropriada. A aquisição de dados SEV seguiu a sequência "tradicional" de arranjo-medições Schlumberger, onde os eletrodos de corrente e potencial são mantidos no mesmo espaçamento relativo e todo o arranjo é progressivamente expandido em torno de um ponto central fixo. **Resultados**: Gráficos log-log e pseudosseção foram devidamente gerados a partir dos dados adquiridos, dos quais se decifrou a estrutura convencional de três camadas com desejável resistividade de 193 Ωm para a Estação SEV 4 na terceira camada. **Discussão**: Os dados adquiridos e processados para este estudo foram submetidos a um conjunto de procedimentos empíricos baseados em regras práticas para interpretação de dados SEV na província geológica do Complexo Basal Nigeriano, com a Estação SEV 4 apresentando o resultado mais encorajador de 100%. **Conclusão**: Recomenda-se perfuração até profundidade de 100 m na Estação 4 com base no embasamento fraturado identificado nesta profundidade.

**Palavras-chave**: *Geoelétrico; SEV; travessia; água subterrânea; aquíferoPalavras-chave: Geoelétrico; SEV; travessia; água subterrânea; aquífero*

## 1. INTRODUCTION

A client who owns a limited-extent real estate property at the upmarket Lawu Estate requires pinpoint information to determine the best location to drill a potable-water borehole, even after his lot has undergone extensive built-up development. The client's challenge becomes the heart of the problem the survey crew of this project must solve, given that, aside from the lot already being built-up, the property is located on an upslope rocky knoll within this Estate.

This study aims to conduct a purpose-specific survey to pinpoint the best location within the upmarket Lawu Estate that is suitable for a drilling regime targeted for household consumption.

The specific objectives herein are to determine the subsurface layer structure, to identify fracture zones with potential for water accumulation, and to estimate the depths of potential aquifers. The designated area of interest here, a 30 m x 20 m lot located on an upslope rocky knoll, was heavily built-up; thus, the survey crew designated a four-station traverse, segmented into 1 x 4 = 4 vertical electrical sounding (VES) survey stations at the frontage of the built-up compound. The VES survey regime was planned for a total depth of 100 m at each survey location. The wider study area of Lawu Estate is shown in the satellite imagery map of Figure 1. On this map, the built-up area forming the backdrop of the study area has been appropriated demarcated based on the georeferenced information of its edges: Point A at 09°39′50.6″;006°30′50.3″, Point B at 09°39′49.7″;006°30′49.0″, Point C 09°39′49.9″;006°30′49.8″, Point D at 09°39′50.7″;006°30′49.8″. Also indicated in Figure 1 are the four individual points along a linear stretch of the frontage earmarked for survey (alas, the plotted solid red triangles for the frontage-traverse are slightly skewed laterally in the northeasterly direction).


***Figure 1****. Satellite imagery map showing the under-construction and partially built-up Lawu Estate, with the core study area appropriately demarcated by solid red triangles*

According to Obaje (2009), the geology of Nigeria comprises three major litho-petrological components: the *Basement Complex*, *Younger Granites*, and *Sedimentary Basins*. The Basement Complex, which is Precambrian in age, comprises the Migmatite-Gneiss Complex, the Schist Belts, and the *Older Granites.* The Younger Granites comprise several Jurassic magmatic ring complexes centered on Jos and other parts of north-central Nigeria. They are structurally and

petrologically distinct from the Older Granites. The Sedimentary Basins, containing sediment fill of Cretaceous to Tertiary ages, comprise the Niger Delta, the Anambra Basin, the Lower, Middle, and Upper Benue Trough, the Chad Basin, the Sokoto Basin, the Mid-Niger (Bida-Nupe) Basin, and the Dahomey Basin.

The Basement Complex forms a part of the Pan-African mobile belt and lies between the West African and Congo Cratons and south of the Tuareg Shield (Black, 1980). It is intruded by the Mesozoic calc-alkaline ring complexes (Younger Granites) of the Jos Plateau and is unconformably overlain by Cretaceous and younger sediments.

The Nigerian basement was affected by the 600 Ma Pan-African orogeny, and it occupies the reactivated region which resulted from plate collision between the passive continental margin of the West African Craton and the active Pharusian continental margin (Burke and Dewey, 1972; Dada, 2006). The basement rocks are believed to result from at least four major orogenic cycles of deformation, metamorphism, and remobilization, corresponding to the Liberian (2,700 Ma), Eburnean (2,000 Ma), Kibaran (1,100 Ma), and Pan-African (600 Ma) cycles. The first three cycles were characterized by intense deformation and isoclinal folding, accompanied by regional metamorphism, followed by extensive migmatization.

The Pan-African deformation was accompanied by regional metamorphism, migmatization, and extensive granitization and gneissification, which produced syntectonic granites and homogeneous gneisses (Abaa, 1983). Late tectonic emplacement of granites and granodiorites, along with associated contact metamorphism, accompanied the end stages of this last deformation. The end of the orogeny was marked by faulting and fracturing (Gandu *et al*., 1986; Olayinka, 1992).

Jonah *et al.* (2013) were tasked with locating an aquifer at a lot on the Dan Zaria Academic Estate, opposite the Gidan Kwano Campus of the Federal University of Technology, Minna. The team members adopted a different approach from the conventional to conduct reconnaissance for the planned survey at this estate; a resistivity geoelectrical survey in the VES mode of the Schlumberger array was employed for the reconnaissance and final stages of this investigation. This “unconventional” approach was the acquisition of VES data at shallow depths (i.e. progressively down to 10m) over the area of study in order to determine the point of lowest resistivity, instead of the approach to determine the lateral variation of resistivity at these shallow depths using the constant separation traversing (CST) method. The point of lowest resistivity thus identified was surveyed to a final depth of 100m. The authors observed that the 30-40m depth interval at this point was the possible groundwater yield zone.

In fidelity to the “conventional” approach, Jonah *et al.* (2014[a]) prospected for an aquifer at a lot located on a granitic knoll in Minna. At the outset, the client’s property was visually reconnoitered; the extent and preferred traverse directions were noted. The survey crew proposed a north-south (i.e., longitudinal traverse, LT) profiling scheme with 10 m separation between survey stations and 10 m separation between profile lines for the constant-separation traversing reconnaissance phase to a depth of 15 m. Thence, detailed vertical electrical sounding surveys were conducted for locations of “low-ohmic interest” to a depth of 100 m. The result of the reconnaissance phase indicated the lowest resistance value of 1.6348 Ω at “LT4-1.” Upon final VES surveys, it was concluded that the prospect of aquifers of good yield in the area of study was very poor indeed; this conclusion corroborated the one drawn from the initial survey that the crew was unaware of.

A third approach in the series of surveys undertaken by Jonah *et al.* (2014[b]) was the “No CST” format, informally described as “not carrying out any reconnaissance survey in order to determine the lateral variation of resistivity.” For this field technique, a VES survey to a depth of 100 m is carried out at each selected location. The survey crew adopted this method to prospect for the suitable location for a desired borehole at a built-up compound of an enclosed bungalow with a self-contained sewage system; only the three corners of the brick fence away from the corner where the cesspool was situated defined in one north-south (longitudinal traverse, LT) and two east-west (transverse traverse, TT) modes were suitable for this survey. Since the client requested that a borehole be drilled on her property, the survey crew considered it inexpedient to conduct a CST survey; hence, the “No CST” format.

The derived continuous variation of resistivity with depth model indicated that a four-layer sequence was identified for VES TT1, a four-layer sequence for VES LT1, and a three-layer sequence for VES TT2. The authors based their interpretation of the aquifer prospect at the three VES locations on a combination of informal, but fairly successful, empirical rules to determine the

likely presence of groundwater in the basement complex geological province. Based on these rules, TT1 indicates the best prospect for groundwater yield in the area of survey with good showings from the 30m-depth mark down to the 50 m-depth; LT1 could be discounted in water yield terms with respect to TT1, and TT2 satisfies the criteria at the 20m-depth mark and discontinuously still, at the 50 m-depth mark before a spike in "ohmic" values. Also, it was observed that the 50 m depth mark for TT1 and TT2 correlates very well with a prospective aquifer zone. If drilling must be done at all, then it was recommended that point TT1 be considered a good prospect for groundwater yield over the 20-m "yield window." Because of the smoothly changing continuum of resistivity values down to the 100 m-depth mark, it was recommended that drilling should be terminated at this maximum or total depth (TD) of survey in order to tap into the fractured basement at this TD. Incidentally, TT1 was upslope of the sewer pit, which was a plus for this VES station over the possible prospect of TT2.

In order to carry out a geoelectrical investigation for groundwater development at a wetland lot at the Bosso Estate, Minna, Nigeria, this location being some 350 m south of Lawu Estate, Jonah *et al.* (2014[c]) started off by visually reconnoitering the target objective (i.e. client's property); the extent, local geology, and preferred traverse directions of the area of survey were noted. The survey crew proposed a southwest-southeast profile as the longitudinal traverse (LT), with 10 m separation between survey stations and 10 m between profile lines, for the initial low-resistance reconnaissance scheme to a depth of 15m.

Thence, a detailed vertical electrical sounding (VES) survey was conducted for locations of "low-ohmic interest" to a depth of 70 m. In essence, the team treated this exercise as a blind geoelectrical prospecting, since the client had exclusive access to the results of an earlier, independent survey conducted for an aquifer prospect at this lot. On-the-field inspection of the CST dataset revealed that the lowest resistance value of 2.1919 Ω was obtained at "LT3-5" corresponding to the following geographic coordinate: $09^{0}39'15.8"$, $006^{0}30'46.6"$; an arbitrary field benchmark of <3 Ω was selected for this fieldwork. The survey crew based their interpretation of the aquifer prospect at the VES locations on an informal, but fairly successful, empirical rule to determine the likely presence of groundwater in the basement complex geological province. Based on this standardization, the survey crew observed that the prospect for groundwater yield is encouraging at location "LT3-5." This location is actually approximately 5-6m displaced from the position of the initial survey carried out 2 years earlier, as verified by the client. The survey party recommended sinking a borehole to a depth of 50 m at this location.

In the desire to explore approaches that are not generally conventional, but ones that have a good foundational basis, Jonah *et al.* (2015) conducted a wet-season geoelectrical investigation for groundwater development at a built-up property at the Western Bypass, Minna, Nigeria, this location being *circa* 200 m away due southwest along the Western Bypass from Lawu Estate. The client had already commissioned a dry-season spell survey at the same built-up property, but the result was not known to the present survey crew beforehand. The result of the present endeavour would be essentially corroborative. The vertical electrical sounding (VES) mode of the resistivity-type geoelectrical survey employing the Schlumberger array was the preferred format for this exercise. The survey schedule called for VES to a total depth of 100 m, where possible. However, that depth was well beyond the effective water-bearing subsurface environment and into the local bedrock proper.

Nonetheless, the built-up nature of the neighbourhood around the survey locations precluded the 100 m target. In interpreting possible groundwater locations, two constraints are used: the "ideal" log-log plot and the "Olasehinde Protocol." Such a log-log plot must have almost all plotted points alternately "rising-and-falling" along the curve, and the Olasehinde Protocol states that resistivity values between 180 Ωm and 250 Ωm at the 20 m to 25 m depth mark is indicative of a possible groundwater prospect. Only the third and last survey location approximated these impositions at the 20 m–30 m depth range, with a smoothly varying resistivity profile extending to 40 m, and its corresponding plot indicated a three-layer sequence. Based on the imposed constraints, the survey crew concluded that the location at 09°39′36.2″ N and 006°30′30.2″ E was the best prospect identified in this survey. If drilling must be done at all, the survey crew recommended drilling this location to a total depth (TD) of 50 m.

According to Yaman *et al.* (2020), the Minna Area is mainly underlain by rocks of the Basement Complex. The authors observed that the main lithological unit underlying the area is granites (over 90%), which virtually cover the entire map, whilst the other lithological unit is

schist, which occurs in the southeastern part of the area. The cross-section indicates a terrain that is not very rugged, but gentle, with schists forming the higher elevations. The elevation ranges from 240 m to 300 m, with the highest point near the Police Secondary School. The authors remarked that the granites are the youngest of the two rock types.

Ibeneme *et al.* (2014) remark that the different aquifer units within the Lower Orashi River Sub-Basin, Southeastern Nigeria, were delineated using the Vertical Electrical Sounding (VES) technique. The authors observe that twenty-two (22) VES soundings were carried out using the ABEM SAS 4000 Terrameter. The generated data were analyzed using the Zohdy software, which produced modeled curves for depth and resistivity. According to the authors, six profiles were collected in the northeast–southwest and northwest–southeast directions to cover the entire study area. Four to six geoelectric layers comprising the top soil, clayey sand, dry sandstone, saturated sandstone, shaley sand, and sandy shale were delineated, with the latter usually occurring as the last layer. The third and fourth layers underlying dry sandstone form the aquiferous unit. This unit was found to have an average resistivity of 10.7–6060 Ωm and an average thickness of 32 m. It was observed that most of the aquifer units in the area are unconfined, with static water levels ranging from 10.6 to 62.8 m. Some aquifer units are shallow, with static water levels below 40 m, while others are deeper, with static water levels above 60 m. It was advised that care should be taken when drilling and casing in shallow aquiferous areas to maintain proper sanitary conditions and reduce the risk of groundwater contamination.

Bahri *et al.* (2016) note that they endeavored to evaluate the quality of groundwater and the associated pollution of aquifers at Sukolilo, Surabaya, East Java, Indonesia. They pointed out that the vertical electrical sounding procedure is a geoelectric method for measuring rock resistivity, and the associated instrumentation is used to obtain subsurface information on aquifer depth. The authors used a water-quality tester to measure pH, conductivity, salinity, oxidation-reduction potential, and total dissolved solids. The authors reported that the prevailing aquifer thickness in the study area is in the region of 3.17 m, with a depth range of 0.45 m to 3.62 m. They also noted that the local lithology is alluvial and changes toward the north, as indicated by the varying depths of the observed rock layers. The authors note that seawater has intruded into the groundwater in the Sukolilo area, a finding corroborated by high salinity and total dissolved solids readings. Thus, the authors concluded that water from the unconfined Sukolilo aquifer was polluted and unsuitable for consumption.

Asta and Prasetia (2020), in MATEC Web of Conferences 331, discussed the application of vertical electrical sounding with a resistivity meter powered by a boost converter to estimate groundwater potential in Karang Anyar, Tarakan City, Indonesia. The authors noted that the vertical electrical sounding method can be used to predict geological and hydrogeological conditions. The authors observed that, as a result of the investigation using a resistivity meter powered by a boost converter, their results indicated the presence of groundwater at depths of 7.91m to 44.33 m, with a characteristic resistance of 27.22 Ωm, consistent with an estimated lithology of sand.

Pacheco *et al.* (2023) explained that, in recent years, the occurrence of unexpected meteorological events during the dry season and population growth have led to shortages in the city of Pampas, Peru, in the supply of drinking water. This situation prompted the authors to look for new search strategies for natural water sources, including underground sources. The authors observed that faced with this problem, the possibility of detecting and parameterizing these sources was raised, while the design of a tubular well that allows the economic extraction of water from the aquifer was also raised studied; both of these objectives were achieved through the use of geophysical techniques, generating profile images of geological maps of the strata and the location of the possible water table of the study area.

The authors noted that preferred locations for groundwater collection are alluvial fans and fractured valley bottoms. Using the Schlumberger array, eleven (11) vertical electrical soundings were completed up to a depth of 150 m. The acquired resistivity values range from 6.32 Ωm to 125.23 Ωm. The PQWTS-150-Water Detector equipment was also used to measure the depth of the semi-confined aquifer and to know its groundwater flow. The authors further noted that the geological map was described, and that in this profile, clayey, silty, sandy, and gravelly soils, and combinations of them, were found. Of particular interest, according to the authors, was VES Point 11, which was surveyed at the nursery of Daniel Hernández district, an area that is flat and humid. The authors noted that the aquifer at VES Point 11 has good hydrogeological conditions, enabling surface recharge. The water table was also determined to be between 4 m and 8 m.

Subsequently, the tubular well was designed. The authors concluded that the well was designed for a total depth of 115 m.

At the upmarket Lawu Estate in Minna, there is no luxury of conducting an unimpeded wide-area survey, as the Estate is built up almost in its entirety. Therefore, the constrained area required to be surveyed necessitated the adoption of the “electrical drilling,” or the vertical electrical sounding mode, of the geoelectrical method in order to make the inquiry requested by the client.

In general, the Bosso Estate-Lawu Estate-Western Bypass triangulate tranche of the larger Minna Area has not been an encouraging neighborhood for sustained large-scale groundwater exploitation from boreholes drilled into its near-surface, solid-rock substratum. Thus, as a result of lessons learnt from previous observations, a survey regime of the kind herein is more formally structured to gather relevant information from greater depths, which could be encouraging.

## 2. MATERIALS AND METHODS

### 2.1 Materials

#### *2.1.1 Hand-Held Global Positioning System (GPS) Unit*

The hand-held Garmin GPSmap78® global positioning system unit, shown in Figure 2, was employed to georeference the four corners of the lot to be surveyed, as well as the individual locations selected for occupation for the VES data acquisition scheme. The GPSmap78® is a high-sensitivity GPS with proprietary HotFix® coordinate-fixing software, featuring an in-built 3-axis compass and barometric altimeter. This GPS unit also features 1.7 GB of internal memory and up to 20 hours of battery life (dual AA batteries, that is).

.


***Figure 2**. Hand-held Garmin GPSmap78® global positioning system unit*

#### *2.1.2 Resistivity Meter*

The resistivity meter employed for the survey herein, the locally built Vineyard Geological Survey brand, is shown in Figure 3. This terrameter brand is based on the generic design of PIOS Hydrogeophysical Services (PHG), with its head office in Ilorin, Nigeria. The PIOS suite of locally-built geophysical equipment is managed by PHG, a company founded by the late Prof. P. I. Olasehinde. Thus, the locally built vineyard geological survey brand employs a highly durable multi-conductor field cable set with strong electrodes and provisions to measure current, I, and voltages V1 and V2 separately. Resistance, R, is thus calculated by dividing the potential difference $\Delta V$ by the observed current I. An in-built 12V Ni-Cd battery pack powers the equipment. It can also run from an external 12V DC source (e.g., a lead-acid car battery) via an external battery port. If fully charged, it can provide one working day of electrical soundings, provided it is turned off between soundings.

***Figure 3**. Resistivity meter employed for survey*

### 2.2 Methods

#### *2.2.1 Survey Design*

Owing to extensive build-up in the study area, only a four-point traverse along the 30-meter dimension of the building's frontage was demarcated in a northwesterly direction, thereby limiting the survey crew's ability to define an appropriate survey grid.

#### *2.2.2 Field Procedures*

At the outset, the survey crew reconnoitered the study area to georeference the locations to be occupied for the VES survey within the 30 m x 20 m lot. Unable to define a preferred grid pattern, the four-point traverse along the 30-

meter dimension of the building's frontage was duly identified by its latitude and longitude coordinates. Such a survey-design procedure has precedents from the works of Jonah *et al.* (2014[a]), Jonah *et al.* (2014[b]), and Jonah *et al.* (2015).

#### *2.2.3 Data Acquisition Parameters*

The VES data acquisition procedure adopted for this study, in the Schlumberger array mode, is the "electrical drilling" or "expanding probe" technique, used mainly to study horizontal or near-horizontal interfaces, which is the assumed geological character of the local basement region of the study area. The current and potential probes were maintained at the same relative spacing and the whole spread was progressively expanded about a fixed central point (Koefoed, 1979; Kearey and Brooks, 1984; Parasnis, 1986).

The initial potential electrode separation was 0.5 m whilst the initial current electrode separation was 1 m. The 0.5 m potential electrode separation was maintained for the next five measurement sequences, with the current electrode separation progressively increased by 1 m after each sequence. At the 6$^{th}$ meter current separation spread, the VES measurement was repeated as the potential probe distance was increased from 0.5 m to 1 m to ensure that these metallic probe-electrodes could detect a sufficiently measurable potential difference, $\Delta V$.

This format was repeated until a second repeated measurement for current electrode separation of 10 m was obtained, by which time the potential probe separation was increased to 2.5 m. Another repeat measurement was at a 40 m current electrode separation, by which time the potential probe separation had increased to 7.5 m. The final repeat measurement was at a current electrode separation of 80 m, by which time the potential probe separation had been increased to 15 m. The final measurement for a survey point was 100 m with the current electrode separation.

The accompanying tables during the measurement sequences at the four survey points record information regarding "AB/2" (that is, half current electrode separation), "MN/2" (that is, half potential electrode separation), geometrical factor for the Schlumberger array, the first and second potential readings and their computed differences, the amount of current sent into the ground for each measurement, the computed resistance and thence the resistivity values.

#### *2.2.4 Data Processing Method*

The conversion of each computed resistance value into its corresponding resistivity value is achieved by simply multiplying the resistance value by the corresponding geometrical factor.

## 3. RESULTS AND DISCUSSION

### 3.1 Results

#### *3.1.1 Generation of Log-Log Plots*

Usually, after determining the resistivity values from the field resistance values, it is desirable to generate curves, commonly log-log plots, showing the variation of resistivity values with the total depth surveyed at that particular sequence for each VES station. It is recognised that the effective depth of penetration is equal to half the current electrode spacing (i.e., AB/2, where AB separates the current electrodes). According to Zohdy (1989), a continuous variation of resistivity with depth curve can be easily derived from a multilayer step-function curve by drawing a curve that passes through the logarithmic midpoint of each vertical and horizontal line on the multilayer step-function model. Given that the layer depths are logarithmically spaced, the derived continuous variation of resistivity with depth model is equivalent to the original model. This approach makes it easy to construct maps of contoured resistivity values at different depths and to construct contoured geoelectric sections.

The field resistivity values were initially subjected to the log-log plot routine in the Windows-compatible WinResist® software, from which corresponding field curves for all occupied stations were produced. The initial outputs were the "default" graphs. These were further smoothed through layer-by-layer iterations, resulting in final "modelled" outputs. The smoothed graphs connect all the plotted points and are presented in Figures 4-7. The log-log plots of VES Stations 1, 2, 3, and 4, presented in Figures 4, 5, 6, and 7, have been conveniently (though erroneously) labelled as those of VES Stations 13, 14, 15, and 16, which do not exist in the archive. Each WinResist® log-log plot provides information on the number of layers, the average resistivity of each layer, the depth of each layer, and its approximate thickness.

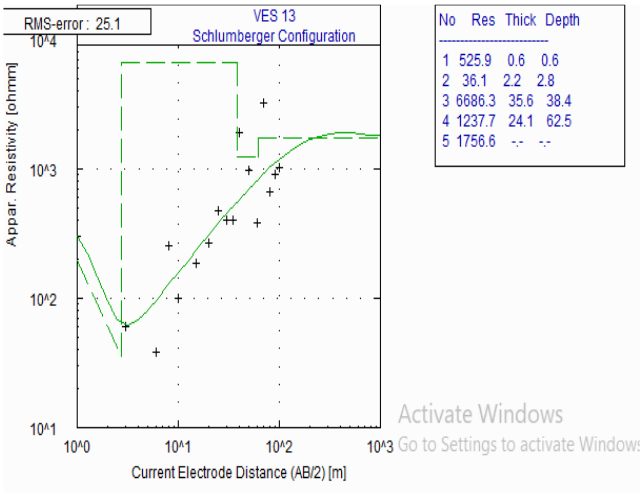


***Figure 4**. Log-log plot of Station 1*

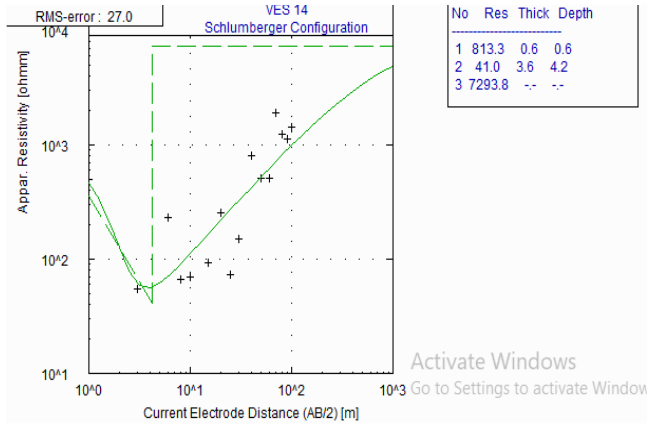


***Figure 5**. Log-log plot of Station 2*

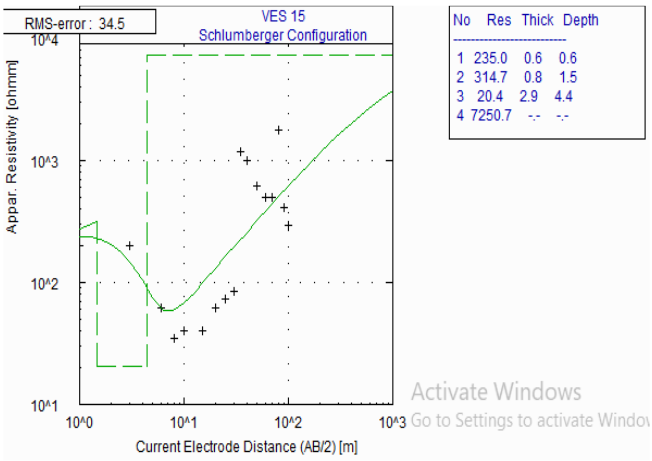


***Figure 6**. Log-log plot of Station 3*

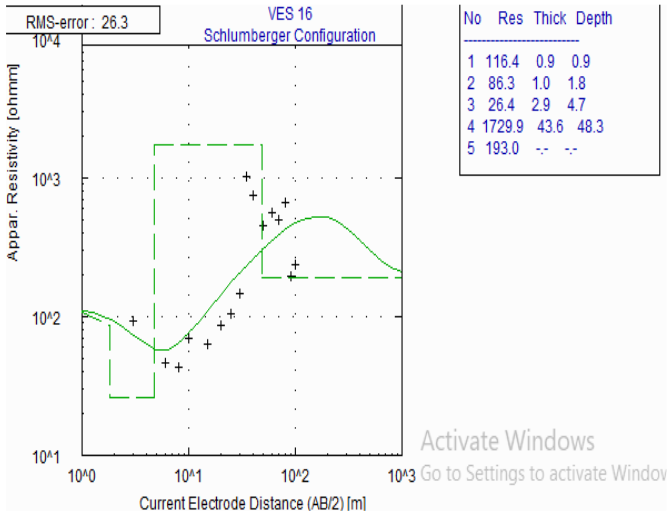


***Figure 7**. Log-log plot of Station 4*

### *3.1.2 Production of Pseudosection Plot*

To show the resistivity cross-section along the survey traverse line in the study area, a pseudosection plot was generated and is shown in Figure 8.

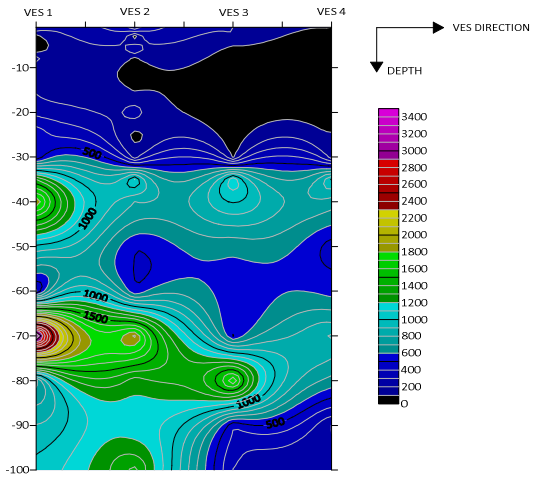


***Figure 8**. Pseudosection plot of study area*

## 3.2 Discussions

### *3.2.1 "Tricks" for Groundwater Search at the Nigerian Basement Complex*

For the Nigerian Basement Complex, empirical rules (as complements to the "traditional" interpretation sequences taught in schools) exist by which workers can reliably make deductions regarding the presence of sustainable groundwater at VES survey points along a line or across an area of study. Loke (2001) quoted Acworth (1981) as stating that, "the weathered layer is thicker in areas with fractures in the

bedrock." Jonah and Jimoh (2016) examined the validity of an empirical rule for delineating aquifer prospects at the Gidan Kwano Campus Development Phase II, Federal University of Technology, Minna, and this reliable route has been christened "Geoexplore Empirical Standardisation for Minna Area;" The Geoexplore Empirical Standardisation for Minna Area states that resistivity values between 200 Ωm and 300 Ωm at the 20 m depth and less than 200 Ωm at depths greater than 20 m are indicative of possible groundwater prospects. These recognised empirical rules, the veritable "tricks" for groundwater search in the Nigerian Basement Complex, are at the core of the rules-of-thumb employed to determine the location of groundwater in the first and fourth-stage interpretation instances, according to Jonah (2024).

#### *3.2.2 The Log-Log Plots*

The log-log plots indicate that, along the four stations of the traverse-line of survey, only one station is designated as a three-layer location, only one as a four-layer location, whilst two stations are designated as five-layer locations. According to Olasehinde (personal communication), the three-layer structure is the expected norm at the local basement geological province. Whereas, too, the norm is to have a comparatively high resistivity value for the third layer of a discerned three-layer geological structure in a general survey area of the local basement complex geological province, in ordinal format; this condition is satisfied for VES Station 2, albeit not in ordinal format. The mid-section layers of the inferred four-layer locations of Figure 6 corresponding to VES Station 3 could be "compressed" into a single layer in order to achieve fidelity to the three-layer specification at the local geological province. In a similar vein, the mid-section layers of the inferred five-layer locations of Figure 4 and Figure 7, corresponding to VES Station 1 and VES Station 4 could be "compressed" into a single layer.

#### 3.2.3 Fidelity to the Log-Log Plots of the First Rule-of-Thumb Schedule to Determine a Groundwater Location

The first rule-of-thumb is recognised herein to be the "traditional" or the "desired outcome" interpretation schedule whence the resistivity of the third layer in a three-layer geological sequence suddenly drops to the below-1000 Ωm values that indicates presence of fracture for where the prevailing resistivity values of the second layer in this sequence are greater than the 1000 Ωm values that correspond to those for fresh basement.

#### *3.2.4 Fidelity to the Log-Log Plots of the Second Rule-of-Thumb Schedule to Determine a Groundwater Location*

The second rule-of-thumb is recognised herein as the Acworth Protocol (1981), henceforth called the Acworth Protocol.

#### *3.2.5 Fidelity to the Log-Log Plots of the Third Rule-of-Thumb Schedule to Determine a Groundwater Location*

The third rule-of-thumb is recognised herein to be the Geoexplore Empirical Standardisation for the Minna Area.

#### *3.2.6 The Pseudosection Plot*

The pseudosection plot of the four-station traverse-line study area shows discernible three-resistivity layers, with a predominantly low-resistivity trend generally occurring at depths shallower than 30 m but also discernible at greater depths, especially at the fourth VES station. However, a low-resistivity zone of interest is present at depth beneath the first VES station. The next high-resistivity trend predominates across the traverse line from the 30 m depth downwards, whilst the highest-resistivity trend of unmistakable fresh basement character seems to "juts" from VES Station 1 at the 70 m to 80 m depth, seemingly terminating at VES Station 3.

## 4. CONCLUSIONS

### 4.1 The Log-Log Plots

#### *4.1.1 Fidelity to the Log-Log Plots of the First Rule-of-Thumb Schedule to Determine a Groundwater Location*

As per the constraint of the first rule-of-thumb schedule to determine a groundwater location, VES Station 1 is not in fidelity to the first rule-of-thumb schedule and it is therefore designated as not "hydro-centric." The term "hydro-centric" is used herein to indicate "water-bearing." Based on the same argument, VES Station 2 and VES Station 3 are also not "hydro-centric." However, VES Station 4 is tagged "hydro-centric" based on its conformity to the first rule-of-thumb schedule.

#### 4.1.2 Fidelity to the Log-Log Plots of the Second Rule-of-Thumb Schedule to Determine a Groundwater Location

With respect to the second rule-of-thumb schedule, VES Station 1, VES Station 2, and VES Station 3 are not "hydro-centric." VES Station 4 meets the "hydro-centric" classification under the

"relaxed" condition of assuming that a 4.7 m thickness regime of the assumed second layer is relatively "thick." Moreover, the "hydro-centric" nature and designation of VES Station 4 is assured from fidelity to the first rule-of-thumb schedule.

#### 4.1.3 Fidelity to the Log-Log Plots of the Third Rule-of-Thumb Schedule to Determine a Groundwater Location

VES Station 1, VES Station 2, and VES Station 3 are not "hydro-centric" under this scheme. VES Station 4 is tagged "hydro-centric" based on its conformity to the third rule-of-thumb schedule. VES Station 4 compliance with this schedule, by and large, occurs at the depth regimes of 20–30 m mark and at the greater depth of 90 m and beyond.

#### 4.1.4 Percentage Fidelity of VES Stations to the Three Rules-of-Thumb

Table 1 presents the percentage weights for the four stations based on their fidelity to the three rules of thumb.

***Table 1.*** *Percentage weighting with respect to fidelity to the three rules of thumb*

| VES Station | Percentage |
|---|---|
| Station 1 | 0% |
| Station 2 | 0% |
| Station 3 | 0% |
| Station 4 | 100% |

#### *4.1.5. Deductive Inference Regarding VES Stations*

Based on percentage fidelity to the three rules-of-thumb, VES Station 1, VES Station 2, and VES Station 3 are not groundwater locations.. However, VES Station 4 is an "assured" groundwater location or a "strongly aquiferous" location, "aquiferous" being a term coined by S.A. Jonah to indicate association with the likelihood of an aquifer in the subsurface.

### 4.2. The Pseudosection Plot

The pseudosection plot validates the "assured" groundwater and "strongly aquiferous" location inferences for VES Station 4. The reason for not designating VES Stations 1, 2, and 3 as "aquiferous" locations is obvious from the pseudosection plot. A 75% "fail" margin for this survey does not come across as a surprise because of the location of the traverse line of the survey in an area of prominent and profuse granitic outcrop showings. In spite of the high 75% "fail" margin for this survey, VES Station 4 "checks off" all the constraints of the groundwater-determination rules-of-thumb for 100% assurance. Thus, it is strongly recommended that VES Station 4 be used in the client's planned drilling programme. Drilling to a depth of 100 m at Station 4 is recommended based on the identified fractured basement at this depth.

## 5. DECLARATIONS

### 5.1. Study Limitations

This study presents several limitations that should be considered when interpreting the results. The extensive build-up at the surveyed lot severely constrained the survey design, limiting data acquisition to only four VES stations along a single traverse direction (northeasterly) at the building frontage. This constraint prevented the establishment of an appropriate two-dimensional survey grid that would have enabled more comprehensive lateral mapping of subsurface resistivity variations across the entire 30 m × 20 m lot. The absence of perpendicular or oblique traverses limits the three-dimensional understanding of subsurface geological structures and the potential extent of aquifers.

The study relied exclusively on the VES geoelectrical method without complementary geophysical techniques such as seismic refraction, ground-penetrating radar, or electromagnetic surveys. Multi-method approaches typically provide more robust subsurface characterization and reduce interpretation ambiguities inherent in single-method investigations. Additionally, the interpretation of VES data was based primarily on empirical rules-of-thumb developed for the Nigerian Basement Complex geological province, which, while proven useful, may not capture site-specific geological complexities at this upslope rocky knoll location.

The investigation depth was limited to 100 meters, which may not fully characterize deeper aquifer systems if present. Furthermore, no borehole drilling or pumping tests were conducted to validate the geophysical interpretations, verify the presence and productivity of the identified fractured basement aquifer at VES Station 4, or determine actual groundwater quality and sustainable yield rates. The study also did not include hydrochemical analysis, seasonal water

level monitoring, or assessment of recharge mechanisms, all of which are essential for comprehensive groundwater resource evaluation and sustainable exploitation planning.


### 5.2. Acknowledgements

The authors express their sincere gratitude to the Federal University of Technology, Minna, for providing the institutional support and research facilities that made this study possible.

The authors also acknowledge support from the University's research infrastructure, especially library resources, which were essential for data analysis and manuscript preparation.

### 5.3. Funding Source

This research was conducted with personal funding from the authors, without securing any external grants or institutional research funding. The authors acknowledge that the research team's personal resources covered all fieldwork expenses, laboratory analyses, and equipment use.

The authors confirm that no commercial interests, external funding bodies, or third-party organizations influenced the design, execution, or interpretation of this research. This independence ensures that all findings and conclusions presented herein reflect solely the scientific evidence gathered and analyzed by the research team, maintaining complete integrity in the research process and data interpretation.

In accordance with the ethical guidelines of the Southern Journal of Sciences, which do not allow donations from authors with manuscripts under evaluation (even when research funds are available), or in cases of authors' financial constraints, publication costs were fully absorbed by the journal under our Platinum Open Access policy, through the support of the Araucária Scientific Association (https://acaria.org/). This policy aims to ensure complete independence between the editorial process and any financial aspects, reinforcing our commitment to scientific integrity and equity in knowledge dissemination.

### 5.4. Competing Interests

The authors declare that there exists no conflict of interest whatsoever arising from the preparation of this manuscript for publication with any other competing interests, whether they be of the authors' or of second parties and third parties thereof. The data employed in the enunciation of the textual material herein are original, having been duly acquired by the authors as part of the annual undergraduate schedule of project supervision here at the Federal University of Technology, Minna, Nigeria. This body of data field, duly archived for validation and reference purposes, is available for integrity checks anytime.




### 5.6. Author Contributions

S.A.J. conceived the study design, supervised fieldwork, and wrote the manuscript. O.A. and S.G.A. conducted VES measurements and data collection. F.O.O. and V.C.O. assisted with field surveys and GPS measurements. J.A.A. and M.A. contributed to data processing and analysis. E.E.E. assisted with equipment setup and calibration. S.S. provided geographical expertise and site reconnaissance. All authors contributed to the manuscript review and approved the final version.

## 6. HUMAN AND ANIMAL-RELATED STUDIES

### 6.1. Ethical Approval

Not applicable.

### 6.2. Informed Consent

Not applicable.

## 7. REFERENCES:


1. Abaa, S.I. (1983). The structure and petrography of alkaline rocks of the Mada Younger Granite Complex, Nigeria. Journal of African Earth Science, 3,107–

113.
2. Acworth, R.I. (1981). The Evaluation of Groundwater Resources in the Crystalline Basement of Northern Nigeria, PhD Thesis, Univ. of Birmingham.
3. Asta*, & Prasetia, A.M. (2020). Application of vertical electrical sounding (VES) method with resistivity meter based on boost converter to estimate the potential of groundwater aquifers in Karang Anyar of Tarakan City. MATEC Web of Conferences 331, https://doi.org/10.1051/matecconf/202033106001. (*Single-named Indonesian author.)
4. Bahri, F.A., Rismayanti, H.F., & Warnana, D.D. (2016). Groundwater analysis using vertical electrical sounding and water quality tester in Sukolilo Area, Surabaya, East Java: Significant information for groundwater resources. Second International Seminar on Science and Technology, Postgraduate Program, Institut Teknologi Sepuluh Nopember ("the Tenth of November Institute of Technology"), Surabaya, Indonesia.
5. Black, R. (1980). Precambrian of West Africa. Episodes, 4, 3-8.
6. Burke, K.C., & Dewey, J.F. (1972). Orogeny in Africa. In Dessauvagie, T.F.J., & Whiteman, A.J. (editors), Africa Geology. University of Ibadan Press, Ibadan, pp 583-608.
7. Dada, S.S. (2006). Proterozoic evolution of Nigeria. In Oshi, O. (editor), The Basement Complex of Nigeria and its Mineral Resources (A Tribute to Prof. M. A. O. Rahaman), Akin Jinad & Co., Ibadan, pp 29-44.
8. Gandu, A.H., Ojo, S.B., & Ajakaiye, D.E. (1986). A gravity study of the Precambrian rocks in the Malumfashi area of Kaduna State, Nigeria. Tectonophysics, 126, 181–194.
9. Ibeneme, S.I., Okereke C.N., Iroegbu C., & Etiefe E.O. (2014). Vertical electrical sounding for aquifer characterization around the Lower Orashi River Sub-Basin, Southeastern Nigeria. Communications in Applied Sciences, 2(1), 36–51.
10. Jonah, S.A. (2024). Dual Geoelectrical Survey Regime to Profile Groundwater Occurrence at an East-Central Tranche of the Gidan Kwano Campus, Minna, Nigeria, Unpublished Synopsis for PhD Thesis, Federal University of Technology, Minna, Nigeria.
11. Jonah, S.A., & Jimoh, M.O. (2016). Validity of an empirical rule for delineating aquifer prospects at the Gidan Kwano Campus Development Phase II, Federal University of Technology, Minna, Northcentral Nigeria. Journal of Science, Technology, Mathematics, and Education (JOSTMED), 12(2), 18-24.
12. Jonah, S.A., James, G.O., Adeku, D.E., Ahmed, F., Alhassan, A., Hamza, S., ...Umoh, U.E. (2013). A survey for groundwater at a lot at the Dan Zaria Academic Estate, Federal University of Technology, Minna, Central Nigeria. Journal of Science, Technology, Mathematics, and Education, 9(3), 26–38.
13. Jonah, S.A., James, G.O., Adeku, D.E., Ahmed, F., Alhassan, A., Hamza, S., ...Umoh, U.E. (2014[b]). Pre-drilling geoelectrical survey at a built-up compound at Barkin-Sale Ward, Minna, Niger State, Nigeria. Journal of Information, Education, Science, and Technology, 1(2), 86–97.
14. Jonah, S.A., Jimoh, M.O., & Umar, M. (2015). A wet-season geoelectrical investigation for groundwater development at a built-up property at the Western Bye-Pass, Minna, Nigeria. Journal of Science, Technology, Mathematics, and Education, 11(1), 109-117.
15. Jonah, S.A., Umoh, S.E., James, G.O., Adeku, D.E., Ahmed, F., Alhassan, A., ... Umoh, U.E. (2014[a]). A blind geoelectrical survey commissioned to affirm or deny the presence of aquifer at a compound at Minna, Central Nigeria. Journal of Information, Education, Science, and Technology, 1(2), 20–38.
16. Jonah, S.A., Umoh, S.E., James, G.O., Adeku, D.E., Ahmed, F., Alhassan, A., ... Umoh, U.E. (2014[c]). A wetland lot geoelectrical investigation for groundwater development at Bosso Estate, Minna, Central Nigeria. Journal of Information, Education, Science, and Technology, 1(2), 158 –171.
17. Kearey, P., & Brooks, M. (1984). An Introduction to Geophysical Exploration, Blackwell Scientific Publications, Oxford.
18. Koefoed, O. (1979). Geosounding Principles 1: Resistivity Sounding Measurements, Elsevier Science Publishing Company, Amsterdam.
19. Loke, M.H. (2001). Tutorial: 2-D and 3-D Electrical Imaging Surveys, Google search, 8th August 2018, 11:08 a.m.

20. Obaje, N.G. (2009). Geology and mineral resources of Nigeria. In Lecture Notes in Earth Sciences. Springer-Verlag, Berlin.
21. Olayinka, A.I. (1992). Geophysical siting of boreholes in crystalline basement areas of Africa. Journal of African Earth Science, 14,197–207.
22. Pacheco, M. del P.C., Flores, J.A.C., Salvador, D.J.J., & Capcha, T.M. (2023). Vertical electrical sounding method to detect groundwater and design of a tubular well for the Pampas District, Peru. Civil Engineering and Architecture, 11(4), 1984-2006. DOI: 10.13189/cea.2023.110423.
23. Parasnis, D.S. (1986). Principles of Applied Geophysics (4th Edition), Chapman and Hall, London.
24. Yaman, A., Idris-Nda, A., Goro, A.I., and Ejepu, J.S. (2020). The geology and hydrogeology of parts of Minna Sheet 164 NE. Minna Journal of Geosciences, 4(2), 96-107.
25. Zohdy, A.A.R. (1989). A new method for the automatic interpretation of Schlumberger and Wenner sounding curves. Geophysics, 54(2), 245-253.

SOUTHERN JOURNAL OF SCIENCES

*ESTABLISHED IN 1993*

*Original research paper*

# HIGH BURDEN OF VITAMIN D DEFICIENCY AND FERRITIN-LINKED IMPACT IN B-THALASSEMIA MAJOR

SHARBA, Intisar R.[1]*; ABDULRAHMAN, Baneen Ali[2]; SARHAN, Dhamya Kadhim[3]

[1]University of Kufa, Faculty of Science, Department of Biology, Iraq. ORCID: 0000-0002-8251-5133

[2]Jabir Ibn Hayyan University for Medical and Pharmaceutical Sciences, Faculty of Pharmacy, Pharmacology and Toxicology Department, Iraq. ORCID: 0009-0006-7979-8271

[3]University of Kufa, Faculty of Science, Department of Biology, Iraq. ORCID: 0009-0008-7768-0119

*Corresponding author: intisar.sharba@uokufa.edu.iq

Received 29 October 2025; received in revised form 05 December 2025; accepted 12 December 2025

## ABSTRACT

**Background:** Background: Vitamin D plays an essential role in bone health and overall physiological function, and its deficiency is common in children and adolescents with β-thalassemia major (βTM). Iron overload, as reflected by elevated ferritin, may further influence vitamin D status. **Aim**: This study aimed to evaluate serum vitamin D levels in βTM patients and determine their association with ferritin levels. **Methods**: A total of 40 βTM patients and 20 age-matched healthy controls (aged 4–25 years) were enrolled between October 2024 and February 2025. Serum vitamin D, calcium, ferritin, and hemoglobin were measured. Statistical analysis, including correlation and logistic regression, was performed using SPSS v.26 to identify predictors of vitamin D deficiency. **Results**: Vitamin D deficiency was highly prevalent among βTM patients (70%) compared with controls. Patients showed significantly lower vitamin D levels (17.32±1.56) than controls (25.34±1.76). Vitamin D levels were positively correlated with age ($r = 0.788$), calcium ($r = 0.772$), and hemoglobin ($r = 0.771$), and negatively correlated with ferritin ($r = –0.517$). Logistic regression demonstrated that ferritin >1000 ng/mL strongly predicted vitamin D deficiency (OR = 17.875; 95% CI: 3.258–98.074; $p = 0.001$), while younger age ( < 10 years) also increased the odds of deficiency (OR = 5.200; $p = 0.018$). **Discussion**: D deficiency is a prevalent and intrinsic metabolic disturbance in β-thalassemia major, closely linked to chronic iron overload and elevated ferritin levels. This interplay disrupts hepatic vitamin D hydroxylation, induces inflammation, and contributes to endocrine and skeletal complications, highlighting ferritin as a key predictor of deficiency in these patients. **Conclusion**: Vitamin D deficiency is highly prevalent in βTM and is strongly associated with elevated ferritin levels, suggesting that iron overload is a significant predictor. Integrating vitamin D assessment into routine monitoring may support better management of disease-related metabolic disturbances in patients with βTM.

**Keywords**:*Beta-thalassemia; Vitamin D deficiency; Serum ferritin; Iron overload; Ineffective erythropoiesis.*

## RESUMO

**Introdução**: A vitamina D desempenha papel essencial na saúde óssea e na função fisiológica geral, e sua deficiência é comum em crianças e adolescentes com β-talassemia maior (βTM). A sobrecarga de ferro, refletida pela ferritina elevada, pode influenciar ainda mais o status da vitamina D. **Objetivo**: Este estudo teve como objetivo avaliar os níveis séricos de vitamina D em pacientes com βTM e determinar sua associação com os níveis de ferritina. **Métodos**: Um total de 40 pacientes com βTM e 20 controles saudáveis pareados por idade (com idades entre 4 e 25 anos) foram incluídos entre outubro de 2024 e fevereiro de 2025. Foram medidos vitamina D sérica, cálcio, ferritina e hemoglobina. A análise estatística, incluindo correlação e regressão logística, foi realizada usando SPSS v.26 para identificar preditores de deficiência de vitamina D. **Resultados**: A deficiência de vitamina D foi altamente prevalente entre pacientes com βTM (70%) em comparação com controles. Os pacientes apresentaram níveis de vitamina D significativamente menores (17,32±1,56) do que os controles

 
DOI: 10.48141/2764-5959.04.v33.n40.2025_04_Sarhan_pgs_62_74.pdf

(25,34±1,76). Os níveis de vitamina D correlacionaram-se positivamente com idade (r = 0,788), cálcio (r = 0,772) e hemoglobina (r = 0,771), e negativamente com ferritina (r = −0,517). A regressão logística demonstrou que ferritina >1000 ng/mL predisse fortemente a deficiência de vitamina D (OR = 17,875; IC 95%: 3,258–98,074; p = 0,001), enquanto idade mais jovem (< 10 anos) também aumentou as chances de deficiência (OR = 5,200; p = 0,018). Discussão: A deficiência de vitamina D é um distúrbio metabólico prevalente e intrínseco na β-talassemia maior, intimamente ligado à sobrecarga crônica de ferro e aos níveis elevados de ferritina. Essa interação interrompe a hidroxilação hepática da vitamina D, induz inflamação e contribui para complicações endócrinas e esqueléticas, destacando a ferritina como um preditor-chave de deficiência nesses pacientes. **Conclusão**: A deficiência de vitamina D é altamente prevalente na βTM e está fortemente associada a níveis elevados de ferritina, sugerindo que a sobrecarga de ferro é um preditor significativo. Integrar a avaliação da vitamina D no monitoramento de rotina pode apoiar melhor manejo dos distúrbios metabólicos relacionados à doença em pacientes com βTM.

**Palavras-chave**: *Beta-talassemia; Deficiência de vitamina D; Ferritina sérica; Sobrecarga de ferro; Eritropoiese ineficaz.*

## 1. INTRODUCTION

Beta-thalassemia major is a severe hereditary blood disorder characterized by defective hemoglobin synthesis, leading to chronic anemia and a lifelong dependence on regular blood transfusions (Bin et al., 2025). While transfusion therapy has dramatically improved survival, it also results in progressive iron overload, which can cause multi-organ dysfunction, particularly affecting the heart, liver, and endocrine system (Pinto & Forni, 2020; Pala *et al.,* 2023). Among the most prevalent and clinically significant complications in these patients is vitamin D deficiency, which has been increasingly recognized as a major contributor to morbidity (Abdelmotaleb *et al.,* 2021; Akram *et al*., 2025).

Recent studies have demonstrated that vitamin D deficiency is highly prevalent in children and adults with beta-thalassemia major, with reported rates ranging from 63% to over 90% (Bin *et al*., 2025; Meshram *et al*., 2025). This deficiency is multifactorial, resulting from decreased cutaneous synthesis, impaired hepatic hydroxylation due to iron-induced liver dysfunction, and possible nutritional inadequacies (Abdelmotaleb *et al.,* 2021; Majid and Sharba, 2025). Iron overload, as measured by elevated serum ferritin and direct organ iron quantification, has been shown to correlate negatively with vitamin D levels, suggesting that iron toxicity may directly impair vitamin D metabolism (Pala *et al.,* 2023; Verma *et al.,* 2020; Meloni *et al*., 2023).

The clinical consequences of vitamin D deficiency in beta-thalassemia major are profound. Patients are at increased risk for bone disease, including osteopenia and osteoporosis, as well as endocrine complications such as hypoparathyroidism and growth retardation (Mohammed *et al*., 2022; Meshram *et al.,* 2025). Furthermore, recent evidence indicates that low vitamin D status is associated with increased cardiac iron uptake and impaired cardiac function, highlighting the importance of regular monitoring and supplementation (Pala *et al.,* 2023; Meloni *et al*., 2023). Given these findings, integrated management strategies that address both iron overload and vitamin D deficiency are essential to improve long-term outcomes in this vulnerable population.

This study aims to determine the prevalence of vitamin D deficiency and its association with ferritin levels in patients with beta-thalassemia. The findings are expected to elucidate shared pathological mechanisms and provide a scientific basis for more effective interventional strategies to prevent and treat bone complications in this patient population, which may ultimately improve their quality of life.

## 2. MATERIALS AND METHODS

### 2.1. Study Design and Participants

This case-control study was conducted between October 2024 and February 2025 and included 60 participants: 40 individuals with beta-thalassemia major (β-TM) and 20 age-matched healthy controls, all aged 4-25 years. Patients were recruited from the Hematology Diseases Center at Al-Zahraa Teaching Hospital in Al-Najaf, whereas controls were selected from healthy staff members of the Faculty of Science, University of Kufa. Written informed consent was obtained from adult participants and from parents or legal guardians of minors, with children's assent obtained when applicable. The study protocol was approved by the Institutional Review Board of the

University of Kufa, Faculty of Science, on September 5, 2024

### 2.2. Data Collection and Clinical Assessment

Clinical information for β-TM patients was collected through a structured questionnaire and a detailed review of medical records. Data included demographic characteristics (age, sex), disease-related variables (duration since diagnosis, age at first transfusion), current management plans (type and schedule of chelation therapy, transfusion frequency), and the presence of any systemic, metabolic, or immunological comorbidities.

### 2.3. Blood Sample Collection and Processing

Following an overnight fast of 8–12 hours, venous blood samples (approximately 3 mL) were drawn using standard aseptic procedures. Samples were divided into two tubes: a $K_2$EDTA tube (BD Vacutainer, USA) for hematological analysis and a serum-separator gel tube (BD Vacutainer, USA) for biochemical tests. Serum samples were allowed to clot for 15–20 minutes, centrifuged at 3000 × g for 10 minutes, then aliquoted into sterile microtubes and stored at –20 °C until batch analysis to minimize analytical variation.

## 2.4. Laboratory Assays

#### *2.4.1. Hematological and Biochemical Assay*

Hematological parameters were measured using an automated hematology analyzer (Abbott CELL-DYN Ruby, USA). Biochemical parameters were measured in serum using commercially supplied kits according to the manufacturers' protocols, with all measurements conducted in duplicate.

#### *2.4.2. 25-Hydroxyvitamin D (Vit. D)*

Serum 25(OH)D levels were determined using a competitive ELISA kit (Cat. No. E-EL-0012, MyBioSource, USA). Vitamin D status was classified according to widely accepted clinical cutoffs:

• Deficiency: < 20 ng/mL

• Insufficiency: 20–29 ng/mL

• Sufficiency: ≥30 ng/mL

This biomarker reflects total body vitamin D stores and is the standard indicator for assessing vitamin D status.

#### *2.4.3. Ferritin*

Serum ferritin concentration, used as a marker of iron stores and iron-overload status, was measured using a quantitative sandwich ELISA kit (Cat. No. MBS843444, MyBioSource, USA).

#### *2.4.4. Calcium*

Total serum calcium was quantified using a colorimetric assay (Cat. No. E-BC-K103-M, Elabscience, USA).

## 2.5. Statistical analysis

All data were analyzed using SPSS version 26. Comparisons between patients and control groups were performed using the Independent t-test for normally distributed variables or the Mann–Whitney U test for non-normally distributed variables. Comparisons among three groups were conducted using one-way ANOVA followed by Tukey's post hoc test. Nominal variables were presented as frequencies and percentages, and the Chi-square test was applied throughout the study. Pearson correlation coefficients were used for parametric variables and Spearman's rho for non-parametric variables. Binary logistic regression analysis was performed to evaluate the association between clinical variables and the outcome measures, and adjusted odds ratios (ORs) with 95% confidence intervals (CIs) were reported. Statistical significance was set at $p \leq 0.05$ and $p \leq 0.01$.

# 3. RESULTS AND DISCUSSION

### 3.1. Results

#### *3.1.1. Distribution of demographic parameters in βTM patients and control groups.*

The statistical analysis in Table 1. Documented the distribution of studied groups, which included 40 patients with beta-thalassemia major βMT whose mean age was about 10.78 (1.12), was compared with 20 healthy controls who matched in age 11.05 (1.23), non-significant ($p = 0.880$). No significant difference ($p = 0.850$) was observed between the two age groups of patients (62.5% age < 10 years and 37.5% age >10 years), compared with 65.0% and 35% in the age < 10 and >10 years, respectively, in the control groups. The distribution of sex in patients was males 52.5% and females 47.5%, compared with females/males 45.0%/55.0 % in the control group, with no significant difference between the two groups ($p = 0.584$). A significant difference in βTM thalassemia with vitamin D deficiency 70.0%, and insufficient 12.5% more than in patients with vitamin D sufficient 17.5% when compared with deficient, insufficient, and sufficient vitamin D 30.0%, 40.0%, and 30.0% in the control groups, $p = 0.009$. According to anemia status, the results showed that βTM with severe and moderate

anemia was about 35.0% and 37.5%, respectively, the highest among patients with mild anemia at 20.0% and nonanemic (normal) at 7.5%, compared with mild 15% and normal 50% in the control groups, respectively, p = 0.0001. In the βTM thalassemia group, 32 individuals (80.0%) had ferritin levels >1000 ng/dL, while only 8 (20.0%) were ≤1000 ng/dL. In contrast, all controls (20 individuals, 100.0%) fell within the ≤1000 ng/dL category, and none had elevated ferritin. This distribution yielded a highly significant association ($\chi^2$ = 34.286, p = 0.0001),

### *3.1.2. Comparison of studied parameters in the βTM patients with control groups.*

The results are in Table 2. Indicated a significant (p < 0.05) decrease in the serum vitamin D levels in the βTM patients, with a mean (SE) of 17.32 (1.56), as compared with the control groups 25.34 (1.76), p = 0.002, Figure 1. Serum Ca levels are significantly lower in the βTM patients (mean (SE) 6.97 (0.26)) compared with the control groups (9.01 (0.14), p = 0.0001, Figure 2. Highly significant elevated serum ferritin levels in the βTM patients as compared with the control group mean (SE) about (2080.76 (194.63) vs. 56.54 (5.08), p = 0.0001), figure 3. In similar results, the βTM patients had a significant (p < 0.05) decrease in Hb levels when compared with the control group mean (SE) about (9.21 (0.30) VS. 11.39 (0.27), P = 0.001)—Figure 4.

### *3.1.3 Comparison of studied parameters among vitamin D status in β-thalassemia major patients (βTM)*

The statistical analysis is in Table 3. Show βTM patients divided into three groups according to vitamin D classification, which includes 7 patients with vitamin D Sufficient, with a mean (SE) of 35.27 (1.41), Insufficient (n = 5) with a mean (SE) of 23.82 (1.38), and 28 patients with Deficient 11.68 (0.64) ng/ml, these results showed significant differences p = 0.0001. Serum Ca levels in βTM patients indicated a significant (p < 0.05) decrease in patients with vitamin D Deficiency (6.36 (0.29)), compared with Insufficient (8.2 (0.35)) and Sufficient (8.54 (0.19)), p = 0.006. Figure 5. Highly significant increase in serum ferritin levels in patients with vitamin D deficiency, with a mean (SE) of 2365.1 (237.96), more than in patients with Insufficient 1529.11 (433.96), as compared with Sufficient patients' mean (SE) of 1260.77 (175.97), p = 0.003. Figure 6. Hb levels in βTM patients showed a significant (p < 0.05) decrease in patients with vitamin D Deficiency (8.59 (0.3) g/dl), compared with Insufficient (9.08 (0.69)) and Sufficient (11.78 (0.25)), p = 0.001. Figure 7. The β-thalassemia major group showed a significant association between ferritin status and vitamin D status, reflected by a Chi-square value of 14.464 and a p-value of 0.0001. Among those with ferritin >1000 ng/mL, 4 patients (80.0%) had insufficient vitamin D, 26 (92.9%) were vitamin D deficient, and 2 (28.6%) were sufficient. In contrast, within the ≤1000 ng/mL ferritin category, only 1 patient (20.0%) had insufficient vitamin D, 2 (7.1%) were deficient, while 5 (71.4%) were sufficient.

### *3.1.4.Correlation and logistic regression analysis of vitamin D with studied parameters in βTM patients.*

The correlation results are shown in Table 4. Vitamin D showed significant positive correlations with age (r = 0.788), Ca (r = 0.772), and Hb (r = 0.771), but a negative correlation with ferritin (r = -0.517). Also, ferritin was inversely associated with Ca (r = -0.610) and Hb (r = -0.597), while a positive correlation was observed between the two last parameters (r = 0.866).

The logistic regression analysis compared vitamin D status across the studied categories in Table 4. For age groups, using individuals older than 10 years as the reference, those younger than 10 years with insufficient vitamin D showed a coefficient of 0.624, corresponding to an odds ratio (OR) of 1.867 with a 95% confidence interval (CI) of 0.392–8.894 and a p-value of 0.433, while those with deficient vitamin D had a coefficient of 1.649, an OR of 5.200 (95% CI: 1.322–20.460), and a p-value of 0.018. For sex, with females as the reference, males with insufficient vitamin D had a coefficient of –0.341, an OR of 0.711 (95% CI: 0.140–3.606), and a p-value of 0.681, whereas males with deficient vitamin D had a coefficient of –1.291, an OR of 0.275 (95% CI: 0.070–1.078), and a p-value of 0.064. Regarding anemia status, taking none–mild anemia as the reference group, participants with moderate to severe anemia and insufficient vitamin D had a coefficient of -0.811, producing an OR of 0.444 (95% CI: 0.137–1.443) with a p-value of 0.0001. In contrast, the deficient vitamin D category showed a coefficient of 1.540 and OR of 4.667 (95% CI: 1.932-11.270), For ferritin status, with < 1000 ng/mL as the reference group, individuals with ferritin >1000 ng/mL and insufficient vitamin D had a coefficient of 0.894, an OR of 2.444 (95% CI: 0.361–16.547), and a p-value of 0.360, whereas those with deficient vitamin D showed a coefficient of 2.883, an OR of 17.875 (95% CI: 3.258–98.074), and a p-value of 0.001.

## 3.2. Discussions

The present study adds to a growing consensus that vitamin D deficiency is a pervasive and clinically significant metabolic disturbance in individuals with β-thalassemia major (β-TM). Our findings, considered alongside previous reports, indicate that this deficiency is an intrinsic aspect of the disease's pathophysiology, rather than a consequence of external factors alone, such as sunlight exposure or dietary intake (Abdelmotaleb *et al.,* 2021; Al-Rubae *et al.,* 2023; Rothchild *et al.,* 2023).

A central feature of β-TM is chronic iron overload, primarily resulting from repeated red blood cell transfusions and from augmented intestinal iron absorption driven by ineffective erythropoiesis (Almousawi & Sharba, 2019). Excess circulating iron is stored in parenchymal tissues, particularly the liver, which is the principal

site for 25-hydroxylation of vitamin D. Iron-mediated hepatocellular injury disrupts the activity of key cytochrome P450 enzymes responsible for converting vitamin D into 25-hydroxyvitamin D, thereby diminishing circulating levels of the biomarker most commonly used to assess vitamin D status (Hamayun *et al.,* 2017; Mogire *et al*., 2020). This pathophysiological mechanism provides a biologically plausible explanation for the inverse association observed between ferritin and vitamin D in our cohort and in other thalassemia populations.

Beyond hepatic conversion, iron overload induces oxidative stress and inflammatory signaling, altering vitamin D metabolism at multiple regulatory points. Elevated ferritin reflects not only iron stores but also a state of chronic inflammation. Inflammatory mediators can suppress the synthesis of vitamin D–D-binding protein, alter receptor expression, and interfere with downstream signaling pathways critical for endocrine function (Urmi *et al.,* 2022). These effects may also modulate parathyroid hormone (PTH) activity, contributing to the secondary endocrine dysregulation observed in thalassemia, as hypothesized in experimental and clinical studies (Saki *et al.,* 2020).

Our logistic regression analysis reinforces the centrality of ferritin in predicting vitamin D deficiency. Elevated ferritin emerged as one of the strongest independent predictors of deficient vitamin D status in multivariable modeling. This analytic outcome aligns with mechanistic insights, indicating that iron burden is more than a correlate of deficiency—it has predictive value in identifying patients at the highest risk of metabolic derangement. Age was also a significant predictor in the model, suggesting that developmental and maturational factors may interact with iron-related metabolic stress to influence vitamin D homeostasis. These statistical associations provide quantitative support for the clinically observed interplay between iron overload and vitamin D deficiency.

The consequences of this metabolic interaction extend to skeletal health. Vitamin D plays an indispensable role in calcium absorption, skeletal mineralization, and bone turnover regulation. When its activation is compromised by iron-induced hepatic dysfunction, calcium homeostasis becomes destabilized. Concurrent iron toxicity in bone marrow and trabecular structures further impairs osteoblastic activity and enhances resorption, fostering an environment conducive to osteoporosis, deformities, and increased fracture risk (Pala *et al.,* 2023; Baird *et al.,* 2022). This synergistic deterioration of bone integrity underscores why bone disease remains a leading cause of morbidity in β-TM despite advances in supportive care.

Moreover, ineffective erythropoiesis and suppressed hepcidin levels create a persistent drive for dietary iron absorption, compounding systemic iron loading even in the context of chelation therapy. Low hepcidin facilitates continuous iron uptake from the gut and mobilization from macrophage stores, further elevating serum ferritin and perpetuating its deleterious metabolic effects (Saad *et al.,* 2021; Cazzola, 2022). Such alterations in iron physiology have implications not only for vitamin D metabolism but also for endocrine axes, glucose regulation, and immune competence.

Taken together, the present findings support a model in which iron overload and vitamin D deficiency are interdependent components of a broader metabolic dysregulation in β-TM. Rather than functioning as isolated abnormalities, they represent convergent pathways that exacerbate skeletal and systemic complications characteristic of this disorder.

## 4. CONCLUSIONS

This study confirms that vitamin D deficiency and elevated ferritin are intertwined metabolic entities in β-thalassemia major, with elevated ferritin serving as a robust predictor of deficient vitamin D status. These findings reinforce the need to incorporate routine monitoring of both parameters into standard care. Vitamin D supplementation should be individualized and closely supervised, particularly in the context of iron-mediated liver dysfunction. In addition, optimizing iron chelation therapy remains essential to mitigate the broader metabolic consequences of iron overload. Longitudinal and interventional studies are required to determine whether correcting vitamin D deficiency can improve bone outcomes and quality of life in patients with β-TM.

## 5. DECLARATIONS

### 5.1. Study Limitations

Case–control studies on vitamin D deficiency and iron overload in β-thalassemia major often face several limitations. Small sample sizes reduce statistical power and generalizability. Matching of cases and controls is sometimes inadequate, especially for age, sex, or disease severity. Variability in laboratory methods and in definitions of deficiency complicates comparisons across studies. Many studies lack detailed clinical or biochemical data, such as parathyroid hormone levels or chelation therapy regimens, limiting mechanistic insights. The absence of long-term follow-up also prevents evaluation of disease progression and intervention outcomes.


### 5.2. Acknowledgements

The authors extend their sincere appreciation to all participants who contributed to this study, with particular gratitude to the patients with β-thalassemia for their cooperation and commitment. Deep thanks are also conveyed to the laboratory staff at the Center for Hematology and Thalassemia at Al-Zahraa Hospital for their dedicated technical support and their essential role in facilitating the laboratory procedures that enabled the completion of this research.

### 5.3. Funding source

The authors funded this research. In accordance with the ethical guidelines of the Southern Journal of Sciences, which do not allow donations from authors with manuscripts under evaluation (even when research funds are available), or in cases of authors' financial constraints, publication costs were fully absorbed by the journal under our Platinum Open Access policy, through the support of the Araucária Scientific Association (https://acaria.org/). This policy aims to ensure complete independence between the editorial process and any financial aspects, reinforcing our commitment to scientific integrity and equity in knowledge dissemination.


### 5.4. Competing Interests

The authors declare no conflict of interest. More information about

### 5.5. Open Access



## 6. HUMAN AND ANIMAL-RELATED STUDIES

### 6.1. Ethical Approval

The study protocol was reviewed and approved by the Institutional Review Board of the University of Kufa, Faculty of Science, on September 5, 2024. As the study used samples collected during patients' routine follow-up and pre-transfusion tests, which occur twice weekly, with no additional procedures performed on participants, informed consent was not required.

## 7. REFERENCES:


1. Abdelmotaleb, G. S., Behairy, O. G., El Azim, K. E. A., El-Hassib, D. M. A., & Hemeda, T. M. (2021). Assessment of serum vitamin D levels in Egyptian children with beta-thalassemia major. Egyptian Pediatric Association Gazette, 69, 1–7.
2. Akram, S., Ghafoor, T., Awan, S., Akram, A., Nawaz, R., & Rahman, A. (2025). Vitamin D status in children with thalassemia major. Pakistan Armed Forces Medical Journal, 75(1), 1–6.

3. Akter, R., Afrose, A., Sharmin, S., Rezwan, R., Rahman, M. R., & Neelotpol, S. (2022). A comprehensive look into the association of vitamin D levels and vitamin D receptor gene polymorphism with obesity in children. Biomedicine & Pharmacotherapy, 153, 113285.
4. Almousawi, A. S., & Sharba, I. R. (2019, September). Erythroferrone hormone, a novel biomarker, is associated with anemia and iron overload in beta thalassemia patients. In Journal of Physics: Conference Series (Vol. 1294, No. 6, p. 062045). IOP Publishing.
5. Al-Rubae, A. M., Ansaf, A. I., & Faraj, S. A. (2023). Evaluation of vitamin D level in thalassemia patients: The experience of a single center. Iraqi Journal of Hematology, 12(2), 141–145.
6. Baird, D. C., Batten, S. H., & Sparks, S. K. (2022). Alpha- and beta-thalassemia: Rapid evidence review. American Family Physician, 105(3), 272–280.
7. Bin, A., Batool, T., Ali, F., Khanzada, M., Kiran, Q., Khan, I. U. D., & Nasir, A. (2025). Evaluation of vitamin D, calcium, LFTs in beta thalassemia patients. Journal of Medical & Health Sciences Review, 9(2), 45–52.
8. Cazzola, M. (2022). Ineffective erythropoiesis and its treatment. Blood, 139(16), 2460–2470. https://doi.org/10.1182/blood.2021011045
9. Hussein, S. Z. (2022). Evaluation of thyroid hormones and ferritin level in patients with β-thalassemia. Medicine and Pharmacy Reports, 95(2), 152–157. https://doi.org/10.15386/mpr-2053
10. Majid, Z., & Sharba, I. R. (2025). Low serum vitamin D levels as a risk factor for peptic ulcer development in Iraqi patients. Pharmakeftiki, 37(2S).
11. Meloni, A., Pistoia, L., Vassalle, C., Spasiano, A., Fotzi, I., Bagnato, S., Putti, M., Cossu, A., Massei, F., Giovangrossi, P., Maffei, S., Positano, V., & Cademartiri, F. (2023). Low vitamin D levels are associated with increased cardiac iron uptake in beta-thalassemia major. Diagnostics, 13(12), 2101.
12. Meshram, R. M., Salodkar, M. A., Yesambare, S. R., Mohite, S. M., Gite, R. B., & Rathod, V. R. (2025). Clinical profile and vitamin D status in beta thalassemia major children at a tertiary care institute of Central India: A cross-sectional study. Nigerian Journal of Clinical Practice, 28(1), 1–7.
13. Mogire, R. M., Muriuki, J. M., Morovat, A., Mentzer, A. J., Webb, E. L., Kimita, W., … & Atkinson, S. H. (2022). Vitamin D deficiency and its association with iron deficiency in African children. Nutrients, 14(7), 1372.
14. Mohammed, M. R., Hamoode, R. H., & Al-Mahdawi, F. K. I. (2022). Hypoparathyroidism due to iron overload in beta-thalassemia patients. Biomedicine, 42(4), 1–8.
15. Rujeerapaiboon, N., Tantiworawit, A., Piriyakhuntorn, P., Rattanathammethee, T., Hantrakool, S., Chai-Adisaksopha, C., Rattarittamrong, E., Norasetthada, L., Fanhchaksai, K., & Charoenkwan, P. (2021). Correlation between serum ferritin and viral hepatitis in thalassemia patients. Hemoglobin, 45(3), 175–179.
16. Pala, M., Bhat, K. G., Manya, S., Joseph, N., & Harish, S. (2023). Vitamin D levels and left ventricular function in beta-thalassemia major with iron overload. European Journal of Pediatrics, 182(4), 1749–1754.
17. Pinto, V., & Forni, G. (2020). Management of iron overload in beta-thalassemia patients: Clinical practice update based on case series. International Journal of Molecular Sciences, 21(21), 1–18.
18. Qwader, M. R., Sherief, L. M., Sherif, A. A., & Baraka, A. M. (2021). Evaluation of osteopathy and vitamin D status in patients with beta-thalassemia major. Zagazig University Medical Journal, 27(5), 776–781.
19. Ribeil, J. A., Arlet, J. B., Dussiot, M., Moura, I. C., Courtois, G., & Hermine, O. (2013). Ineffective erythropoiesis in β-thalassemia. TheScientificWorldJournal, 2013, 394295. https://doi.org/10.1155/2013/394295
20. Rothschild, B. M., Surmik, D., & Bertozzo, F. (2023). Hematologic disease. In Modern Paleopathology, The Study of Diagnostic Approach to Ancient Diseases, their Pathology and Epidemiology: Let there be light, the light of science and critical thinking (pp. 405–416). Cham: Springer International Publishing.
21. Saad, H. K. M., Taib, W. R. W., Ismail, I., Johan, M. F., Al-Wajeeh, A. S., & Al-Jamal, H. A. N. (2021). Reduced hepcidin expression enhances iron overload in patients with HbE/β-thalassemia: A comparative cross-sectional study. Experimental and Therapeutic Medicine, 22(6), 1402. https://doi.org/10.3892/etm.2021.10838

22. Saki, F., Salehifar, A., Kassaee, S. R., & Omrani, G. R. (2020). Association of vitamin D and FGF23 with serum ferritin in hypoparathyroid thalassemia: A case-control study. BMC Nephrology, 21, 1–8.

23. Shah, F., Huey, K., Deshpande, S., Turner, M., Chitnis, M., Schiller, E., Yucel, A., Moro Bueno, L., & Oliva, E. N. (2022). Relationship between serum ferritin and outcomes in β-thalassemia: A systematic literature review. Journal of Clinical Medicine, 11(15), 4448. https://doi.org/10.3390/jcm11154448

24. Urmi, S., Munira, F. T., & Begum, S. (2022). Relationship between serum ferritin and parathyroid function in adult male patients with transfusion-dependent thalassemia. Journal of Bangladesh Society of Physiologist, 17(1), 1–5.

25. Verma, A., Khanna, A., Jangra, B., Nanda, S., & Verma, S. (2020). Association of vitamin D deficiency and bone mass with liver and heart iron overload in transfusion-dependent thalassemia. International Journal of Contemporary Pediatrics, 7(6), 1–6.

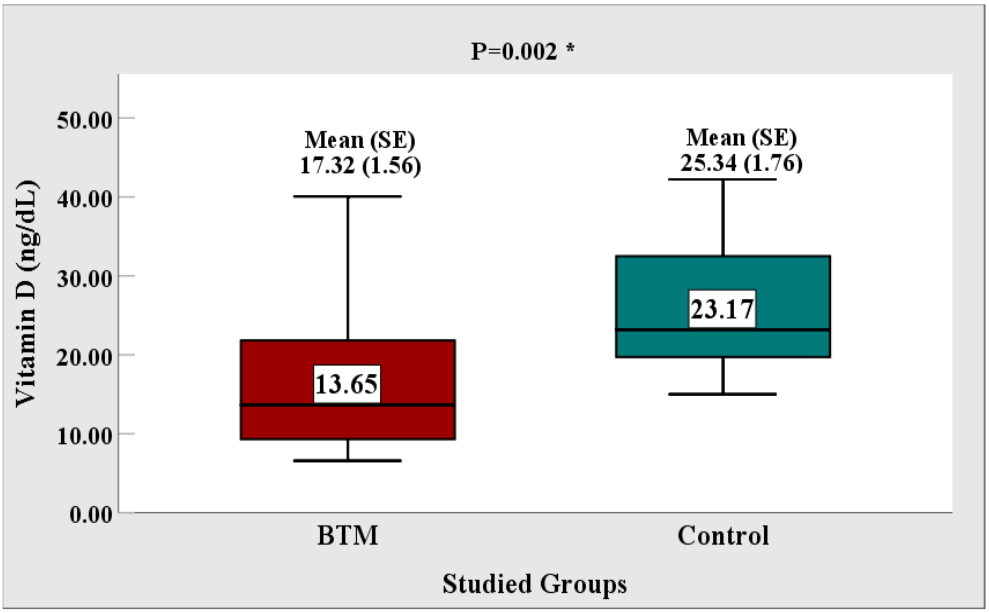


***Figure 1.*** *Serum Vitamin D (ng/dL) levels in the βTM patients and control groups. Significant differences at p-values * < 0.05, ** < 0.01. SEM Standard error of the mean*

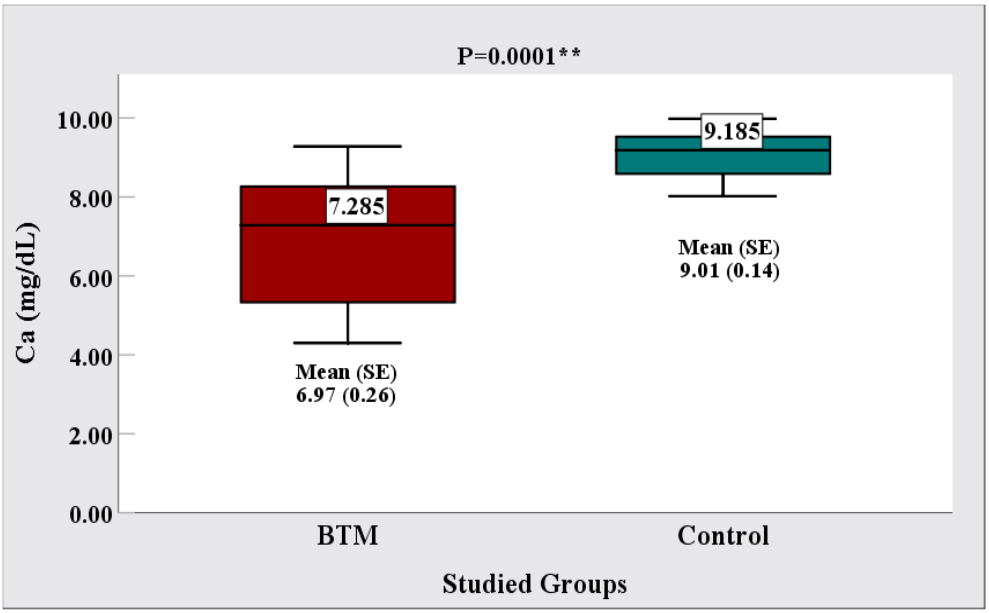


***Figure 2.*** *Serum Ca (mg/dL) levels in the βTM patients and control groups. Significant differences at p-values * < 0.05, ** < 0.01. SEM: Standard error of the mean.*

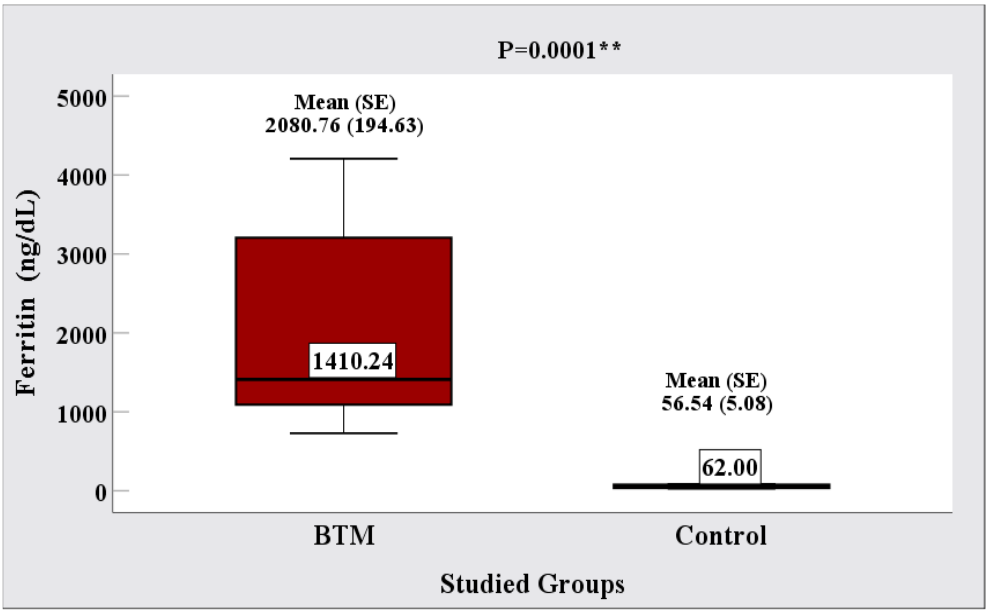


***Figure 3.*** *Serum Ferritin (ng/dL) levels in the βTM patients and control groups. Significant differences at p-values * < 0.05, ** < 0.01. SEM Standard error of the mean*

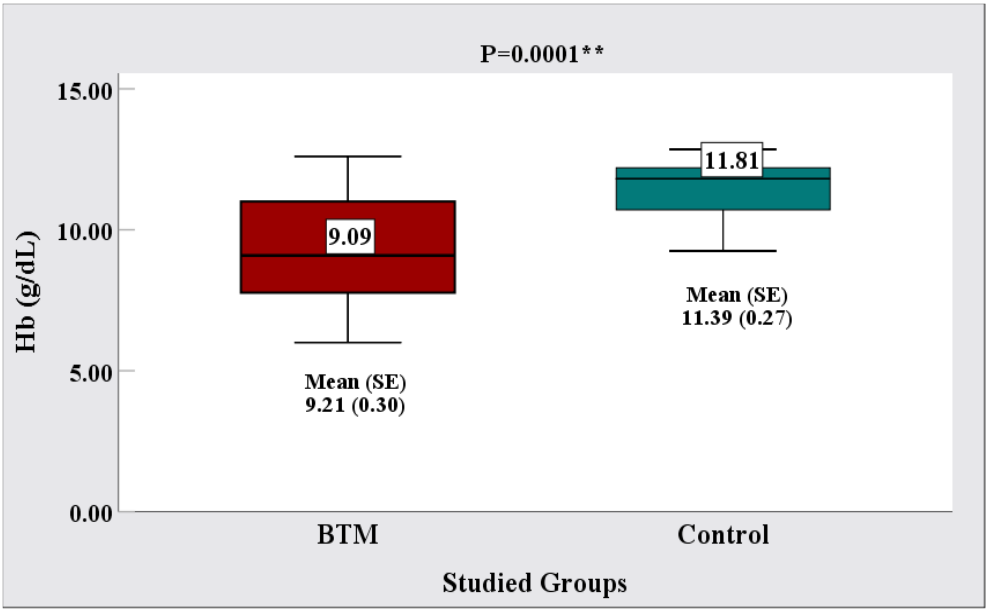


***Figure 4.*** *Hb (g/dL) levels in the βTM patients and control groups. Significant differences at p-values * < 0.05, ** < 0.01. SEM Standard error of the mean*

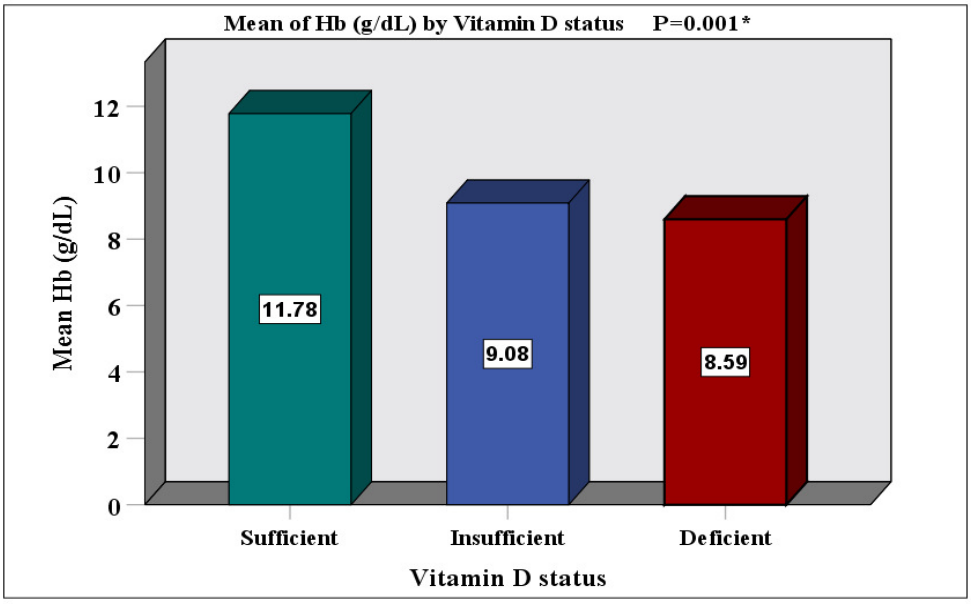


***Figure 5.*** *Hb (g/dL) levels associated with vitamin D status in patients βTM. Significant differences at p-values * < 0.05, ** < 0.01. SEM Standard error of the mean*

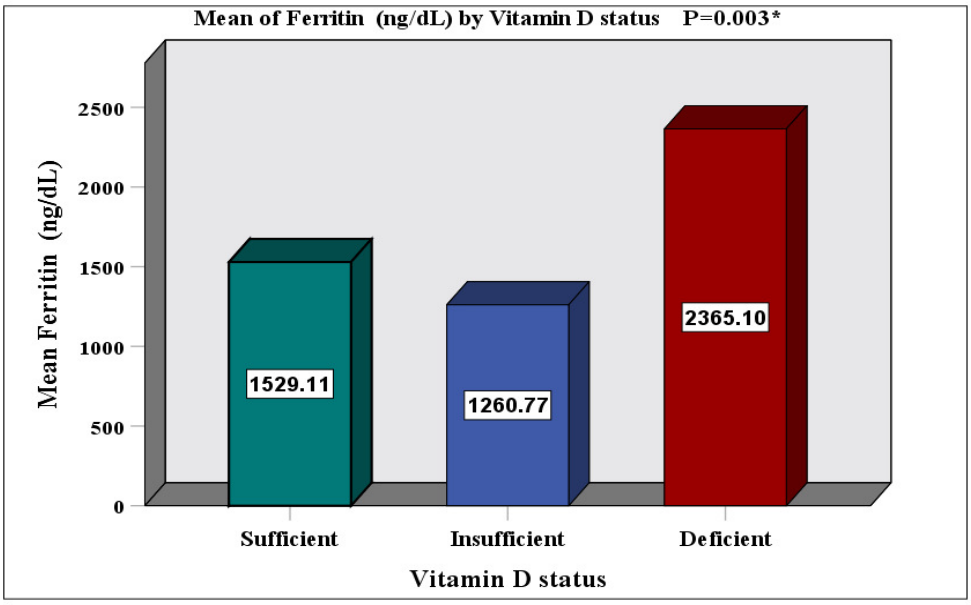


***Figure 6.*** *Serum Ferritin (ng/dL) levels associated with vitamin D status in patients βTM. Significant differences at p-values * < 0.05, ** < 0.01. SEM Standard error of the mean*

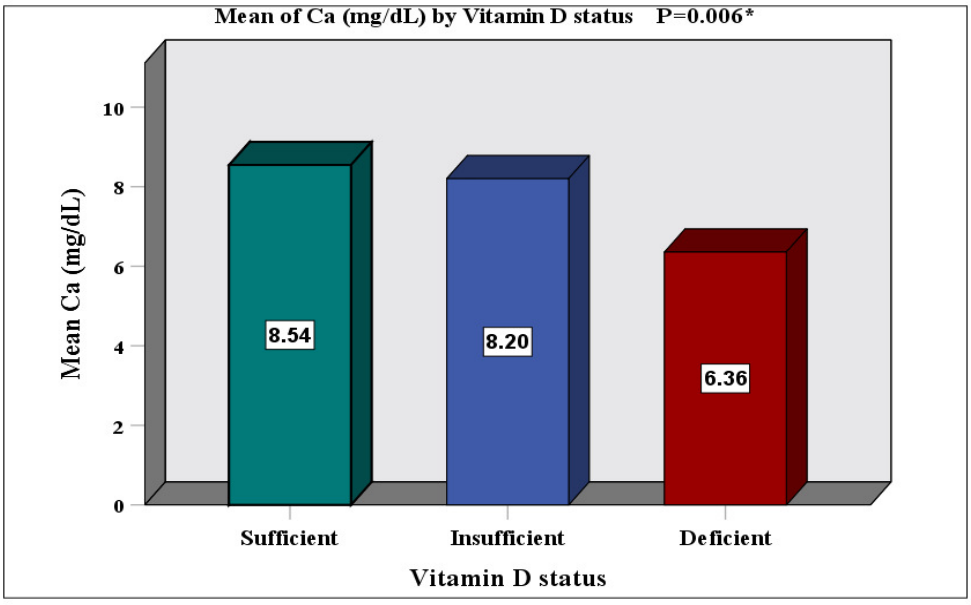


***Figure7.*** *Serum Ca (mg/dL) levels associated with vitamin D status in patients βTM. Significant differences at p-values * < 0.05, ** < 0.01. SEM Standard error of the mean*

**Table 1. Distribution of demographic parameters in βTM patients and control groups**.

| Variables | Categories | βTM | Control | Total | p-value |
|---|---|---|---|---|---|
| Age (year) | Mean (SE) | 10.78(1.12) | 11.05(1.23) | | 0.880 ns |
| | < 10 years | 25 | 13 | 38 | |
| | | 62.5% | 65.0% | 63.3% | 0.036 [a] |
| | >10 years | 15 | 7 | 22 | 0.850 ns |
| | | 37.5% | 35.0% | 36.7% | |
| Sex | Male | 21 | 9 | 30 | |
| | | 52.5% | 45.0% | 50.0% | 0.300[a] |
| | Female | 19 | 11 | 30 | 0.584 ns |
| | | 47.5% | 55.0% | 50.0% | |
| Vitamin D status | Deficient | 28 | 6 | 34 | |
| | | 70.0% | 30.0% | 56.7% | |
| | Insufficient | 5 | 8 | 13 | 9.380[a] |
| | | 12.5% | 40.0% | 21.7% | 0.009* |
| | Sufficient | 7 | 6 | 13 | |
| | | 17.5% | 30.0% | 21.7% | |
| Anemia status | Non-anemia | 3 | 7 | 10 | |
| | | 7.5% | 35.0% | 16.7% | |
| | Mild | 8 | 10 | 18 | |
| | | 20.0% | 50.0% | 30.0% | 19.300[a] |
| | Moderate | 15 | 3 | 18 | 0.0001** |
| | | 37.5% | 15.0% | 30.0% | |
| | Severe | 14 | 0 | 14 | |
| | | 35.0% | 0.0% | 23.3% | |
| Ferritin status | ≤1000 (ng/dL) | 8 | 20 | 28 | |
| | | 20.0% | 100.0% | 46.7% | 34.286[a] |
| | > 1000 (ng/dL) | 32 | 0 | 32 | 0.0001** |
| | | 80.0% | 0.0% | 53.3% | |
| Total | | 40 | 20 | 60 | |
| | | 100.0% | 100.0% | 100.0% | |

**Significant differences at p-value * < 0.05, ** < 0.01. a: Chi-Square test. Ns: non-significant.**

***Table 2.*** *Comparison of studied parameters in the βTM patients with control groups.*

| Variables | Control n = 20 | βTM n = 40 | P-value |
|---|---|---|---|
| **Age (year)** | 11.05 (1.23) | 10.78 (1.12) | 0.880 ns |
| **Vitamin D (ng/dL)** | 25.34 (1.76) | 17.32 (1.56) | 0.002* |
| **Ca (mg/dL)** | 9.01 (0.14) | 6.97 (0.26) | 0.0001** |
| **Ferritin (ng/dL)** | 56.54 (5.08) | 2080.76 (194.63) | 0.0001** |
| **Hb (g/dL)** | 11.39 (0.27) | 9.21 (0.30) | 0.0001** |

Different letters have significant differences at p-values * < 0.05, ** < 0.01. SEM: Standard error of the mean. Independent T-test, or Mann-Whitney.

***Table 3.*** *Comparison of studied parameters among vitamin D status in β-thalassemia major patients*

| Variables | Sufficient N = 7 | Insufficient N = 5 | Deficient N = 28 | p-value |
|---|---|---|---|---|
| **Vitamin D (ng/dL)** | 35.27 (1.41) A | 23.82 (1.38) B | 11.68 (0.64) C | 0.0001** |
| **Ca (mg/dL)** | 8.54 (0.19) A | 8.2 (0.35) A | 6.36 (0.29) B | 0.006* |
| **Hb (g/dL)** | 11.78 (0.25) A | 9.08 (0.69) B | 8.59 (0.3) C | 0.001* |
| **Ferritin (ng/dL)** | 1529.11 (433.96) A | 1260.77 (175.97) B | 2365.1 (237.9) A | 0.003* |
| **>1000** | 2 (28.6%) | 4 (80.0%) | 26 (92.9%) | 14.464[a] |
| **≤1000** | 5 (71.4%) | 1 (20.0%) | 2 (7.1%) | 0.0001** |

**Different letters have significant differences at p-values * < 0.05, ** < 0.01. SEM: Standard error of the mean. ANOVA test. a: Chi-Square test**

***Table 4.*** *Correlation of vitamin D with studied parameters in βTM patients.*

| | | Vitamin D | Ca | Ferritin | Hb |
|---|---|---|---|---|---|
| **Age (year)** | **r** | 0.788** | 0.493** | -0.293 | 0.463** |
| | **p-value** | 0.0001 | 0.001 | 0.066 | 0.003 |
| **Vitamin D (ng/dL)** | **r** | 1 | 0.772** | -0.517** | 0.772** |
| | **p-value** | | 0.0001 | 0.001 | 0.0001 |
| **Ca (mg/dL)** | **r** | | | -0.610** | 0.866** |
| | **p-value** | | | 0.0002 | 0.0001 |
| **Ferritin (ng/dL)** | **r** | | | 1 | -0.597** |
| | **p-value** | | | | 0.0001 |

Significant differences at p-value * < 0.05, ** < 0.01. r: Pearson correlation

***Table 5:*** *Logistic Regression Analysis of Factors Associated with Vitamin D Status in β-Thalassemia Major Patients*

| Variables | **Vitamin D Status** | **B** | **OR (95% CI)** | **P-value** |
|---|---|---|---|---|
| **Age Group (Ref: >10 yr.)** | Deficient | 1.649 | 5.200 (1.322–20.460) | 0.018* |
| | Insufficient | 0.624 | 1.867 (0.392–8.894) | 0.433 |
| | Sufficient | 0 (ref.) | — | — |
| **Sex (Ref: Female)** | Deficient | –1.291 | 0.275 (0.070–1.078) | 0.064 |
| | Insufficient | –0.341 | 0.711 (0.140–3.606) | 0.681 |
| | Sufficient | 0 (ref.) | — | — |
| **Anemia Status (Ref: None to Mild)** | Deficient | 1.540 | 4.667 (1.932-11.270) | 0.001* |
| | Insufficient | -0.811 | 0.444 (0.137–1.443) | 0.177 |
| | Sufficient | 0 (ref.) | — | — |
| **Ferritin Status (Ref: < 1000 ng/mL)** | Insufficient | 0.894 | 2.444 (0.361–16.547) | 0.360 |
| | Deficient | 2.883 | 17.875 (3.258–98.074) | 0.001* |
| | Sufficient | 0 (ref.) | — | — |

OR: Odds Ratio; CI: Confidence Interval; B: Regression Coefficient; Ref. Reference Group. Asterisk (*) Statistical significance at P < 0.05.

SOUTHERN JOURNAL OF SCIENCES

*ESTABLISHED IN 1993*

*Original research paper*

# PRIVACY-PRESERVING DATA ANONYMIZATION TOOL FOR MEDICAL DATA

# FERRAMENTA DE ANONIMIZAÇÃO DE DADOS MÉDICOS COM PRESERVAÇÃO DE PRIVACIDADE

BORKAKOTY, Sangeeta[1]; ISLAM, Atowar Ul[2]*; BORA, Kanak Chandra[3]

[1]University of Science & Technology Meghalaya, Department of Computer Science. India. ORCID: 0009-0003-1554-9717

[2]University of Science & Technology Meghalaya, Department of Computer Science. India. ORCID: 0000-0001-5345-0556

[3]University of Science & Technology Meghalaya, Department of Computer Science. India. ORCID: 0009-0009-0491-1235

** Corresponding author: e-mail: atowar91626@gmail.com*

Received xxx; received in revised form xxx; accepted xxx

## ABSTRACT

**Background:** Medical institutions collect a vast amount of sensitive patient data for personalized treatments and health trend analysis. However, this raises concerns regarding the privacy of patient data, as it contains sensitive and confidential information. **Aims:** Develop an anonymization tool using diverse techniques to protect data while preserving its utility. **Methods:** A Python-based data anonymization tool for medical datasets supporting both categorical and numerical data is developed. It employs various methods, including data perturbation, binning, scaling, transformation, and differential privacy. **Results:** The tool was able to anonymize sensitive data, both categorical and numerical, while preserving its utility for further analysis. **Discussion:** The Privacy-Preserving Data Anonymization Tool advances sensitive medical data management by anonymizing both categorical and numerical data using various techniques while retaining data utility. **Conclusions:** The Anonymization Tool addresses patient data privacy concerns by balancing data utility with privacy, enabling secure medical data use in research.

**Keywords**: *anonymization, privacy-preservation, medical dataset, data utility, data analytics.*

## RESUMO

**Introdução**: As instituições médicas coletam vastas quantidades de dados sensíveis de pacientes para tratamentos personalizados e análise de tendências de saúde. No entanto, isso levanta preocupações quanto à privacidade dos dados dos pacientes, pois contêm informações sensíveis e confidenciais. **Objetivos**: Desenvolver uma ferramenta de anonimização usando diversas técnicas para proteger dados enquanto preserva sua utilidade. **Métodos**: Uma ferramenta de anonimização de dados baseada em Python para conjuntos de dados médicos que suporta dados categóricos e numéricos foi desenvolvida. Ela emprega vários métodos, incluindo perturbação de dados, binning, escalonamento, transformação e privacidade diferencial. Resultados: A ferramenta foi capaz de anonimizar os dados sensíveis, tanto categóricos quanto numéricos, preservando ao mesmo tempo sua utilidade para análises posteriores. **Discussão**: A Ferramenta de Anonimização de Dados com Preservação de Privacidade avança o gerenciamento de dados médicos sensíveis ao anonimizar dados categóricos e numéricos usando várias técnicas enquanto mantém a utilidade dos dados. **Conclusões**: A Ferramenta de Anonimização aborda as preocupações com a privacidade dos dados dos pacientes equilibrando utilidade dos dados com privacidade, permitindo o uso seguro de dados médicos em pesquisas.

**Palavras-chave**: *anonimização, preservação de privacidade, conjunto de dados médicos, utilidade de dados, análise de dados.*

 
DOI: 10.48141/2764-5959.05.v33.n40.2025_05_BORA_pgs_75_85.pdf

## 1. INTRODUCTION:

Medical institutions collect sensitive patient information, including personal identification, medical histories, and genetic data, to enable personalized treatments, enhance diagnostic accuracy, and analyze health trends at both individual and population levels. This wealth of data holds the potential to drive significant advancements in medical research, improve patient outcomes, and inform public health policies. However, it also raises serious privacy concerns due to risks of unauthorized access, data breaches, and misuse. These issues are exacerbated by the increasing frequency and sophistication of cyberattacks targeting healthcare facilities, which can compromise patient trust and hinder the adoption of data-driven healthcare innovations.

Moreover, ethical challenges arise from the lack of transparency regarding data usage and sharing. Patients are often unaware of how their data is being stored, processed, or shared with third parties, raising concerns about consent and ownership. This highlights the critical need for robust privacy protections and ethical frameworks to ensure data is handled responsibly. Failure to address these concerns not only jeopardizes patient confidentiality but also threatens the integrity of the healthcare system.

There are two widely accepted methods to combat privacy breaches and ensure data privacy: data encryption and anonymization. In data encryption, the data is transformed into a ciphertext using cryptographic algorithms and keys. This makes the data unreadable to unauthorized. The encrypted data can be decrypted only by authorized parties who possess the corresponding decryption keys. This method ensures that the data remains protected if it is intercepted or accessed without authorization. However, data encryption is generally unsuitable when data needs to be frequently shared after processing. Data encryption and decryption add complexity and computational overhead to data-handling processes. Moreover, key management and ensuring compatibility and interoperability between systems and organizations may pose challenges.

In anonymization, the data is selectively removed or altered to prevent the identification of individuals and other details. However, if done indiscriminately, it can remove or conceal valuable information, thereby reducing the usefulness or accuracy of the data for analysis and decision-making. Various anonymization techniques have been developed to ensure data privacy without compromising its usability. Dhawas *et al.* (2024) have provided a survey of existing anonymization techniques, analyzing their advantages and disadvantages. Olatunji *et al.* (2022) have done an extensive review of anonymization for Healthcare Data.

Similar studies done by Kargupta *et al.* (2003) and Muralidhar & Sarathy (1999) focus on specific data anonymization techniques, like random data perturbation (RDP) methods.

One practical application of data analytics is in recommendation systems, widely used by e-commerce sites to suggest products to customers based on their buying habits. While such data analytics is valuable for business decision-making, it raises serious privacy concerns if it falls into the wrong hands. In this context, Murthy *et al.* (2019) have compared five anonymization techniques using the same dataset, reviewing the strengths and weaknesses of each approach. Marques & Bernardino (2020) have reviewed several anonymization techniques and efficient software tools, aiming to understand which methods offer higher levels of anonymization, along with their respective strengths and weaknesses. In the same lines, Majeed & Lee (2021) conducted a comprehensive survey of anonymization techniques for privacy-preserving data publishing, examining potential attacks on sanitized data and the different stakeholders involved in the anonymization process.

At a very basic level, privacy is about keeping personal information away from unauthorized access. It is essential for individual autonomy, individualism, and respect. There are four types of privacy: information, bodily, territorial, and communication.

This paper focuses on information privacy, which includes systems and infrastructures that collect, analyze, process, and publish users' data.

### 1.1 Aim of the project

To address the challenges of preserving privacy while maintaining the functionality of data, this paper aims to develop a Privacy-Preserving Anonymization tool for medical datasets, designed to safeguard sensitive patient information while enabling its meaningful use in research and healthcare analytics. This tool will employ anonymization techniques such as pseudonymization and binning to protect Personal Identifiable Information (PII) and other sensitive data while ensuring the functionality and utility of the datasets remain intact. Pseudonymization

replaces identifiable attributes with pseudonyms or unique codes, making it difficult to trace the information back to individuals without access to the specific mapping keys. Binning will group continuous or high-resolution data, such as ages or numerical test results, into broader categories or ranges, reducing the risk of re-identification while preserving the dataset's analytical value.

By integrating these techniques, the tool will strike a balance between robust privacy protection and the usability of the data for research and analysis. This approach ensures that medical datasets can be shared or analyzed without compromising patient confidentiality, enabling the secure and ethical use of health information across applications such as medical research, public health studies, and policy development.

## 2. MATERIALS AND METHODS:

### 2.1. Materials

The tool was developed in a Windows environment using Python version 3.12.2, selected for its comprehensive data processing and web application capabilities. Key libraries include Pandas for data manipulation, Flask for creating the web interface, Nest Asyncio for resolving conflicts in the event loop, and Random for pseudonymization. The application was programmed and tested using Jupyter Notebook version 7.1.3.

### 2.2. Methods

The anonymization techniques chosen for this tool are - binning for numerical data and pseudonymization for textual data. These are particularly well-suited given the specific use case and application context. One of the key reasons for their selection is their simplicity and ease of implementation. Unlike advanced techniques such as k-anonymity or differential privacy, binning and pseudonymization are straightforward to apply and require minimal computational resources. This makes them ideal for scenarios where quick, efficient anonymization is necessary, without relying on complex configurations or dependencies.

Additionally, these techniques excel in preserving the utility of the data. Binning obfuscates specific numerical values by grouping them into ranges, ensuring that patterns and trends remain observable, which is essential for exploratory data analysis or visualization. Pseudonymization, on the other hand, replaces text data with randomly generated identifiers while maintaining its structural integrity. This approach preserves categorical distinctions, making it highly effective in cases where understanding groupings or classifications is crucial, even when the actual identifiers are hidden.

The focus of this tool is on lightweight privacy needs, making these techniques particularly suitable. The use case involves anonymizing a dataset for general-purpose sharing or analysis rather than meeting the stringent privacy guarantees demanded in sensitive domains such as healthcare or finance. Advanced methods like differential privacy, while offering robust guarantees, are often unnecessary for simpler datasets and can be challenging to configure correctly. In contrast, binning and pseudonymization provide a practical and efficient solution.

Moreover, these techniques perform well in small-scale applications where computational efficiency is a priority. Methods such as k-anonymity or differential privacy can introduce performance bottlenecks, especially when deployed on lightweight systems or in real-time processing scenarios. The chosen techniques strike a balance between performance and effectiveness, ensuring the tool remains efficient and user-friendly.

The alignment of these techniques with the dataset's data types further justifies their use. Binning works effectively for numeric data by masking specific values while retaining ranges relevant for analysis. Pseudonymization, tailored for string data, successfully anonymizes identifiable text while preserving distinct categories. This alignment ensures that the anonymization process is both meaningful and contextually appropriate. Finally, the scalability and adaptability of these methods make them suitable for varying datasets. Without extensive preprocessing or parameter tuning, they can be applied across different structures and sizes, ensuring the tool's versatility for general-purpose applications.

#### 2.2.1. Implementation of the Tool

The program is a Flask-based web application designed for uploading and processing CSV files. Its primary goal is to provide users with the ability to:

- Upload a CSV file and view its attributes (column names and data types).

- Select specific columns (features) for anonymization or binning:
  - Textual data is pseudonymized by replacing values with random alphanumeric strings.
  - Numeric data is binned into ranges.
- Download the anonymized version of the CSV file.

The program employs user-friendly HTML interfaces and leverages pandas for data manipulation.

### 2.2.2 Source Codes

Firstly, the necessary libraries are imported.

- **pandas:** For CSV file manipulation.
- **Flask:** To create a web application.
- **nest_asyncio:** To handle asyncio event loops, especially in environments like Jupyter Notebook.
- **multiprocessing:** Allows running the Flask app as a separate process.
- **random & string:** Generate random strings for pseudonymization.
- **traceback:** For detailed error logging.

```
import pandas as pd
from flask import Flask, request,
render_template_string, send_file
import nest_asyncio
from multiprocessing import Process
import random
import string
import traceback
```

The nest_asyncio.apply() function is called to resolve potential event loop conflicts, making the application more robust. Then, the Flask app is initialized with app = Flask(__name__), which creates an instance of the web application.

```
# Applying nest_asyncio to avoid event
loop issues in Jupyter Notebook
nest_asyncio.apply()

# Creating the Flask app
app = Flask(__name__)
```

Next, two utility functions are defined to handle data anonymization.

The pseudonymize function replaces sensitive textual data with random strings. For every input text, it generates an 8-character alphanumeric string using Python's random.choices() function. This ensures that text data remains anonymous while maintaining uniformity across the dataset.

```
# Function for pseudonymizing text
(replacing with random strings)
def pseudonymize(text):
    return
''.join(random.choices(string.ascii_letter
s + string.digits, k=8))
```

The binning function divides numerical data into equal ranges, known as bins. The range of values in the dataset is divided into bins (default: 5), and each numeric value is replaced by a range string (e.g., 10-20). This reduces the granularity of numerical data while preserving its distribution pattern.

```
# Function for binning numeric data
def binning(value, bins=5):
    bin_size = (max(value) - min(value))
/ bins
    binned_values = [
        f"{min(value) + (int((val -
min(value)) / bin_size) * bin_size)}-
{min(value) + ((int((val - min(value)) /
bin_size) + 1) * bin_size)}"
        for val in value
    ]
    return binned_values
```

The html_template variable contains an HTML structure for the web interface. It provides:

- A form for uploading a CSV file.
- A table displaying file attributes (column names and data types) after the upload.
- A list of checkboxes allowing the user to select columns for anonymization.

The template uses placeholders ({% ... %}) for dynamic rendering via Flask's render_template_string() function.

```
# HTML template for the web page
html_template = """
<!DOCTYPE html>
<html lang="en">
<head>
    <meta charset="UTF-8">
    <meta name="viewport"
content="width=device-width, initial-
scale=1.0">
    <title>CSV Attribute Viewer</title>
    <style>
        body {
            font-family: Arial, sans-
serif;
            margin: 20px;
        }
        h1 {
            color: #333;
        }
        table {
            width: 100%;
            border-collapse: collapse;
            margin-top: 20px;
        }
        th, td {
            border: 1px solid #ddd;
            padding: 8px;
            text-align: left;
        }
```

```
        th {
            background-color: #f4f4f4;
        }
        .checkbox-container {
            display: flex;
            flex-direction: column;
        }
    </style>
</head>
<body>
    <h1>Upload a CSV File</h1>
    <form action="/" method="POST"
enctype="multipart/form-data">
        <input type="file" name="file"
accept=".csv" required>
        <button
type="submit">Upload</button>
    </form>
    {% if attributes %}
    <h2>Select Features to
Anonymize</h2>
    <form action="/anonymize"
method="POST">
        <div class="checkbox-container">
            {% for attr, dtype in
attributes %}
                <label>
                    <input
type="checkbox" name="features"
value="{{ attr }}"> {{ attr }} ({{ dtype
}})
                </label>
            {% endfor %}
        </div>
        <button
type="submit">Anonymize</button>
    </form>
    {% endif %}
</body>
</html>
"""
```

The upload_file route handles both GET and POST requests.

- For a GET request, the route simply renders the initial web page, displaying a form to upload a CSV file.
- For a POST request, the program retrieves the uploaded file using request.files.get("file") and processes it. The file is read into a pandas DataFrame using pd.read_csv(file), and its columns and data types are extracted into a list of tuples (attributes). These attributes are dynamically displayed in the web interface.
- If an error occurs while reading the file (e.g., an invalid CSV format), the program logs the error and displays a message indicating that the file could not be processed.

```
@app.route("/", methods=["GET", "POST"])
def upload_file():
    attributes = None
    if request.method == "POST":
        file = request.files.get("file")
        if file:
            try:
                # Read the CSV file into a
DataFrame
                df = pd.read_csv(file)
                # Extract columns and data
types
                attributes = [(col,
str(dtype)) for col, dtype in
df.dtypes.items()]
            except Exception as e:
                app.logger.error(f"Error
reading file: {e}")
                attributes = [("Error",
f"Unable to process file: {e}")]
    return
render_template_string(html_template,
attributes=attributes)
```

The /anonymize route is responsible for anonymizing the uploaded file.

- First, the selected features (columns) for anonymization are retrieved using request.form.getlist("features").
- The uploaded file is read into a pandas DataFrame. If the file loads successfully, the program iterates through the selected columns. Depending on the column's data type:
    - Textual columns (object or string type) are pseudonymized using the pseudonymize function.
    - Numeric columns (int64 or float64 type) are binned into ranges using the binning function.
- Once the anonymization is complete, the modified DataFrame is saved as a new CSV file (output.csv) using df.to_csv(output_file, index=False).
- A success message, *"Anonymized file saved as output.csv. You can download it below."*, is displayed on the web page. The page also provides a link to download the file by directing users to the /download route.
- The /download route allows users to download the anonymized file. The route uses Flask's send_file() function to serve the saved output.csv file as an attachment, enabling the user to save it locally. This ensures a seamless download experience directly from the web interface.

```
@app.route("/anonymize", methods=["POST"])
def anonymize_file():
    selected_features =
request.form.getlist("features")
    file = request.files.get("file")
```

```
    if file:
        try:
            # Read the CSV file into a
DataFrame
            df = pd.read_csv(file)
            app.logger.info(f"File loaded
successfully. Features selected:
{selected_features}")

            # Apply anonymization based on
feature type
            for feature in
selected_features:
                if feature in df.columns:
                    if df[feature].dtype
== 'object' or df[feature].dtype ==
'string':  # Text data
                        df[feature] =
df[feature].apply(pseudonymize)
                    elif df[feature].dtype
in ['int64', 'float64']:  # Numeric data
                        df[feature] =
binning(df[feature])

            # Save the anonymized
DataFrame to a new CSV file
            output_file = "output.csv"
            df.to_csv(output_file,
index=False)

app.logger.info(f"Anonymization completed.
Output saved to {output_file}")

            # Render a success message in
the HTML
            message = "Anonymized file
saved as output.csv. You can download it
below."
            download_link = f'<a
href="/download" target="_blank">Download
Anonymized File</a>'
            return
f"<p>{message}</p><p>{download_link}</p>"

        except Exception as e:
            app.logger.error(f"Error
during anonymization: {e}")

app.logger.error(traceback.format_exc())
            return "Error: An error
occurred while anonymizing the file."
    return "No file uploaded."
```

The run_app function initializes the Flask app on port 5000 in debug mode. To ensure the web server runs independently, the program uses Python's multiprocessing module. This allows the Flask app to run in a separate process without blocking other operations. By using the Process class, the Flask app starts in parallel with the main Python program, making it suitable for environments that might require additional processing tasks.

```
# Function to run Flask app in a separate
process
def run_app():
    app.run(port=5000, debug=True)

# Start the Flask app in a separate
process
if __name__ == "__main__":
    process = Process(target=run_app)
    process.start()
```

The proposed approach has been implemented as a web-based application to facilitate practical evaluation and reproducibility. The live application is publicly accessible at:

https://csv-anonymizer.onrender.com

The complete source code, including implementation details and documentation, is available in a public GitHub repository at:

https://github.com/sborkakoty-ustm/csv-anonymizer

## 3. RESULTS AND DISCUSSION:

### 3.1. Results

Upon executing the program, users are prompted to upload a CSV file containing data.

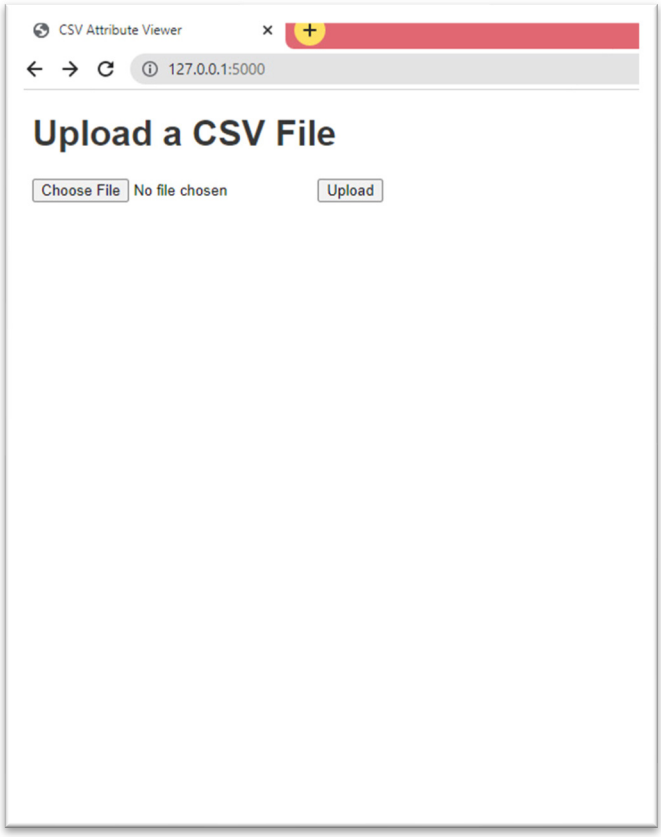


*Figure 1: Interface to upload CSV file*

After uploading the file, the application reads and processes the file, displaying the attributes (column names and data types) of the dataset. Users can then select which features

(columns) they wish to anonymize.

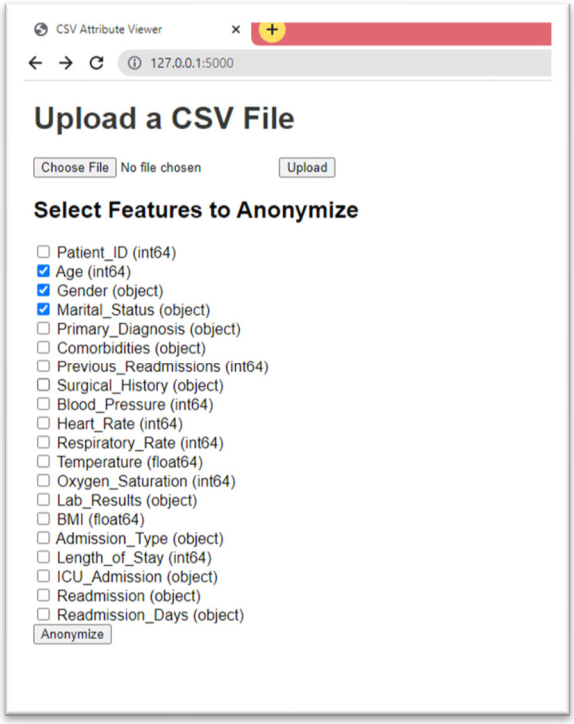


*Figure 2: Interface to select features to anonymize*

After anonymizing the selected features, the modified dataset is saved as output.csv, and the user is provided with a download link. A confirmation message is displayed, stating, "Anonymized file saved as output.csv. You can download it below." This seamless workflow enables users to efficiently anonymize their datasets while providing the necessary feedback about the operation's success.

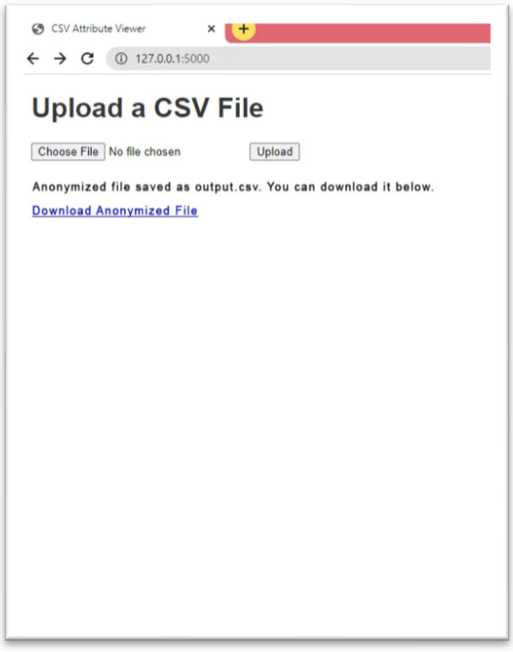


*Figure 3: Interface to download nonymized file*

### 3.2. Discussion

The implementation of pseudonymization and binning as anonymization techniques effectively reduces the risk of re-identifying individuals within a dataset while maintaining the analytical usefulness of the data. These techniques are particularly relevant for scenarios where data privacy and confidentiality are paramount, such as in healthcare.

1. **Pseudonymization**: Pseudonymization is a widely recognized technique for safeguarding personal data. By replacing sensitive textual data (such as names, addresses, or identifiers) with randomized strings, the application prevents unauthorized access to personal information. However, pseudonymization does not fully anonymize the data, as the generated pseudonyms can still be traced back to the original data if additional information is available. Therefore, it is critical to ensure that pseudonymization is combined with other privacy measures, such as secure storage or data encryption, to achieve a higher level of security.
2. **Binning**: The binning technique effectively reduces the precision of numeric data while preserving the overall distribution and patterns. It mitigates the risks associated with sharing fine-grained numerical values that could potentially lead to the identification of individuals. However, binning also introduces a trade-off between privacy and data utility. For example, while a binned dataset may obscure exact values, it may also make certain types of analysis, such as precise trend analysis or regression modeling, more difficult. The choice of the number of bins and their sizes is crucial to ensuring that the binning process effectively balances privacy and data usefulness.
3. **User Experience**: The user interface is designed to be simple and user-friendly. Users can easily upload CSV files, select features for anonymization, and download the processed file with minimal effort. This design ensures that non-technical users can perform data anonymization tasks without needing extensive programming knowledge. Furthermore, including feedback messages, such as confirmation that the anonymized file has been saved, enhances the overall user experience by providing clarity on the operation's status.

### 3.2.1 Areas of improvement

While the system has achieved positive results during the testing phase, there are certain areas of future scope and potential improvements that can further enhance its effectiveness:

1. **Integration of Advanced Anonymization Techniques**: To enhance the system's privacy guarantees, future work could explore integrating more sophisticated anonymization methods. Techniques such as **differential privacy** (Friedman & Schuster, 2010; Geng & Viswanath, 2016), which add noise to data to make it harder to trace back to individuals, could be implemented to further protect privacy. Additionally, incorporating **generalization** (i.e., transforming data into broader categories) could help to mitigate the risks of re-identification while maintaining data utility. (Ahsan *et al.*, 2021; Evans, 2005).
2. **Scalability Improvements**: To better handle large datasets, future improvements could focus on optimizing the application's performance. Techniques such as **chunk-based processing** (Sharma, 2022), where large files are processed in smaller, manageable segments, can be incorporated to reduce memory consumption and enhance efficiency. Additionally, parallel or distributed computing techniques could be explored to speed up the processing of large datasets, making the application more scalable and suitable for enterprise-level use cases (Sedgwick, 2022).
3. **Automated Feature Selection**: The current system requires users to manually select features for anonymization. To improve the user experience and reduce errors, automated feature-selection algorithms could be integrated to recommend which features should be anonymized based on predefined privacy rules or data sensitivity levels. Machine learning algorithms could be used to classify and prioritize sensitive attributes, streamlining the process for non-technical users.
4. **Extended Data Formats**: The current implementation supports only CSV files. Future iterations of the system could expand its functionality to support additional file formats, such as Excel and JSON, and to enable database connections, making the application more versatile and accessible to a wider range of users and industries.
5. **Enhanced User Interface and Experience**: Future versions of the application could improve the user interface (UI) by providing more granular control over the anonymization process, such as allowing users to define custom binning ranges or pseudonymization patterns. Additionally, incorporating a more intuitive UI with visual feedback (e.g., progress bars and alerts for successful anonymization) could enhance the overall user experience, especially for users with limited technical expertise.

## 4. CONCLUSIONS:

This paper presents an anonymization tool designed to protect the privacy of individuals in medical datasets, specifically focusing on pseudonymization and binning techniques for text and numeric data. By integrating Flask for web-based file uploads and processing, the tool provides an intuitive interface that lets users upload CSV files, select anonymization features, and download the modified dataset. By applying pseudonymization to text-based data and binning to numeric values, the system reduces the risk of re-identification while preserving the dataset's general structure and utility.

While the tool demonstrates the feasibility and effectiveness of basic anonymization techniques, it also highlights several limitations, including potential loss of data precision, reversibility of pseudonymization, and scalability challenges with large datasets. Additionally, the current implementation does not address advanced privacy threats, such as inference attacks, and lacks support for data formats beyond CSV.

Despite these limitations, the tool represents a valuable step toward ensuring data privacy in the era of big data and analytics. Future work in this area could expand the system’s capabilities by incorporating advanced anonymization techniques, improving scalability, automating feature selection, and ensuring compliance with international privacy regulations. By building on the current framework, this tool can evolve into a more robust, secure solution that addresses the growing concerns about data privacy in an increasingly connected world.

## 5. DECLARATIONS

### 5.1. Study Limitations

a) **Loss of Data Precision**: One key limitation of the current anonymization method, particularly the binning technique, is the potential loss of precision in numeric data. By grouping numerical values into bins, exact values are obscured, which may reduce the ability to perform certain analyses that require precise numerical data. For example, regression models or detailed statistical analyses may be less accurate because finer data details are lost during binning.

b) **Reversibility of Pseudonymization**: While pseudonymization is an effective method for anonymizing text-based data, it remains vulnerable to reversibility if the pseudonymization key or algorithm is exposed. When the mapping between original and pseudonymized data is known or can be inferred, the pseudonymized data can be linked back to individuals. Therefore, this technique alone may not be sufficient to fully safeguard privacy in high-risk environments.

c) **Limited Anonymization Techniques**: The current system employs only pseudonymization for textual data and binning for numerical data. These two techniques may not be robust enough for certain complex privacy concerns. The application does not address advanced privacy threats, such as inference or linkage attacks, where anonymized data may still be linked to individuals using external information.

d) **Scalability and Performance**: While the application performs effectively on small to medium-sized datasets, it may experience performance issues when handling large volumes of data. The current implementation loads the entire dataset into memory before applying anonymization, which could lead to high memory consumption and slow processing times for large datasets. As the dataset size increases, this could affect the application's responsiveness and efficiency.


### 5.2. Acknowledgements

I want to express my sincere gratitude to everyone who has offered their support during the research journey. While not directly involved in this project, the indirect contributions and unwavering support from various individuals have greatly contributed to its success. I also want to acknowledge the reviewers and editors for their valuable feedback and suggestions, which have significantly enhanced the quality of this research paper.

### 5.3. Funding source

The authors funded this research. In accordance with the ethical guidelines of the Southern Journal of Sciences, which do not allow donations from authors with manuscripts under evaluation (even when research funds are available), or in cases of authors' financial constraints, publication costs were fully absorbed by the journal under our Platinum Open Access policy, through the support of the Araucária Scientific Association (https://acaria.org/). This policy aims to ensure complete independence between the editorial process and any financial aspects, reinforcing our commitment to scientific integrity and equity in knowledge dissemination.


### 5.4. Competing Interests

The authors declare no potential conflict of interest in this publication.

### 5.5. Open Access



### 5.6. AI usage declaration

The authors declare that no Artificial Intelligence (AI) or AI-assisted technologies were used in the conception, data analysis, or preparation of this manuscript. All content presented is the original

work of the authors.

### 5.7. Author's contribution

All authors contributed to the design and implementation of the research, to the analysis of the results, and to the writing of the manuscript.

## 6. HUMAN AND ANIMAL-RELATED STUDIES

#### 6.1. Ethical Approval

Not applicable.

#### 6.2. Informed Consent

Not applicable.

## 7. REFERENCES:


1. Majeed, A., & Lee, S. (2021). Anonymization techniques for privacy preserving data publishing: A comprehensive survey. *IEEE Access*, *9*, 8512–8545. https://doi.org/10.1109/access.2020.3045700
2. Marques, J., & Bernardino, J. (2020). Analysis of data anonymization techniques. In *Proceedings of the 12th International Joint Conference on Knowledge Discovery, Knowledge Engineering and Knowledge Management* (pp. 235–241). SCITEPRESS – Science and Technology Publications. https://doi.org/10.5220/0010142302350241
3. Murthy, S., Abu Bakar, A., Abdul Rahim, F., & Ramli, R. (2019). A comparative study of data anonymization techniques. In *2019 IEEE 5th International Conference on Big Data Security on Cloud (BigDataSecurity)* (pp. 306–309). IEEE. https://doi.org/10.1109/bigdatasecurity-hpsc-ids.2019.00063
4. Kargupta, H., Datta, S., Wang, Q., & Sivakumar, K. (2003). On the privacy preserving properties of random data perturbation techniques. In *Proceedings of the Third IEEE International Conference on Data Mining* (pp. 99–106). IEEE Computer Society. https://doi.org/10.1109/icdm.2003.1250908
5. Muralidhar, K., & Sarathy, R. (1999). Security of random data perturbation methods. *ACM Transactions on Database Systems*, *24*(4), 487–493. https://doi.org/10.1145/331983.331986
6. Dhawas, P., Dhore, A., Bhagat, D., Pawar, R. D., Kukade, A., & Kalbande, K. (2024). Big data preprocessing, techniques, integration, transformation, normalisation, cleaning, discretization, and binning. In *Advances in Business Information Systems and Analytics* (pp. 159–182). IGI Global. https://doi.org/10.4018/979-8-3693-0413-6.ch006
7. Ahsan, M., Mahmud, M., Saha, P., Gupta, K., & Siddique, Z. (2021). Effect of data scaling methods on machine learning algorithms and model performance. *Technologies*, *9*(3), 52. https://doi.org/10.3390/technologies9030052
8. Evans, P. (2005). Scaling and assessment of data quality. *Acta Crystallographica Section D Biological Crystallography*, *62*(1), 72–82. https://doi.org/10.1107/s0907444905036693
9. Sharma, V. (2022). A study on data scaling methods for machine learning. *International Journal for Global Academic & Scientific Research*, *1*(1). https://doi.org/10.55938/ijgasr.v1i1.4
10. Sedgwick, P. (2012). Log transformation of data. *BMJ*, *345*, Article e6727. https://doi.org/10.1136/bmj.e6727
11. Dwork, C. (2006). Differential privacy. In *Lecture Notes in Computer Science* (pp. 1–12). Springer Berlin Heidelberg. https://doi.org/10.1007/11787006_1
12. Friedman, A., & Schuster, A. (2010). Data mining with differential privacy. In *Proceedings of the 16th ACM SIGKDD International Conference on Knowledge Discovery and Data Mining* (pp. 493–502). Association for Computing Machinery. https://doi.org/10.1145/1835804.1835868
13. Geng, Q., & Viswanath, P. (2016). The optimal noise-adding mechanism in differential privacy. *IEEE Transactions on Information Theory*, *62*(2), 925–951. https://doi.org/10.1109/tit.2015.2504967
14. Olatunji, I. E., Rauch, J., Katzensteiner, M., & Khosla, M. (2022). A review of anonymization for healthcare data. *Big Data*. Mary Ann Liebert Inc. https://doi.org/10.1089/big.2021.0169

# EDITORIAL DE TRANSIÇÃO - SOUTHERN JOURNAL OF SCIENCES

Caros autores, revisores, leitores e colaboradores,

Após 32 anos de publicação contínua e ininterrupta no Brasil, o **SOUTHERN JOURNAL OF SCIENCES** inicia um novo capítulo em sua história. Esta é a última edição sob gestão brasileira, marcando o início de uma nova fase internacional.

Iniciado em 1993 pelo Dr. Lavinel Ionescu como **Southern Brazilian Journal of Chemistry**, posteriormente continuado pelos Drs. Luis Alcides Brandini De Boni (2017-2021), Walter José Peláez e Cristián Andrés Quintero (2022-2025), este periódico atravessou mais de três décadas de contribuições científicas significativas nas áreas de Química, Física, Matemática, Biologia, Farmácia, Medicina, Engenharia e áreas interdisciplinares correlatas.

Ao longo desses anos, o jornal evoluiu: mudou de nome (de Southern Brazilian Journal of Chemistry para Southern Journal of Sciences em 2021), ampliou seu escopo multidisciplinar, adotou políticas de acesso aberto sem taxas de publicação, manteve rigorosos padrões de revisão por pares em formato duplo-cego, e consolidou sua indexação em bases internacionais.

**SOBRE O FUTURO DO SJS:**

Temos a satisfação de anunciar que o **Southern Journal of Sciences** será transferido para a **Universidad de Mendoza, Argentina**, onde continuará sua missão como publicação científica internacional. A doação do periódico foi oficialmente aceita pela Unidad de Gestión del Conocimiento (UGC) e pela Editorial Idearium (EdIUM) da Universidad de Mendoza.

Esta transição, que envolve aspectos técnicos editoriais e legais, será conduzida com o apoio do Dr. Cristián Andrés Quintero a partir de fevereiro de 2025. O jornal passa, assim, de uma publicação brasileira para uma publicação argentina, ampliando seu alcance e fortalecendo a colaboração científica na região latino-americana.

Este não é um fim, mas uma renovação e expansão internacional do projeto. O legado construído ao longo de três décadas no Brasil continuará vivo sob nova gestão, mantendo os mesmos valores de excelência científica, rigor na revisão por pares e compromisso com o acesso aberto ao conhecimento.

**AGRADECIMENTOS:**

A todos os autores que confiaram suas pesquisas a este periódico, aos revisores que dedicaram seu tempo e expertise para manter a qualidade científica de nossas publicações, aos membros do conselho editorial que orientaram nossas decisões, e aos leitores que acompanharam nossa jornada – nosso mais profundo agradecimento.

Esta não é uma despedida da ciência, mas uma transformação que fortalece nosso projeto. O legado construído ao longo desses 32 anos permanecerá acessível e continuará contribuindo para o avanço do conhecimento científico. Os artigos publicados estão preservados digitalmente via Portico e permanecem disponíveis em acesso aberto.

O futuro do SJS na Universidad de Mendoza honrará a missão estabelecida em 1993: promover a excelência científica, facilitar o acesso ao conhecimento e contribuir para o desenvolvimento da ciência em âmbito internacional. Que esta nova fase traga benefícios mútuos e contribua significativamente para a ciência em toda a região latino-americana.



10.48141/2764-5959.06.v33.n40.2025_06_WALTER_pgs_86_91.pdf

A todos, nossa gratidão eterna.



*Southern Journal of Sciences*
*ISSN: 2764-5959 (Online) | ISSN: 2764-5967 (Print)*
*DOI: 10.48141/2764-5959*
*Nova Prata - RS, Brasil*
*1993 - 2025*

# TRANSITION EDITORIAL - SOUTHERN JOURNAL OF SCIENCES

Dear authors, reviewers, readers, and collaborators,

After 32 years of continuous and uninterrupted publication in Brazil, the **SOUTHERN JOURNAL OF SCIENCES** begins a new chapter in its history. This is the last issue under Brazilian management, marking the beginning of a new international phase.

Started in 1993 by Dr. Lavinel Ionescu as the **Southern Brazilian Journal of Chemistry**, later continued by Drs. Luis Alcides Brandini De Boni (2017-2021), Walter José Peláez, and Cristián Andrés Quintero (2022-2025), this journal has crossed more than three decades of significant scientific contributions in Chemistry, Physics, Mathematics, Biology, Pharmacy, Medicine, Engineering, and related interdisciplinary areas.

Throughout these years, the journal has evolved: it changed its name (from Southern Brazilian Journal of Chemistry to Southern Journal of Sciences in 2021), expanded its multidisciplinary scope, adopted open-access policies with no publication fees, maintained rigorous double-blind peer-review standards, and consolidated its indexation in international databases.

**ABOUT THE FUTURE OF SJS:**

We are pleased to announce that the **Southern Journal of Sciences** will be transferred to the **Universidad de Mendoza, Argentina**, where it will continue its mission as an international scientific publication. The donation of the journal has been officially accepted by the Unidad de Gestión del Conocimiento (UGC) and Editorial Idearium (EdIUM) of Universidad de Mendoza.

This transition, involving editorial technical and legal aspects, will be conducted with the support of Dr. Cristián Andrés Quintero starting in February 2025. The journal thus transitions from a Brazilian publication to an Argentine publication, expanding its reach and strengthening scientific collaboration in the Latin American region.

This is not an end, but a renewal and international expansion of the project. The legacy built over three decades in Brazil will continue to thrive under new management, maintaining the same values of scientific excellence, rigorous peer review, and commitment to open access to knowledge.

**ACKNOWLEDGMENTS:**

To all authors who entrusted their research to this journal, to reviewers who dedicated their time and expertise to maintain the scientific quality of our publications, to editorial board members who guided our decisions, and to readers who followed our journey – our deepest gratitude.

This is not a farewell to science, but a transformation that strengthens our project. The legacy built over these 32 years will remain accessible and continue contributing to the advancement of scientific knowledge. Published articles are digitally preserved via Portico and remain available in open access.

The future of SJS at Universidad de Mendoza will honor the mission established in 1993: promoting scientific excellence, facilitating access to knowledge, and contributing to the development of science internationally. May this new phase bring mutual benefits and contribute significantly to science throughout the Latin American region.



10.48141/2764-5959.06.v33.n40.2025_06_WALTER_pgs_86_91.pdf

To all, our eternal gratitude.

**Walter José Peláez**
Editor-in-Chief

**Cristián Andrés Quintero**
Co-Editor

**Luis Alcides Brandini De Boni**
Managing editor

*Southern Journal of Sciences*
*ISSN: 2764-5959 (Online) | ISSN: 2764-5967 (Print)*
*DOI: 10.48141/2764-5959*
*Nova Prata - RS, Brazil*
*1993 - 2025*

# EDITORIAL DE TRANSICIÓN - SOUTHERN JOURNAL OF SCIENCES

Estimados autores, revisores, lectores y colaboradores,

Después de 32 años de publicación continua e ininterrumpida en Brasil, el **SOUTHERN JOURNAL OF SCIENCES** inicia un nuevo capítulo en su historia. Esta es la última edición bajo gestión brasileña, marcando el inicio de una nueva fase internacional.

Iniciado en 1993 por el Dr. Lavinel Ionescu como **Southern Brazilian Journal of Chemistry**, posteriormente continuado por los Dres. Luis Alcides Brandini De Boni (2017-2021), Walter José Peláez y Cristián Andrés Quintero (2022-2025), esta revista ha atravesado más de tres décadas de contribuciones científicas significativas en las áreas de Química, Física, Matemática, Biología, Farmacia, Medicina, Ingeniería y áreas interdisciplinarias relacionadas.

A lo largo de estos años, la revista ha evolucionado: cambió de nombre (de Southern Brazilian Journal of Chemistry a Southern Journal of Sciences en 2021), amplió su alcance multidisciplinario, adoptó políticas de acceso abierto sin cargos por publicación, mantuvo rigurosos estándares de revisión por pares en formato doble ciego, y consolidó su indexación en bases de datos internacionales.

## SOBRE EL FUTURO DEL SJS:

Tenemos la satisfacción de anunciar que el **Southern Journal of Sciences** será transferido a la **Universidad de Mendoza, Argentina**, donde continuará su misión como publicación científica internacional. La donación de la revista ha sido oficialmente aceptada por la Unidad de Gestión del Conocimiento (UGC) y la Editorial Idearium (EdIUM) de la Universidad de Mendoza.

Esta transición, que involucra aspectos técnicos editoriales y legales, será conducida con el apoyo del Dr. Cristián Andrés Quintero a partir de febrero de 2025. La revista pasa así de una publicación brasileña a una publicación argentina, ampliando su alcance y fortaleciendo la colaboración científica en la región latinoamericana.

Este no es un final, sino una renovación y expansión internacional del proyecto. El legado construido a lo largo de tres décadas en Brasil continuará vivo bajo nueva gestión, manteniendo los mismos valores de excelencia científica, rigor en la revisión por pares y compromiso con el acceso abierto al conocimiento.

## AGRADECIMIENTOS:

A todos los autores que confiaron sus investigaciones a esta revista, a los revisores que dedicaron su tiempo y expertise para mantener la calidad científica de nuestras publicaciones, a los miembros del consejo editorial que orientaron nuestras decisiones, y a los lectores que acompañaron nuestro recorrido – nuestra más profunda gratitud.

Esta no es una despedida de la ciencia, sino una transformación que fortalece nuestro proyecto. El legado construido a lo largo de estos 32 años permanecerá accesible y continuará contribuyendo al avance del conocimiento científico. Los artículos publicados están preservados digitalmente vía Portico y permanecen disponibles en acceso abierto.



10.48141/2764-5959.06.v33.n40.2025_06_WALTER_pgs_86_91.pdf

El futuro del SJS en la Universidad de Mendoza honrará la misión establecida en 1993: promover la excelencia científica, facilitar el acceso al conocimiento y contribuir al desarrollo de la ciencia en ámbito internacional. Que esta nueva fase traiga beneficios mutuos y contribuya significativamente a la ciencia en toda la región latinoamericana.

A todos, nuestra gratitud eterna.

**Walter José Peláez**
Editor-in-Chief

**Cristián Andrés Quintero**
Co-Editor

**Luis Alcides Brandini De Boni**
Managing editor

*Southern Journal of Sciences*
*ISSN: 2764-5959 (Online) | ISSN: 2764-5967 (Print)*
*DOI: 10.48141/2764-5959*
*Nova Prata - RS, Brasil*
*1993 - 2025*


Call for papers
www.sscon.org
CNPq
Conselho Nacional de Desenvolvimento Científico e Tecnológico
Process: 440182/2025-5
UNIVERSIDADE DE VASSOURAS
SOUTHERN SCIENCE CONFERENCE
SOUTHERN SCIENCE CONFERENCE
UM
UNIVERSIDAD DE MENDOZA
UNIVERSIDADE DE VASSOURAS

SOUTHERN JOURNAL OF SCIENCES

*ESTABLISHED IN 1993*

*ATR - 2025*

# SOUTHERN JOURNAL OF SCIENCES ANNUAL TRANSPARENCY REPORT

Walter José Pelaez[1]; Luis Alcides Brandini De Boni[2]

[1] INFIQC, Departamento de Fisicoquímica. Facultad de Ciencias Químicas, Universidad Nacional de Córdoba, Córdoba, Argentina.

[2] Southern Journal of Sciences, Brazil.

** Correspondence author*
*email: sjofsciences@sjofsciences.com*

Accepted 28 December 2025

In 2022, the Southern Journal of Science introduced the practice of producing an annual transparency report to give authors and institutions access to useful information about the journal. The main facts were presented in bullet format to make the report succinct.

- **Current Editor-in-Cheife**: Dr. Walter José Pelaez.
- **Past Editors**: Dr. Lavinel G. Ionescu; Dr. Luis A. B. De Boni.
- **Currently Edited by:** Aruacária Scientific Association CNPJ # 52.968.321/0001-8
- **Number of countries represented in the journal council**: 12.
- **Number of conferences the journal was invited to publish the resulting material**: 1.
- **Number of conferences that the journal published the resulting material**: 0.
- **Number of manuscripts received in 2024**: 26
- **Number of manuscripts published in 2024**: 12
- **Amount of manuscripts that will continue the publication process in 2025**: 2
- **Amount of improper submissions**: 2
- **Amount of rectified submissions**: 2
- **Innovative tools introduced in the journal**
    - *Abstract Maker tool*: <https://www.sjofsciences.com/Abstract-maker.php>
    - *Manuscript Sketch Tool*: <https://www.sjofsciences.com/manuscript-sketch-maker.php>
    - *Reference formatting tool**: <https://www.sjofsciences.com/doi_to_apa.htm>. This tool reflects the page https://citation.crosscite.org/
- **Financial support received from other institutions (in USD):** $ 0,00. An independent journal.
- **Indexed in:** Index Copernicus International; Crossref; Google Scholar; ROAD (Directory of Open Access Scholarly Resources); Internet Archive Scholar (FATCAT); OpenAlex; SUDOC (French University Documentation System); ISSN Portal.
- **Transition from Brazil to Argentina:** Process initiated.

 
DOI: 10.48141/2764-5959.08.v33.n40.2025_08_ATR_pgs_93.pdf